158

THESE

PRESENTEE A L'UNIVERSITE DE PARIS XI

POUR L'OBTENTION DU DOCTORAT DE 3ème CYCLE

par

François HYAFIL

Spécialité : Enzymologie

Sujet : Le rôle de l'ion métallique dans la réaction d'adénylation de la méthionine catalysée par la méthionyl tARN synthétase d'*Escherichia coli*.

Soutenue le 12 octobre 1976 devant la Commission composée de :

Pr. Jeannine	YON	Président
Dr. Antoine	DANCHIN	Rapporteur
Dr. Georges	COHEN	Examinateurs
Dr. Sylvain	BLANQUET	
Dr. Jean-Pierre	WALLER	

THESE

PRESENTEE A L'UNIVERSITE DE PARIS XI

POUR L'OBTENTION DU DOCTORAT DE 3ème CYCLE

par

François HYAFIL

Spécialité : Enzymologie

Sujet : Le rôle de l'ion métallique dans la réaction d'adénylation de la méthionine catalysée par la méthionyl tARN synthétase d'*Escherichia coli*.

Soutenue le 12 octobre 1976 devant la Commission composée de :

Pr. Jeannine	YON	Président
Dr. Antoine	DANCHIN	Rapporteur
Dr. Georges	COHEN	Examinateurs
Dr. Sylvain	BLANQUET	Examinateurs
Dr. Jean-Pierre	WALLER	Examinateurs

UNIV.
LEIDEN
BIBL.

A Sophie

Ainsi comme les historiens qui décrivent la terre en figure (...) ont accoutumé de supprimer aux extrémités de leurs cartes les régions dont ils n'ont point de connaissance, et en conter quelques telles raisons par endroit de la marge : outre ces pays-ci n'y a plus que profondes sablonnières sans eau, pleines de bêtes venimeuses, ou de la vase que l'on ne peut naviguer, ou la Scythie déserte pour le froid, ou bien la mer glacée.

PLUTARQUE
La vie des hommes illustres
Traduction de Jacques Amyot.

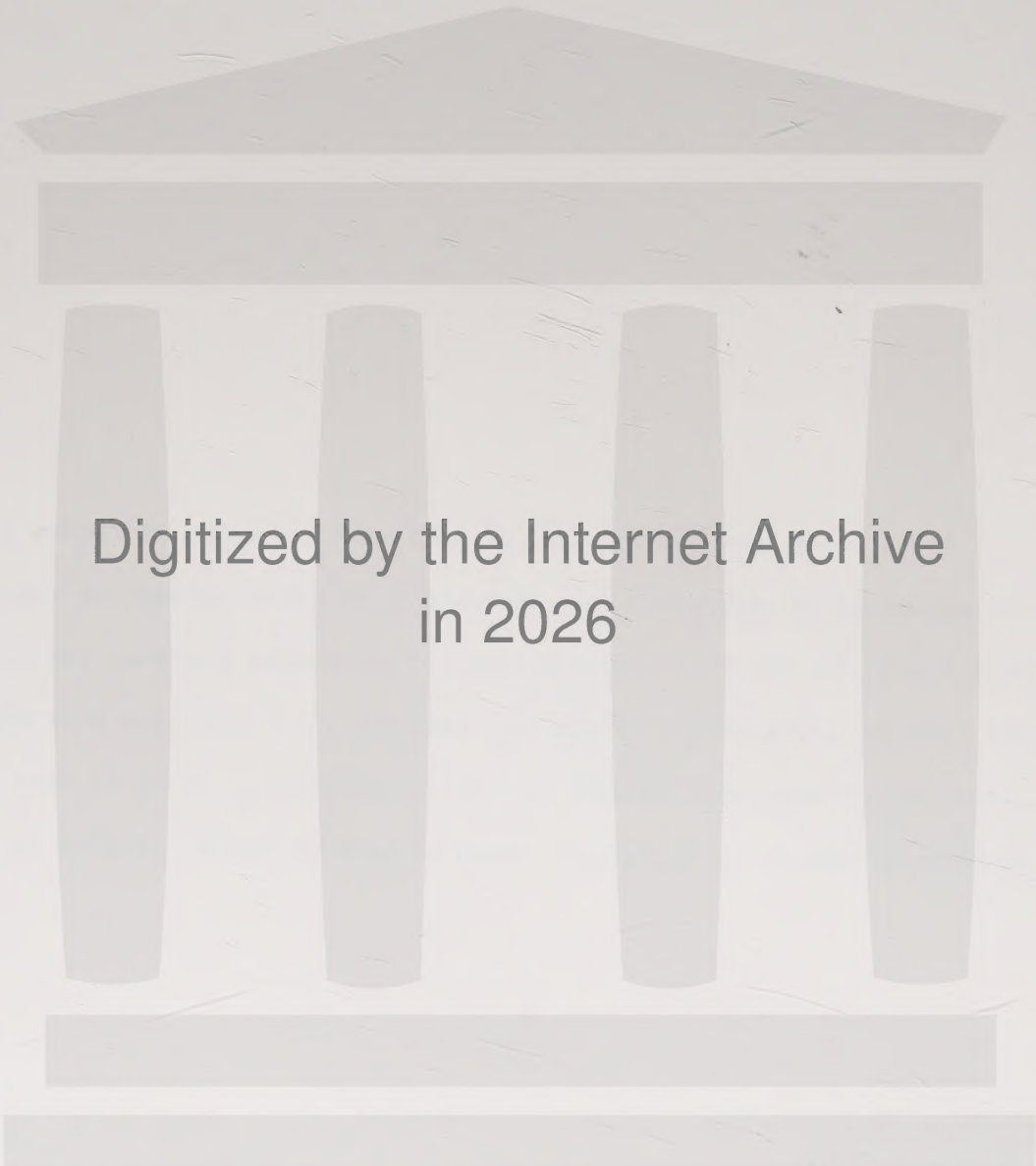
Digitized by the Internet Archive
in 2026

https://archive.org/details/IA41548120_0015

Je voudrais tout d'abord remercier Monsieur Jean-Pierre WALLER qui m'a accueilli au Laboratoire d'Enzymologie du C.N.R.S. à Gif-sur-Yvette puis, à sa création, au Laboratoire de Biochimie de l'Ecole Polytechnique. Son intérêt constant pour mon travail, ses nombreux conseils et les nombreuses discussions scientifiques que nous avons pu avoir m'ont stimulé et aidé durant les deux années passées sous sa direction.

Je voudrais également remercier Monsieur Sylvain BLANQUET qui a guidé mes premiers pas en biochimie et qui par sa sollicitude constante a permis la réalisation de ce travail. Je suis également très reconnaissant à tous mes collègues du laboratoire et plus particulièrement à Monsieur Guy FAYAT qui m'a fait partager un peu de sa précieuse expérience de la manipulation biochimique. Je ne voudrais pas quitter le laboratoire sans exprimer ma gratitude à Mesdames Ornella FOURNIER et Elisabeth MOTTA qui ont habilement et patiemment assuré la frappe de mes manuscrits.

A l'extérieur du laboratoire, ma reconnaissance va tout d'abord aux voisins géographiques et plus particulièrement à Monsieur Maurice GUERON, Directeur du Laboratoire de Biophysique avec qui j'ai eu de nombreuses et stimulantes discussions. Je suis également redevable à Monsieur Marcel FETIZON, Directeur du Laboratoire de Synthèse Organique, de l'intérêt pris à mon travail qui m'a permis de collaborer avec Monsieur Jean-Marie BERNASSAU. Ce dernier, avec lequel j'ai travaillé pendant la dernière partie de cette thèse, m'a initié à la pratique de la RMN et m'a permis de collaborer en un travail fructueux tant du point de vue théorique que pratique. Quelques

expériences de "stopped-flow" ont pu être effectuées grâce à l'obligeance de Monsieur Motohiro IWATSUBO (C.G.M., Gif-sur-Yvette).

Last but not least, je voudrais remercier Mademoiselle Jeannine YON d'assurer la présidence de cette thèse de 3ème Cycle et Messieurs Georges COHEN et Antoine DANCHIN d'avoir accepté de juger mon travail.

TABLE DES MATIERES

INTRODUCTION GENERALE p. 1

PREMIERE PARTIE

INTRODUCTION A L'ARTICLE 1. p. 7

ARTICLE 1 : Méthionyl tRNA synthetase from *Escherichia coli* : Active stoichiometry and stopped-flow analysis of methionyl adenylate formation. p. 11

DEUXIEME PARTIE

INTRODUCTION A L'ARTICLE 2. p. 19

ARTICLE 2 : Methionyl tRNA synthetase from *Escherichia coli* : substituting magnesium by manganese in the L-methionine activating reaction. p. 21

TROISIEME PARTIE

INTRODUCTION A L'ARTICLE 3. p. 75

ARTICLE 3 : The L-methionine activation site of methionyl tRNA synthetase from *Escherichia coli* : absence of interaction between the metal ion and the purine ring of ATP. p. 79

ANNEXE

INTRODUCTION A L'ARTICLE 4. p. 95

ARTICLE 4 : Choice of the τ sequence in T_1 measurements by inversion recovery. p. 97

INTRODUCTION GENERALE

Les nucléotides triphosphates (NTP) sont une des principales sources d'énergie de la cellule vivante. Ils participent de plus au métabolisme intermédiaire en tant que donneurs de deux catégories de groupements.

Dans un transfert de phosphoryl (I), le clivage de la liaison β-γ phosphate du nucleotide triphosphate permet de transférer un groupement phosphate sur l'autre substrat de la réaction. Les kinases et certaines synthétases catalysent de telles réactions. Elles peuvent procéder par un mécanisme de type SN_1 avec comme intermédiaire un métaphosphate planaire ou par un mécanisme de type SN_2 avec comme intermédiaire un phosphore pentacoordinné.

(I) Transfert de phosphoryl :

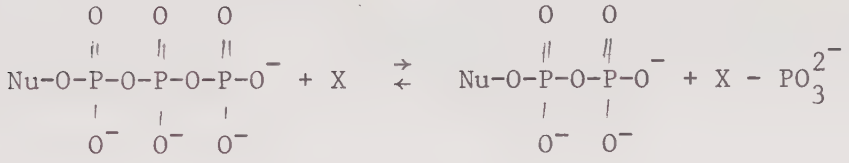

Dans un transfert de nucléotidyl (II), le NTP subit une attaque nucléophile (généralement par un mécanisme SN_2) au niveau du phosphate α de la chaîne triphosphate et la réaction aboutit à l'élimination de pyrophosphate inorganique. Les ADN et ARN polymérases catalysent des transferts de nucléotidyls.

(II) Transfert de nucleotidyl :

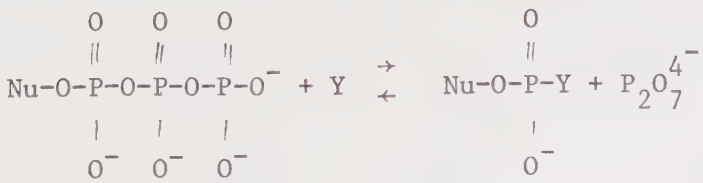

Aussi bien le transfert de phosphoryl que celui de nucléotidyl nécessite la participation d'un ion bivalent, généralement le magnésium. Le transfert de nucléotidyl peut n'être qu'une étape de la réaction dans laquelle un substrat X est activé par sa liaison covalente avec le NMP avant de réagir avec un autre substrat Y (III). Ainsi est réalisé le couplage entre la rupture d'une liaison riche en énergie et la synthèse de X-Y. Comme l'a montré Stadtman [1],

la voie III est plus favorable énergétiquement que la voie IV qui passe par un transfert de phosphoryl.

(III) Transfert de nucléotidyl comme intermédiaire :

$$NTP + X \rightleftarrows NMP - X + PPi$$

$$NMP - X + Y \rightleftarrows X - Y + NMP$$

(IV) Transfert de phosphoryl comme intermédiaire.

$$NTP + X \rightleftarrows NDP + X - P$$

$$X - P + Y \rightleftarrows X - Y + Pi$$

De nombreuses études utilisant des composés modèles ont cherché à élucider la base chimique du transfert de nucléotidyl et surtout de celui de phosphoryl (comme revue voir par exemple [2]). Les rôles possibles de l'ion divalent dans la catalyse ont été soulignés par Cooperman. [3].

Une idée intuitive de Szent Györgyi [4] était que les complexes ATP-ion divalent existaient dans des conformations repliées, le métal chélatant des oxygènes de la chaîne phosphate et des azotes de la base purique. Une telle conformation peut permettre des transferts d'énergie des phosphates à la purine à travers l'ion métallique et favoriser certaines réactions enzymatiques. De tels types de conformation ont été confirmés pour des complexes binaires ATP-métal, tout au moins avec des métaux paramagnétiques pour lesquels les expériences de R.M.N. sont moins ambigues qu'avec le magnésium ou le calcium. Certains auteurs ont postulé, sans confirmation expérimentale, de telles configurations dans des sites actifs d'enzymes.

Cependant les premiers résultats concernant la conformation des nucléotides dans des sites actifs enzymatiques ne semble pas indiquer d'interaction entre le métal et la base [7,8] . Un résultat similaire sera obtenu dans ce travail et nous sommes conduits à penser que le caractère "universel" de l'ATP comme cofacteur de réactions enzymatiques n'est pas lié à la possibilité d'interactions métal-base. Le rôle du nucléoside pourrait plus probablement être expliqué autrement (cf. infra pour le cas des aminoacyl tARN synthétases), en particulier en le considérant comme permettant, par de nombreux points d'attaches possibles sur les protéines, d'augmenter l'affinité du groupement triphosphate important du point de vue de la catalyse.

La synthèse par les aminoacyl-tARN synthétases d'une liaison ester entre le carboxyl d'un acide aminé et le 3' (ou 2') OH de l'adénosine 3' terminale d'un des tARN accepteurs de cet aminoacide a comme intermédiaire l'activation de l'aminoacide grâce à un transfert de nucléotidyl. Pour toutes les enzymes ou un groupement carboxylate est activé par transfert de nucléodidyl,

l'acyl-AMP ainsi formé ne se dissocie pas de l'enzyme. Ce phénomène pourrait n'être qu'une conséquence de l'addition des énergies libres de fixation du groupement acylant et du nucléotide pour contribuer à la stabilité du complexe enzyme : acyl-AMP. La haute spécificité de la synthèse protéique exigeant une haute spécificité dans la formation de l'aminoacyl-tARN, il a été postulé [5] que la stabilisation d'un aminoacyl adénylate sur l'enzyme pouvait permettre un système de vérification de l'aminoacide. Une autre utilisation de l'aminoacyl adénylate pourrait être de stabiliser l'extrémité 3' du tARN près du carboxylate activé grâce, par exemple, à l'empilement entre la base de l'adénosine terminale et celle de l'aminoacyl-AMP. On sait en effet que l'extrémité C-C-A du tARN est extrêmement mobile et, par comparaison entre le tARN-C-C-A et le tARN-C-C, que l'adénosine terminale du tARN n'a que peu d'énergie d'interaction avec l'enzyme et par conséquent probablement pas de points spécifiques de fixation.

Ces deux exemples montrent l'importance de la réaction d'activation, non seulement pour activer le carboxylate de l'acide aminé mais aussi pour contribuer à la spécificité de la charge et de l'interaction protéine-acide nucléique.

On peut souligner que les aminoacyl-tARN synthétases forment une classe qui tant au point de vue des réactions catalysées que de la structure primaire par exemple présente une uniformité certaine. La connaissance des mécanismes communs à la classe des synthétases pourrait donc être étayée par l'étude d'un petit nombre d'enzymes prototypes.

La méthionyl-tARN synthétase d'*Escherichia coli* apparaît comme un bon modèle pour une étude fine du site d'activation des synthétases. En effet le fragment monomérique obtenu par protéolyse ménagée de cette enzyme (fragment trypsique) est actuellement l'objet d'études visant à élucider sa structure

primaire (à Cambridge) et tertiaire (à Gif-sur-Yvette). D'autre part, les travaux antérieurs du laboratoire ont permis de mettre au point des méthodes d'étude de la physico-chimie de ses interactions avec ses substrats.

D'autres travaux en cours s'attachent à la caractérisation des résidus impliqués dans le site d'adénylation. Le but de cette thèse est de chercher à comprendre les rapports entre la présence et la nature d'un ion divalent et la réaction d'activation de la méthionine. D'autre part les couplages entre substrats et/ ou analogues de substrats récemment mis en évidence dans le site d'activation de la méthionine [6] dépendent en partie de la présence d'un ion divalent. La compréhension du rôle de cet ion divalent dans la promotion de ces couplages et la connaissance de leur thermodynamique permettront de décrire des analogues abortifs d'intermédiaires dans la réaction d'activation de la méthionine. Ces analogues seront alors susceptibles de se prêter à une étude par résonance magnétique pour en préciser la géométrie.

REFERENCES

[1] STADTMAN E.R. (1973). In the Enzymes Vol. VIII (P.D. Boyer, Ed.) Academic Press (N.Y.-London) pp. 1-49.

[2] BENKOVIC S.J. and SCHRAY K.J. In the Enzymes Vol. VIII (P.D.Boyer Ed.) Academic press (N.Y.-London) pp. 201-238.

[3] COOPERMAN B.S.(1976). In metal ions in biological systems, Vol.5 (H.Sigel Ed) Marcel Dekker New-York, pp. 79-125.

[4] SZENT GYÖRGY A. (1958). Bioenergetics p. 64.

[5] HOPFIELD J.J. (1974). P.N.A.S. 71, 4135-4139.

[6] BLANQUET S., FAYAT G. and WALLER J.P. (1975). J.Mol.Biol. 94, 1-15.

[7] SLOAN D.L., LOEB A.L., MILDVAN A.S. and FELDMANN R.S. (1975). J. Biol. Chem. 250 , 8913-8920.

[8] SLOAN D.L. and MILDVAN A.S. (1976). J. Biol. Chem. 251, 2412-2420.

PREMIERE PARTIE

INTRODUCTION A L'ARTICLE 1

La méthionyl tRNA synthétase d'*Escherichia coli* est un dimère de poids moléculaire 2 x 86.000 daltons. Une protéolyse ménagée par la trypsine (1) conduit à une enzyme modifiée monomérique de poids moléculaire 64.000 daltons qui ne s'associe plus en dimères. Cette enzyme, facilement cristallisable (2) (par opposition à l'enzyme native) , est actuellement l'objet d'analyses de structures primaires (3) et tertiaires (4) et a été choisie comme prototype pour l'étude du site d'activation de la méthionine. Les premiers résultats obtenus sur la structure primaire de la méthionyl tARN synthétase et d'autres aminoacyl-tARN synthétases de poids moléculaire équivalent montrent une large homologie interne de séquence. Cette homologie paraît être due à la duplication d'un gène ancestral codant pour une aminoacyl-tARN synthétase de taille moitié suivie d'un processus de fusion. Chaque sous-unité de la méthionyl-tARN synthétase a donc potentiellement deux sites d'adénylation et le problème se pose de savoir si les deux sites sont toujours actifs ou si l'un a été inactivé au cours du processus de fusion ou lors de l'évolution post-fusionnelle. Une partie de l'article suivant se consacre à démontrer par différentes techniques à l'équilibre et hors d'équilibre qu'un seul site d'activation de la méthionine est exprimé par l'enzyme modifiée et par chacune des sous-unités de l'enzyme native. De plus les paramètres thermodynamiques pour l'activation de la méthionine de l'enzyme modifiée sont identiques à ceux de chacune des sous-unités de l'enzyme native. L'enzyme modifiée apparaît donc comme ayant conservé quant au site d'activation, toutes les propriétés de l'enzyme native et peut donc être utilisée comme modèle.

Les études à l'état stationnaire (5) sur le mécanisme d'action de la méthionyl tARN synthétase avaient permis de caractériser les complexes binaires entre l'enzyme et ses substrats (substrat est pris ici au sens de substrat ou produit) et de préciser la constante globale de la réaction d'activation de la méthionine. Cependant les complexes ternaires productifs et les états intermédiaires de la réaction étaient englobés dans une espèce unique (appelée X). La levée de la dégénérescence recouvrant les espèces comprises dans X n'est possible qu'à l'aide d'études à l'état préstationnaire. L'article n° 1 montre que les états intermédiaires de la réaction peuvent être décrits par deux espèces en interconversion lente, avec une constante d'équilibre de 1. La connaissance à l'état préstationnaire du mécanisme d'activation de la méthionine permet de montrer que les fixations de méthionine et d'ATP-Mg^{2+} ne sont pas couplées dans le site actif, c'est-à-dire que la présence de l'un de ces substrats sur l'enzyme n'affecte pas la constante de fixation de l'autre. Ce résultat peut être rapproché d'une part, du couplage positif (synergique) entre le méthioninol (aminoalcool correspond à la méthionine) et ATP-Mg^{2+} et d'autre part du couplage allergique entre méthionine et AMP. La conclusion majeure est que le couplage synergique dans le site entre le noyau nucléotidique et l'acide aminé (6) permet de surmonter la répulsion électrostatique entre le carboxylate de la méthionine et le phosphate α de l'ATP et permet donc la présence simultanée des substrats dans le site actif, condition évidemment nécessaire à la réaction.

REFERENCES

[1] CASSIO D. and WALLER J.P. (1971).
Eur. J. Biochem. 20, 283-300.

[2] WALLER J.P., RISLER J.L., MONTEILHET C. and ZELWER C. (1971).
Febs Letters 16, 186-188.

[3] BRUTON C.J., JAKES R. and KOCH G.L.E. (1974).
Febs Letters 45, 26-28.

[4] ZELWER C., RISLER J.L. and MONTEILHET C. (1976).
J. Mol. Biol. 102, 93-101.

[5] BLANQUET S., FAYAT G. and WALLER J.P. (1974).
Eur. J. Biochem. 44, 343-351.

[6] BLANQUET S., FAYAT G. and WALLER J.P. (1975).
J. Mol. Biol., 94, 1-15.

ARTICLE 1

BIOCHEMISTRY (1976) 15, 3678-3685.

Methionyl-tRNA Synthetase from *Escherichia coli:* Active Stoichiometry and Stopped-Flow Analysis of Methionyl Adenylate Formation†

François Hyafil, Yannick Jacques, Guy Fayat, Michel Fromant, Philippe Dessen, and Sylvain Blanquet*

ABSTRACT: Native dimeric methionyl-tRNA synthetase and its monomeric proteolytic fragment are shown to form and to bind 1 mol of methionyl adenylate per polypeptide chain. Moreover, at 25 °C, each monomer of the dimeric native enzyme behaves independently, exhibiting the same parameters for the methionine activation reaction as does the monomeric modified enzyme. These results were obtained using several independent methods including equilibrium and nonequilibrium dialysis, active site and tryptophan fluorescence titrations, and stopped-flow by fluorescence. Stopped-flow resolution of the reversible methionine activation reaction also demonstrates that methionine and ATP-Mg^{2+} react without coupling to form a ternary enzyme·methionine·ATP-Mg^{2+} complex. This complex readily converts to enzyme·methionyl~adenylate·PP-Mg^{2+} with a standard free energy close to zero. It is concluded that the uncoupled enzyme·methionine·ATP-Mg^{2+} complex may resemble the transition state of the reaction at the expense of the additional synergistic binding energy provided by reciprocal coupling, within the site, of the methionine molecule with the adenosine and PP-Mg^{2+} parts of the ATP-Mg^{2+} molecule (Blanquet, S., Fayat, G., and Waller, J. P. (1975), *J. Mol. Biol. 94,* 1).

Recent studies have demonstrated that several aminoacyl-tRNA synthetases exhibit extensive sequence duplication. Enzymes so far shown to possess this property are either monomeric proteins composed of a polypeptide chain having twice the normal subunit size (i.e., approximately 100 000 daltons) (Kula, 1973; Koch et al., 1974; Waterson and Konigsberg, 1974; Bruton, 1975a) or else dimeric enzymes composed of two such large protomers (Bruton et al., 1974). The existence of these large protomers, which may have arisen through duplication and fusion of adjacent genes coding for normal sized subunits (i.e., approximately 45 000 daltons), raises the important issue of their functional significance.

In the case of tyrosyl-tRNA synthetase from prokaryotic origin, composed of two normal, 45 000-daltons subunits in noncovalent association, it has been shown that the subunits exhibit anticooperativity for substrate binding to the tyrosine adenylating sites, while on the other hand both subunits are able to synthesize tyrosyl adenylate at different rates (Fersht, 1975; Jakes and Fersht, 1975). In an attempt to extrapolate this property to the synthetases which possess the sequence duplication feature, these authors have performed experiments which tend to indicate that, in spite of the loss of symmetry resulting from covalent associations, remains of this anticooperativity have been preserved during the fusion process. The rationale of the two sets of binding sites for amino acid and ATP in such twice repeated sequences has been proposed in terms of a general mechanism for enhancement of specificity for the amino acid in the esterification of tRNA (Fersht, 1975).

However, the specificity of interaction with tRNA itself plays a role at least as crucial as that involving amino acid in

† From Ecole Polytechnique, Laboratoire de Biochimie, Laboratoire Associé n° 240 du Centre National de la Recherche Scientifique, 91120 Palaiseau, France. *Received December 31, 1975.* This study was supported in part by the Commissariat à l'Energie Atomique (Saclay, France) and by the Délégation Générale à la Recherche Scientifique et Technique.

determining the accuracy of protein synthesis. Therefore, repeating sequences, acquired by synthetases during evolution, may also provide an advantage for specific binding of tRNA. Indeed it has been suggested that an internal pseudo-symmetry could appear in some parts of the tRNA structure which bind both the "unit domains" of the enzymes (Kim, 1975). Such a "two-point" binding process would be capable of better discriminating between cognate and noncognate tRNAs by amplifying the difference in their free energy of binding.

The present report deals with the demonstration that, in the case of the native methionyl-tRNA synthetase composed of two large protomers, as well as in the case of its monomeric tryptic fragment, no more than one binding site for the adenylation of methionine per single polypeptide chain can be detected, at least in the absence of tRNA.

Investigations on the primary structure of native dimeric methionyl-tRNA synthetase indicate that each monomer of molecular weight 86 000 contains about 200 amino acid residues in repeated sequences (Bruton et al., 1974; Bruton, 1975b). Proteolysis of the native enzyme by trypsin generates two molecules of modified monomer with a molecular weight of 64 000 (Cassio and Waller, 1971b). Sequence analysis reveals that cleavage occurs exclusively at the carboxyl-terminal extremity of the polypeptide chain and that no more than 50 amino acid residues remain duplicated in the modified enzymatically active fragment (Bruton, 1975b). The monomeric tryptic fragment is, therefore, unlikely to have conserved intact a hypothetical second set of binding sites. The demonstration, in the present study, that this modified enzyme exhibits thermodynamic parameters which are identical with those of the native enzyme also argues against the existence of two sets of binding sites per subunit of this enzyme.

Materials and Methods

Homogeneous native methionyl-tRNA synthetase was purified using a published procedure from *E. coli* strain EM 20031 carrying the F 32 episome (Cassio and Waller, 1971a). Homogeneous trypsin-modified methionyl-tRNA synthetase was derived from the purified native enzyme as described earlier (Cassio and Waller, 1971b). The enzymes were stored in 50% glycerol at −15 °C at concentrations of the order of 15 mg/ml. Enzyme concentrations were determined from their absorbancies at 280 nm as indicated elsewhere (Blanquet et al., 1973). It was verified that the enzyme solutions were devoid of contaminating pyrophosphatase activity (Blanquet et al., 1974). Yeast inorganic pyrophosphatase (Boehringer) (EC 3.6.1.1) has a specific activity of 200 units/mg. Adenosine and ATP (Na) are purchased from Boehringer (Mannheim). L-Methionine, PP (Na), and imidazole are from Merck. The latter was recrystallized from methanol. The labeled [α-^{32}P]ATP (93 mCi/mmol) and [^{14}C]methionine (53 mCi/mmol) are from the Commissariat à l'Energie Atomique (France). Purity of the labeled methionine was checked by paper chromatography in 2-propanol-H_2O (7:3, v/v); its sulfoxide content was evaluated by counting the radioactivity of the corresponding spots. Purity of the nucleotide was verified by thin-layer chromatography on cellulose, using the solvent system isobutyric acid-water-ammonia (66:33:1, v/v/v). The [γ-^{32}P]ATP (1789 mCi/mmol) was purchased from the Radiochemical Centre, Amersham.

The experiments mentioned in this article have been performed at 25 °C in standard buffer containing 20 mM imidazole hydrochloride at pH 7.6, 0.1 mM EDTA, and 10 mM 2-mercaptoethanol. The magnesium content was 7 mM, unless specified.

Equilibrium Dialysis. Equilibrium dialysis measurements were performed in slowly rotating cells equipped with IRIS 3069 membranes (Société des Usines Rhône-Poulenc, Paris). The cell chamber which received the ligands was filled to 0.4 ml, while the enzyme chamber was filled with 0.050 ml (Blanquet et al., 1975a). In one set of experiments, 6.25 ng of yeast pyrophosphatase (Boehringer-Mannheim) was added to the enzyme chamber. In this case the labeled methionine concentration was varied from 20 to 200 μM, while in the other cases it was from 2 to 200 μM. Equilibration of ligands was achieved in 2 h. At the end of the experiments, portions from each compartment were counted in a liquid scintillation counter after addition of 12 ml of Bray's solution.

Active Site Titration. [γ-^{32}P]ATP, enzymes, and yeast inorganic pyrophosphatase (1.25 μg) were incubated at 25 °C in standard buffer (1.8 ml) containing 7 mM magnesium chloride. Synthesis of methionyl adenylate was started by adding an aliquot of methionine. Control experiments were performed in parallel without adding the requisite amino acid. From zero time, 100-μl aliquots of this mixture were periodically mixed with 2.5 ml of 0.35% perchloric acid in 50 mM sodium acetate (pH 4.5) containing 0.4% w/v activated charcoal plus 100 mM PP_i and 100 mM P_i. After adsorption of the labeled ATP, the Norit was filtered on Whatman no. 1 filter paper disks, washed, and counted on an IDL crystal scintillation counter.

Nonequilibrium Dialysis. The apparatus consists of a lucite dialysis cell (kindly provided by Dr. Pantaloni) with an open-to-the-air upper chamber containing the enzyme and labeled substrates, separated by an IRIS 3069 membrane (Société des Usines Rhône-Poulenc) from a lower chamber through which buffer is pumped at a constant rate and from which the effluent is sampled for measurements of radioactivity. The upper chamber (1 ml) was filled with 0.5 ml of a solution containing the enzyme and α-^{32}P-labeled ATP in standard buffer with 10 mM magnesium chloride and 0.1 μg of yeast inorganic pyrophosphatase.

The formation and subsequent reversion of methionyl adenylate were initiated by adding 5-μl aliquots of stock solutions (200 mM) of methionine and pyrophosphate, respectively. Pumping of the effluent into the lower chamber (0.4 ml) was ensured by a perfusor (B. Braun Melsungen S. A.) working at a constant rate (30 ml/h). This rate was controlled using a flowmeter (Sho-rate, Brooks) equipped with a sapphire ball. The dialysis cell was connected to the perfusor and to the collector with the shortest lengths of polyethylene catheter no. 1 from Biotrol (inner diameter of 0.30 mm). Stirring of the upper and lower chambers was respectively ensured by a bent rotating Pasteur pipet and a magnet. During the course of the experiment, the volume contained in the upper chamber was controlled by taking 5-μl aliquots each 15 min and comparing their radioactivity content with the measured distribution of the radioactivity between the two chambers at the same time. Finally the dialysis cell was thermostated at 10 °C. Fractions obtained during dialysis (1.5 ml) were directly counted in an SL30 Intertechnique spectrometer, using the Czerenkov effect.

Fluorescence at Equilibrium. The excitation light (295 nm) is provided by a stabilized 450-W Osram xenon source analyzed by a HRS2 monochromator (Jobin & Yvon). The emission of fluorescence is registered at 332 nm using another HRS2 monochromator followed by an EMI 6456 photomul-

[1] Abbreviations used: E, enzyme; AA, L-methionine; PP, pyrophosphate; AA~AMP, methionyl adenylate; P_i, inorganic phosphate.

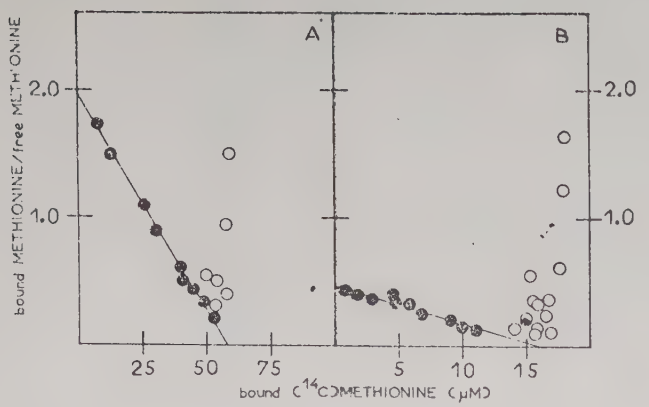

FIGURE 1: Equilibrium dialysis. Native (panel A) and trypsin-modified (panel B) methionyl-tRNA synthetases at concentrations of 27 and 19 μM, respectively, are titrated by [^{14}C]methionine in the presence of 1.85 mM ATP with 2 mM pyrophosphate (-●-) or pyrophosphatase (-○-). All experiments are performed in the presence of 7 mM magnesium chloride.

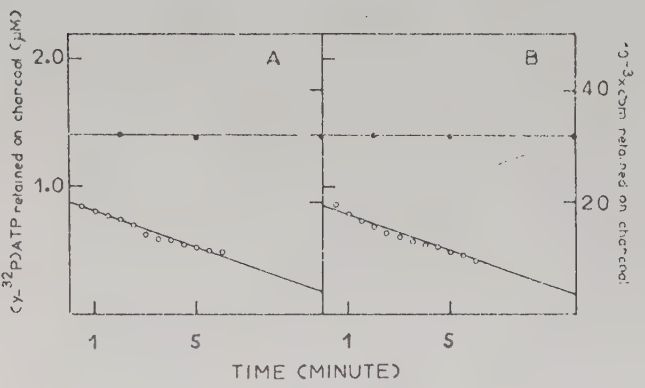

FIGURE 2: Active site titration. Native (0.25 μM) (panel A) and trypsin-modified (0.57 μM) (panel B) methionyl-tRNA synthetases have been incubated with 1.55 μM [γ-^{32}P]ATP in the presence of magnesium and yeast inorganic pyrophosphatase at 25 °C. At time zero, adenylate synthesis was started by adding a final concentration of 1.25 mM methionine. The resulting time-dependent variations of the intact labeled ATP (-○-) are plotted in comparison with the parallel experiment in which the amino acid has been omitted (-●-). Extrapolations to zero time of the steady-state ATP consumption provide initial bursts of ATP hydrolysis when methionine is added. These initial bursts correspond to 2.1 and 0.95 ATP molecules hydrolyzed respectively per molecule of native and trypsin-modified enzyme.

tiplier. Both monochromators are equipped with diffraction gratings blazed at 340 nm. The quartz cell (1 cm × 0.4 cm, Hellma) was filled with 0.8 ml of the enzyme solutions. Saturation curves were obtained by adding successive aliquots of 0.005 ml of the buffer containing the ligand under study. Levels of fluorescence are expressed as percentage of the fluorescence of the free enzyme at the beginning of titration. In the case where stabilities of the enzyme-methionyl adenylate complexes were followed as a function of time, unnecessary exposure of the synthetase complexes to the excitation light was avoided.

Stopped-Flow Fluorescence. Rapid mixing experiments are performed at 25 °C in a Durrum-Gibson stopped-flow spectrometer equipped with fluorescence detection. Excitation at 295 nm of the tryptophan fluorescence is ensured by a 450-W Osram xenon lamp followed by a Jobin-Yvon HRS2 monochromator. The slit width of the excitation monochromator is 2 mm. The observation cell is a quartz tube of 2-mm diameter and 20-mm length. The emission is observed with an aperture at 90° after passing MTO (A 340 b) and Corning CS 0.54 filters, using an Hammamatsu R 376 photomultiplier. The dead time of the spectrometer is 2.5 ms.

Relaxations were obtained by 1:1 mixing of 0.2-ml volumes of reactants. The registered oscillograms were fitted to single exponentials using a multiparameter iterative least-squares procedure on a Wang 2200 B computer.

Results

1. Stoichiometry of the Methionyl Adenylate Molecules Formed and Bound on the Dimeric Native Methionyl-tRNA Synthetase or Its Monomeric Trypsin-Modified Derivative. (a) Equilibrium Dialysis. Methionine reacts with ATP-Mg^{2+} on the enzyme to yield methionyl adenylate with concomitant release of pyrophosphate. This reaction has been carefully studied in the past using different methods (Blanquet et al., 1974). It is characterized by a central complex symbolized elsewhere by X, which contains the E·AA·ATP-Mg^{2+} and E·AA~AMP·PP-Mg^{2+} complexes in equilibrium. The pyrophosphate molecule may dissociate from the X species thus giving the E·AA~AMP complex in equilibrium with free PP-Mg^{2+}. Equilibrium dialysis experiments performed in this study deal with the stoichiometry of ^{14}C-labeled amino acid in the X and E·AA~AMP complexes formed with native and trypsin-modified methionyl-tRNA synthetases. The Scatchard plots presented in panels A and B of Figure 1 represent the formation of the X species by titrating the enzymes with amino acid in the presence of saturating amounts of ATP-Mg^{2+} and PP-Mg^{2+}. The formation of the E·AA~AMP species by titrating the E·ATP-Mg^{2+} complex by amino acid in the presence of yeast inorganic pyrophosphatase is presented on the same figure. The results clearly show that in both cases the stoichiometry of adenylate formation and binding corresponds to the subunits composition of the enzyme species, i.e., respectively two and one methionyl adenylate molecules per mole of native and trypsin-modified enzymes. These experiments are independent of the stability of the adenylate since both experiments are performed in the presence of unlimiting amounts of ATP-Mg^{2+}. Finally it must be noted that the dissociation constants of methionine from the X species, (E·ATP-Mg^{2+})·(AA)/(X), the values of which are respectively 28 and 32 μM with the native and trypsin-modified enzymes, are in excellent agreement with the values published elsewhere using the isotopic ATP-PP exchange or fluorescence titration (Blanquet et al., 1974).

(b) Active Site Titration. Such a technique has been already applied to the native methionyl-tRNA synthetase by others (Fersht et al., 1975). The resulting stoichiometry (two sites per mole of dimeric enzyme) was in excellent agreement with our previous binding stoichiometries (Blanquet et al., 1974). In the present work, we apply this method to both the native and the trypsin-modified methionyl-tRNA synthetases under our standard conditions. The results of Figure 2 demonstrate that the initial bursts of labeled ATP depletion correspond to two and one molecules of ATP consumed respectively in the case of the native enzyme and of its derivative. Moreover, in both cases the initial methionyl adenylate synthesis is followed by similar steady-state ATP hydrolysis corresponding to the lability of the enzyme-adenylate complex. The corresponding turnover rates are in good agreement with the results of the fluorescence section presented later.

(c) Nonequilibrium Dialysis. This technique provides a very rapid and useful method for titration of the active sites of activating enzymes. Such a titration experiment is presented in Figure 3 where at zero time native or trypsin-modified methionyl-tRNA synthetase, α-^{32}P-labeled ATP, and pyrophos-

tase are mixed in the upper chamber of the dialysis appa-
us in standard buffer containing magnesium. At the same
e collection of the effluent from the lower chamber (0.5
/min) was started. The radioactivity contained in the re-
ing fractions was proportional to the amount of the free
eled ATP in the upper chamber since this radioactivity
asures the unidirectional diffusion of the ligand across the
mbrane. In Figure 3 the histogram which represents the
mpled radioactivity follows the free ligand concentration in
upper chamber, while the continuous line reflects the
responding concentration of total labeled ATP concentra-
remaining in the chamber containing the enzyme. This line
s obtained by calculation using the balance of radioactivity
ween the two chambers from zero time. It has been verified
t, at the concentrations used, ATP-Mg^{2+} does not bind
nificantly the enzymes. Adenylate formation is started by
ling a saturating aliquot of methionine to the solution in the
er chamber. Its synthesis results in a rapid depletion of free
eled ATP diffusing across the membrane. The magnitude
his effect allows determination of stoichiometries of 1.9 ±
and 0.9 ± 0.1 adenylate molecules respectively bound per
le of native and trypsin-modified methionyl-tRNA syn-
tases. In the course of the same experiment, reversion of the
nylate was performed by adding an excess of pyrophosphate
he upper chamber. Under these conditions, the bound la-
ed ATP is instantaneously removed as free ATP, thus in-
asing the rate of diffusion of this ligand across the mem-
ne. As shown in Figure 3, the sampled radioactivity reflects
s effect, the magnitude of which corresponds to the above
chiometries.

d) Fluorescence Titration. As was demonstrated elsewhere,
tryptophan fluorescences of native and trypsin-modified
thionyl-tRNA synthetases are markedly sensitive to the
binations of their various substrates (Blanquet et al., 1972,
4). Indeed methionine binding to the enzymes leads to a
% increase of proteic fluorescence. Moreover, ATP-Mg^{2+}
react with the E·AA complex thus promoting a quenching
he enzyme fluorescence, the final magnitude of which is
% of the free enzyme fluorescence. In the case of both en-
mes, this latter effect has already allowed the determination
the equilibrium constant (E·AA)·(ATP-Mg^{2+})/(E·
~AMP)·(PP-Mg^{2+}) as well as the stoichiometry for
nylate formation. This constant, symbolized by $K_{f_1} = K_{eq}/K_{AA}$ with K_{eq} = (E)·(AA)·(ATP-Mg^{2+})/(E·
~AMP)·(PP-Mg^{2+}), was found very similar with the two
ns of the enzyme while the stoichiometries of synthetized
hionyl adenylate molecules were respectively 2.2 and 1.2
mol of native or trypsin-modified enzyme (Blanquet et al.,
4). A comparison of the corresponding titration curves is
sented again in Figure 4. It is now easy to perform such a
ation in the presence of pyrophosphatase which will shift
above equilibrium toward the E·AA~AMP species. The
responding active titrations are also presented in Figure 4,
ere it is shown that two and one molecules of adenylate are
pectively formed and bound by the dimeric native and the
nomeric trypsin-modified enzymes. In panels C and D, the
bilities of such formed adenylate-enzyme complexes are
mined as a function of time. Respective half-life times of
and 14 min are derived from these experiments, the low
mes of which exclude a significant over-estimation of the
ve stoichiometries due to the unavoidable hydrolysis of the
med adenylate in the course of the titration experiments.
ally it was tested that the presence of adenosine (1.8 mM),
ich is known to bind synergistically the E·AA complex
anquet et al., 1975a), has no measurable effect on the en-

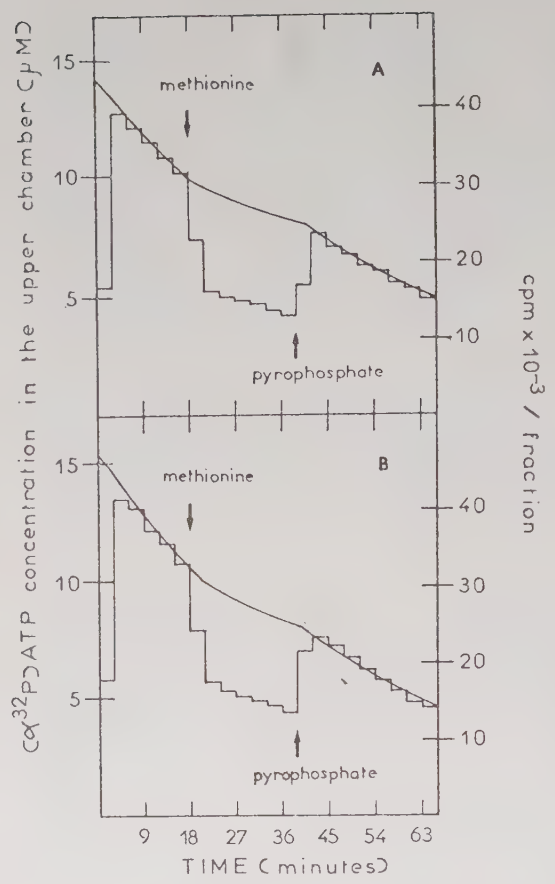

FIGURE 3: Nonequilibrium dialysis. Native (panel A) and trypsin-modified (panel B) methionyl-tRNA synthetases at respective concentrations of 2.5 and 5.2 μM are incubated with 15 μM [α-^{32}P]ATP in the presence of 0.1 μg of yeast pyrophosphatase and 10 mM magnesium chloride. Synthesis of the methionyl adenylate is started by adding methionine at a final concentration of 2 mM. Reversion of the adenylate is ensured by adding 2 mM final pyrophosphate. The histogram follows the sampled radioactivity dialyzing across the membrane (free ATP) which is expressed in cpm/fraction (one fraction is 1.5 ml/3 min). The continuous line indicates the concentration of total ATP remaining in the chamber containing the enzyme and is calculated from zero time using the balance of radioactivity across the membrane. For the sake of clarity, both lines are normalized to coincidence.

zyme-adenylate stabilities. This property reflects the strength of the enzyme-adenylate interaction.

2. Stopped-Flow Analysis of Methionyl Adenylate Synthesis Catalyzed by the Dimeric Native Methionyl-tRNA Synthetase or Its Monomeric Trypsin-Modified Derivative. In the previous section it has been shown that the fluorescence phenomena resulting from the reaction of methionine with ATP-Mg^{2+} on the enzyme are fully relatable to the results obtained by the more direct isotopic methods. Consequently, the tryptophan fluorescence is used with no reservation in this article in order to monitor the reaction scheme corresponding to the enzyme-catalyzed reversible formation of methionyl adenylate from methionine and ATP-Mg^{2+}. This scheme has already been analyzed in part using isotopic ATP-PP exchange as well as fluorescence (Blanquet et al., 1974). However, in the case of these equilibrium methods, the central complex, X, of the reaction was not resolved since it contains isomers in equilibrium. Stopped-flow analysis of the reaction is a useful way to resolve this central complex by measuring its rates of isomerization, provided that reaction of substrates is not rate limiting in the observed rates. Taking into account the fact that when it is formed the adenylate does not dissociate significantly from the enzyme, the analyzed reaction may be formulated as

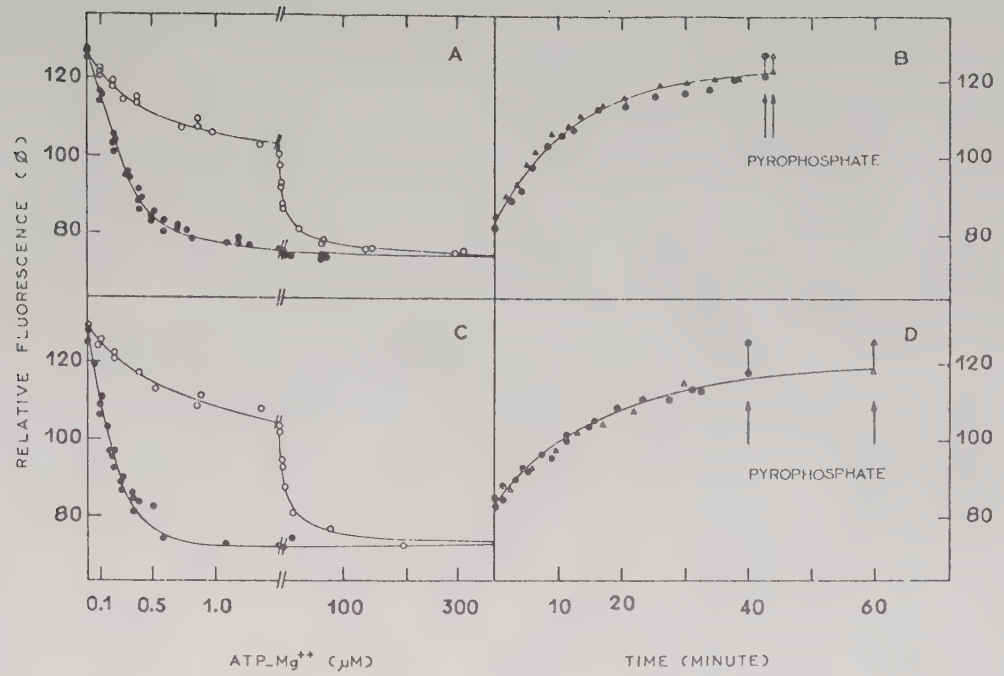

FIGURE 4: Fluorescence at equilibrium. Native (panels A and B) and trypsin-modified (panels C and D) methionyl-tRNA synthetases at concentrations of 0.25 and 0.34 μM, respectively, are titrated by ATP (panels A and C) in the presence of 1.8 mM methionine with (-●-) or without (-○-) 0.1 μg of yeast inorganic pyrophosphatase. In the presence of pyrophosphatase (-●-), the stoichiometries are obtained by calculating the ATP concentrations which correspond to the intersections of the final plateau with the initial slope of the titration curves. In panels B and D, stabilities of the enzyme-methionyl-AMP complexes are followed as a function of time in the absence (-●-) or in the presence of 1.14 mM adenosine (-△-). These complexes are previously formed by reacting native and trypsin-modified methionyl-tRNA synthetases with limiting ATP (respectively 0.5 and 0.4 μM) in the presence of 1.8 mM methionine, and yeast pyrophosphatase. At the end of kinetics, reversion to the enzyme-methionine complex was ensured by adding excess pyrophosphate (1.2 mM). In addition, all the solutions contained 10 mM magnesium chloride.

shown in Scheme I. The symbols used in this scheme are those defined in Table I.

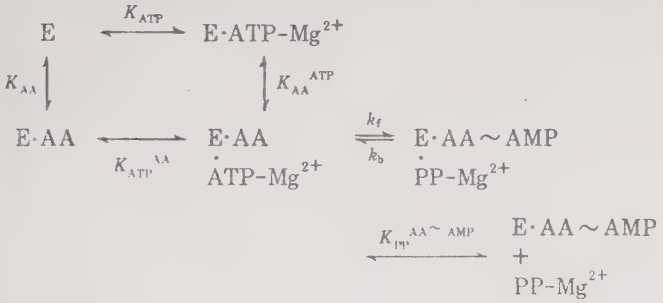

As indicated in the previous section, when ATP-Mg^{2+} reacts with the enzyme-methionine complex, the tryptophan fluorescence of the enzyme is markedly decreased upon the formation of enzymatically bound methionyl adenylate. Thus a rate constant for adenylate formation can be measured in these conditions. According to the above reaction scheme, in the general case where each species of the reaction has a different quantum yield of fluorescence ($F_0, F_1, F_2 \ldots$), the total fluorescence, F, can be expressed as:

$$(\mathrm{E})_0 F = (\mathrm{E}\cdot\mathrm{AA}\sim\mathrm{AMP}\cdot\mathrm{PP}\cdot\mathrm{Mg}^{2+})F_1 + (\mathrm{E}\cdot\mathrm{AA}\sim\mathrm{AMP})F_2 + (\mathrm{E}\cdot\mathrm{AA})F_3 + (\mathrm{E}\cdot\mathrm{AA}\cdot\mathrm{ATP})F_4 + (\mathrm{E})F_0$$

which can be transformed into the following equation:

$$(\mathrm{E})_0 F = (\mathrm{A})\frac{(F_1(\mathrm{PP}) + F_2 K_{\mathrm{PP}}^{\mathrm{AA}\sim\mathrm{AMP}})}{((\mathrm{PP}) + K_{\mathrm{PP}}^{\mathrm{AA}\sim\mathrm{AMP}})} + ((\mathrm{E})_0 - (\mathrm{A}))$$

$$\times \frac{(F_3 K_{\mathrm{ATP}}^{\mathrm{AA}}(\mathrm{AA}) + F_4 K_{\mathrm{AA}}^{\mathrm{ATP}}(\mathrm{ATP}) + F_5(\mathrm{AA})(\mathrm{ATP}) + F_0 K_{\mathrm{AA}} K_{\mathrm{ATP}}^{\mathrm{AA}})}{(K_{\mathrm{ATP}}^{\mathrm{AA}}(\mathrm{AA}) + K_{\mathrm{AA}}^{\mathrm{ATP}}(\mathrm{ATP}) + (\mathrm{AA})(\mathrm{ATP}) + K_{\mathrm{AA}} K_{\mathrm{ATP}}^{\mathrm{AA}})}$$

where the minimal ((E·AA∼AMP·PP-Mg^{2+}) + (E·AA∼AMP))·species which complexes the adenylate is symbolized by (A).

As shown in the latter formula, F is a linear function of the A variable; thus the fluorescence variations satisfy the same rate constant as the A species. This species is ruled by the following differential equation:

$$\mathrm{d}(\mathrm{A})/\mathrm{d}t = k_f((\mathrm{E})_0 - (\mathrm{A}))G^{-1} - k_b(\mathrm{A})H^{-1}$$

with

$$G = 1 + K_{\mathrm{ATP}}^{\mathrm{AA}}/(\mathrm{ATP}) + K_{\mathrm{AA}}^{\mathrm{ATP}}/(\mathrm{AA}) + K_{\mathrm{ATP}}^{\mathrm{AA}} K_{\mathrm{AA}}/(\mathrm{AA})(\mathrm{ATP})$$

and

$$H = 1 + K_{\mathrm{PP}}^{\mathrm{AA}\sim\mathrm{AMP}}/(\mathrm{PP})$$

The rate constant for adenylate formation can be directly derived from this equation, provided that the substrates concentrations remain unaffected in the course of the reaction:

$$k = k_f G^{-1} + k_b H^{-1}$$

This rate constant (k) has been calculated by assuming that all of the association dissociation processes are in rapid pre-equilibrium. This assumption is verified by the fact that the experimental data and the calculated rate constant (k) are subject to the same substrate dependence. In addition, in the case of methionine, we have verified that in our standard conditions 60 μM of this ligand (a concentration equal to the dissociation constant which theoretically ensures an apparent rate twice that of the kinetical dissociation constant) reacts with the enzyme within the dead time (2.5 ms) of the stopped-flow apparatus. In the case of the other substrates of the reaction, the absence of ligand-induced fluorescence changes precludes direct measurement of their reaction rate.

ABLE I: Stopped-Flow Resolution of the Methionyl-Adenylating eaction Catalyzed by Native Methionyl-tRNA Synthetase or by s Trypsin-Modified Form.[a]

	Native	Trypsin Modified
$_F$ (s^{-1})	342 ± 15	259 ± 9
$_B$ (s^{-1})	226 ± 6	223 ± 7
$= k_F/k_B$	1.52 ± 0.11	1.11 ± 0.07
$_{AA}$ (μM)	63*	59*
$_{ATP}$ (mM)	1.2*	1.5*
$_{AA}^{ATP}$ (μM)	77 ± 5	80 ± 9
$_{ATP}^{AA}$ (mM)	1.50 ± 0.15	1.50 ± 0.10
$_{PP}^{AA\sim AMP}$ (μM)	101 ± 7	214 ± 11
$_X = K_{PP}^{AA\sim AMP}/$ $(1 + K^{-1})$(μM)	61 ± 9 70*	113 ± 11 120*
$_{eq}K_X/K_{AA}$ =	0.6 ± 0.1	0.7 ± 0.1
$K_{ATP}^{AA}/(1 + K)$ (mM)	0.36*	0.63*
$_{eq}K_X/K_{ATP}$ =	30.5 ± 3.5	37.9 ± 5.7
$K_{AA}^{ATP}/(1 + K)$ (μM)	20.2*	24.8*
$_{eq}/K_{AA}$ =	9.7 ± 2.2	6.3 ± 1.1
$K_{ATP}^{AA}/KK_{PP}^{AA\sim AMP}$	6*	5.2*
$_{eq}/K_{ATP}$ =	0.50 ± 0.11	
$K_{AA}^{ATP}/KK_{PP}^{AA\sim AMP}$	0.26*	0.34 ± 0.08

[a] The rate constants (k), calculated according to the reaction cheme postulated in the text, have been fitted to the whole set of experimental data with the use of a nonlinear iterative regression procedure. The resulting parameters are presented in this table with their tandard errors. For the sake of comparison, parameters determined lsewhere (Blanquet et al., 1974) are compiled on this table with asterisks. The parameters are defined as follows: k_F is the rate of omerization from E·AA·ATP-Mg^{2+} to E·AA~AMP·PP-Mg^{2+}, hile k_B is the inverse one. K_{AA} = (E)(AA)/(E·AA), K_{ATP} = E)·(ATP-Mg^{2+})/(E·ATP-Mg^{2+}), K_{AA}^{ATP} = (E·ATP-Mg^{2+})(AA)/(E·AA·ATP-Mg^{2+}), and K_{ATP}^{AA} = (E·AA)(ATP-Mg^{2+})/(E·AA·ATP-Mg^{2+}). The central complex of the reaction hich contains the sum of the minimal isomers E·AA·ATP-Mg^{2+} and ·AA~AMP·PP-Mg^{2+}, is defined by the X symbol used in other ublications (Blanquet et al., 1974, 1975a). K_X = (E·AA~AMP) PP-Mg^{2+})/(X), $K_{PP}^{AA\sim AMP}$ = (E·AA~AMP)(PP-Mg^{2+})/(E·A~AMP·PP-Mg^{2+}), $K_{AA}^{ATP}/(1 + K)$ = (E·ATP-Mg^{2+})·AA)/(X), $K_{ATP}^{AA}/(1 + K)$ = (E·AA)(ATP-Mg^{2+})/(X) with K k_F/k_B and K_{eq} = (E)(AA)(ATP-Mg^{2+})/(E·AA~AMP)(PP-Mg^{2+}).

lowever, based on the results of the kinetic analysis of the TP-PP exchange (Blanquet et al., 1974), we can safely assume that the dissociation-association processes involved are lso in rapid preequilibrium. Resolution of the parameters ... was achieved by monitoring (1) formation of methionyl adenylate from the E·AA complex eacting with ATP-Mg^{2+} in the presence of buffering pyrophosphate concentrations (i.e., the pyrophosphate produced n the course of the catalysis remains negligible in front of the dded pyrophosphate); (2) formation of methionyl adenylate rom the E·ATP-Mg^{2+} complex reacting with methionine in he presence of buffering pyrophosphate concentrations; (3) eversal of the synthetized methionyl adenylate by various mounts of pyrophosphate in the presence of buffering amino cid and ATP-Mg^{2+} concentrations. Part of the results are resented in Figure 6, where the experimental k values are lotted as a function of the ATP-Mg^{2+} concentration for ifferent pyrophosphate concentrations. The data relative to he formation or reversion of the adenylate are shown in the ame figure. At this point, it must be noted that the relaxations ssociated either with the formation or the reversal of the denylate fitted very well single exponential curves. Moreover,

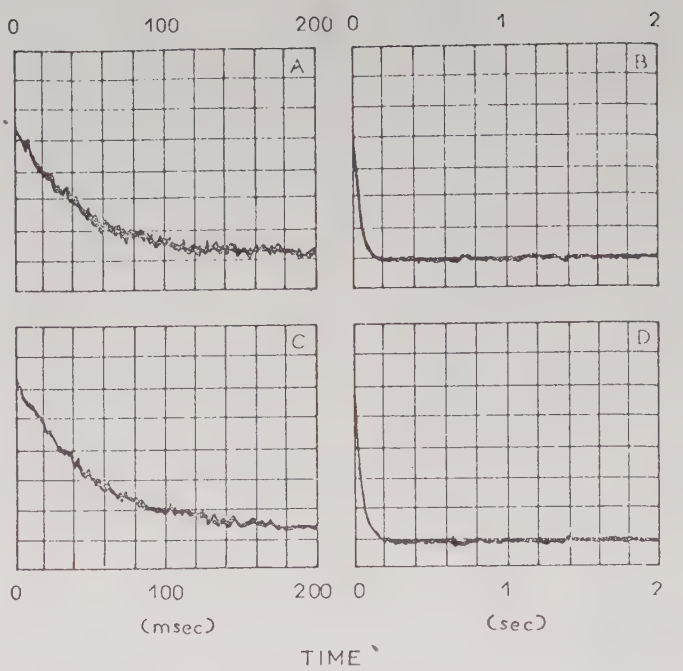

FIGURE 5: Oscillograms for the formation of methionyl-tRNA synthetase-methionyl adenylate complex after rapid 1:1 mixing of a solution containing the enzyme under study plus 2.5 mM methionine and 6.1 μM PP with a solution containing the same concentrations of methionine and PP plus 172 μM ATP. In addition, all solutions contain 7 mM magnesium chloride. Panels A and B present the relaxations obtained on two different base times with native methionyl-tRNA synthetase (concentration after mixing is 0.156 μM). Panels C and D present comparative relaxations obtained with the trypsin-modified enzyme (final concentration is 0.37 μM). Respective rise times of 1 and 5 ms are used with the 20- and 200-ms base times. In all cases the amplitude of signals at equilibrium is equal to 300 mV, after subtracting the blank signal. The voltage unit of the oscillograms is 20 mV/unit.

it is shown in Figure 5 that no secondary effect occurs in the time range of seconds, in the case of either the enzymes examined. This clearly indicates that, under our catalytic conditions (at least in the absence of tRNA), no more than one set of active sites is expressed. In addition, Figures 5 and 6 demonstrate that the native and the trypsin-modified enzymes exhibit very similar rate constants, while as mentioned in the introduction, the proteolytic fragment has a poor chance to preserve intact a hypothetical second binding site.

The whole set of experimental data collected with the two forms of enzyme have been fitted to the calculated rate constant either by a series of independent linear regressions or by a general nonlinear iterative regression. Since both modes of analysis converge on the same values, we adopt the general mode in order to provide related standard errors. The isotherms derived from this fit are presented with the experimental data on Figure 6, while values for the thermodynamical parameters contained in the theoretical expression of the rate constant are summarized with their standard errors in Table I. It must be noted that reactions of the enzyme·AA complex with ATP-Mg^{2+} or of the enzyme·ATP-Mg^{2+} with AA provide identical maximal rates for adenylate formation. This fact argues either for random reaction between these substrates and (or) for the validity of the assumption of rapid preequilibria. The latter would involve equality of $K_{AA}K_{ATP}^{AA}$ and $K_{ATP}K_{AA}^{ATP}$, which is, indeed, verified in Table I.

Conclusion

In the set of experiments presented here, which are restricted to adenylate synthesis in the absence of tRNA, there is no ev-

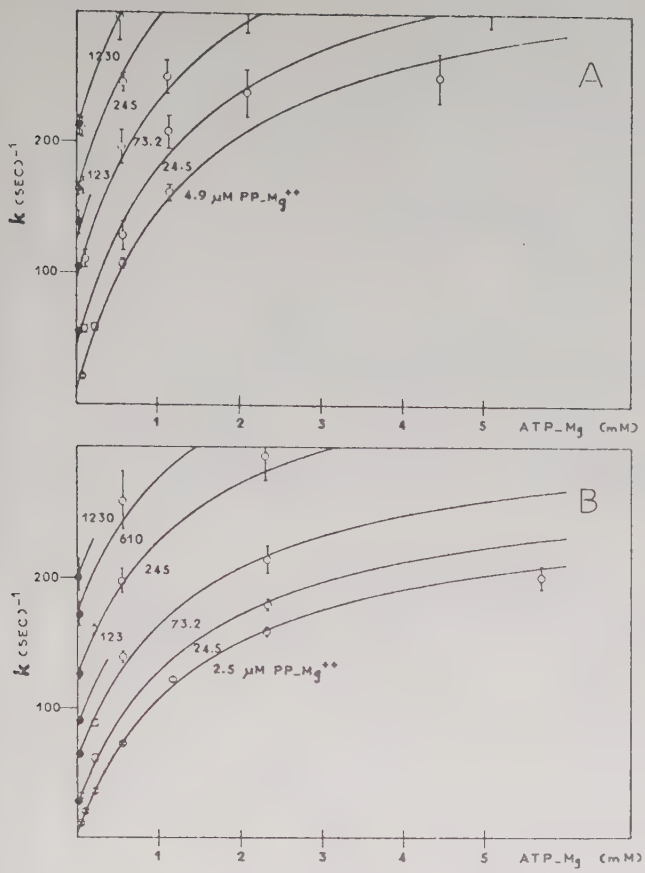

FIGURE 6: Rate constants for the formation or reversion of the methionyl-tRNA synthetase-methionyl adenylate complex. Native (panel A) and trypsin-modified (panel B) methionyl-tRNA synthetases, at the respective concentrations of 0.156 and 0.37 μM after 1:1 mixing, have been reacted in the presence of 2.5 mM methionine and 7 mM magnesium with (1) ATP in the presence of various amounts of PP (-○-); (2) PP in the presence of 22 μM ATP (-●-). The relaxations obtained have been fitted to single exponentials, the rate constants of which are presented on the figure. These data have been analyzed according to the calculated rate constant for the reaction (see Table I). The isotherms derived from this fit are presented as continuous lines with the experimental data.

idence that the existence of repeated sequence within each subunit of methionyl-tRNA synthetase is reflected by binding or reaction at a second site per polypeptide chain. Assuming that repeating sequences within subunits originate from gene duplication followed by fusion of adjacent genes, our results indicate that the process leading to covalent fusion of "monomers" has either abolished or else altered one of the original active site per subunits. In the former case, the advantage of the fusion process may reside in the acquisition of enhanced specificity toward tRNA, as discussed in the introduction. The alternative interpretation is to consider that the polypeptide chains of methionyl-tRNA synthetase derive from two originally noncovalently associated subunits exhibiting anticooperative behavior similar to that of bacterial tyrosyl-tRNA synthetase (Fersht, 1975). As a consequence of covalent linkage between these subunits, the anticooperativity may have grown into a settled "half-of-sites reactivity" due to lack of symmetry in the fused structure. The latter hypothesis would be consistent with the existence of one active site and one unavailable site per polypeptide chain. In this context, it is of interest to recall that in the aminoacylation of tRNA by native as well as trypsin-modified methionyl-tRNA synthetase, methionine displays two K_m values, whereas ATP does not (Lawrence, 1973). Similar effects have been reported in the case of several monomeric synthetases which belong to the class possessing repeated sequences (Yarus and Berg, 1969; Yaniv and Gros, 1969; Rouget and Chapeville, 1971). It is tempting to attribute this behavior to a conditional functioning of the hypothetical closed site in the course of the aminoacylation turnover. Nevertheless, alternative explanations may be suggested, for instance, in terms of competition between the aminoacyl moiety of methionyl-tRNA and free methionine for a common binding site. We intend to resolve this point by studying the methionine dependence, if any, of the transfer rate of the aminoacyl moiety from the adenylate to the tRNA, and of the kinetics of methionyl-tRNA binding.

The first part of the present study deals with the binding and consumption of ligands in the course of the adenylation reaction. Since it is found that neither the native nor the trypsin-modified enzymes express more than one active site per polypeptide chain, it was of interest to refine our analysis with the use of prestationary stopped-flow kinetics. Resolution of the kinetics of the adenylation reaction demonstrates that each of the enzymes catalyzes adenylate synthesis according to a simple scheme which involves a unique set of active sites. In agreement with this scheme, formation and reversal of methionyl adenylate follow single exponential relaxations in the case of both enzymes. This result argues for identical behavior of each of the subunits of native enzyme. Moreover, the values of Table I demonstrate that each of the subunits of the dimer displays the same thermodynamical parameters as does the modified monomer. Thus, it may be safely concluded that the native enzyme has two independent active sites for adenylate synthesis, the catalytic properties of which are unaffected by subunit assembly. Furthermore, as stated in the introduction, the modified fragment has lost a major portion of the duplicated sequence present in each native monomer and is, therefore, unlikely to have conserved a hypothetical second set of binding sites involved in the catalytic process. The identity of the catalytic parameters of the two forms of the enzyme thus provides an additional argument against the occurrence of a second set of binding sites in each monomer of the native enzyme.

Finally, the values of Table I which resolve the kinetics of the adenylation reaction have to be related with other studies dealing with synergism in the binding process of methionine plus adenosine and PP-Mg^{2+} (Blanquet et al., 1975a,b). Indeed, the determination of the K_{AA}^{ATP} and K_{ATP}^{AA} constants, compared with the K_{AA} and K_{ATP} values (Blanquet et al., 1974), demonstrates that the synergistic coupling which appeared between methionine and adenosine plus PP-Mg^{2+} is cancelled out by the introduction of the crucial α-phosphate. Therefore the expense of an additional binding energy of 3 kcal provided by the adenosine and PP-Mg^{2+} parts of the ATP-Mg^{2+} molecule enables this substrate to resemble the transition state despite the electrostatic repulsion between the phosphoryl and carboxyl groups within the reaction center. Mahler and Cordes (1969) have calculated that free acetyl-AMP has a free energy content which is approximately 6 kcal higher than that of ATP in solution. In the case of methionyl-tRNA synthetase, the difference in free energy between adenylate and ATP is strikingly decreased by synergism in the enzymic environment. Indeed, the standard free energy of the reaction is decreased to close to zero (60 -240 cal) when calculated from the k_f/k_b ratio. Similar results have been obtained in the case of isoleucyl-tRNA synthetase from *E. coli* (Holler and Calvin, 1972; Holler et al., 1973). Thus it could be that synergistic leveling of the standard free energy is an essential feature of the mechanism leading to adenylate formation. On the side of the E·AA~AMP·PP-Mg^{2+} species, it is striking to note that

P-Mg^{2+} dissociates from this complex with the same equilibrium constant as in the case of the quaternary dead-end omplex E·AA·adenosine·PP-Mg^{2+} (Blanquet et al., 1975a). his finding clearly indicates that this quaternary complex mulates the transition state of the reaction, and that the A~AMP molecule exerts the same synergistic coupling as ie AA plus adenosine combination on PP-Mg^{2+} binding to ie enzyme. However, the quantum yields of fluorescence for iese E·AA~AMP·PP-Mg^{2+} and E·AA·adenosine·PP-Mg^{2+} pecies are markedly different (respectively 77 and 138% of ie free enzyme fluorescence). The only occurrence of a supplementary covalent link does not account for this effect since ethioninyl adenylate, the alkyl analogue of methionyl adeylate, increases the fluorescence (Blanquet et al., 1972) as ocs methionine in combination with adenosine, or methioninol n combination with AMP (unpublished results).

The major difference between the ester and anhydride bonds xhibited by methioninyl and methionyl adenylate, respecvely, resides in the atomic distances between the carbonyl arbon and the adjacent atoms. Indeed the single bonds C–C nd C–O from a carbon atom are shortened if this carbon atom s double bonded to another atom. Therefore the anhydride ond will be shorter than the ester bond. This fact could be the asis for an enzyme distortion induced by methionyl adenylate vhich would affect the tryptophan radiative process in a way ifferent from that of the relaxed synergistic couples or the onger methioninyl adenylate molecule.

Acknowledgments

This work was carried out in the laboratory of Dr. J. P. Waller, whose continuous support and stimulating criticism re gratefully acknowledged. We are also indebted to Dr. M. watsubo for access to the stopped-flow apparatus.

References

Blanquet, S., Fayat, G., Poiret, M., and Waller, J. P. (1975b), *Eur. J. Biochem. 55,* 567.

Blanquet, S., Fayat, G., and Waller, J. P. (1974), *Eur. J. Biochem. 44,* 343.

Blanquet, S., Fayat, G., and Waller, J. P. (1975a), *J. Mol. Biol. 94,* 1.

Blanquet, S., Fayat, G., Waller, J. P., and Iwatsubo, M. (1972), *Eur. J. Biochem. 24,* 461.

Blanquet, S., Iwatsubo, M., and Waller, J. P. (1973), *Eur. J. Biochem. 36,* 213.

Bruton, C. J. (1975a), *Biochem. J. 147,* 191.

Bruton, C. J. (1975b), Abstract Form, EMBO Workshop on tRNA Structure and Function, Israël, Nof Ginosar.

Bruton, C. J., Jakes, R., and Koch, G. L. E. (1974), *FEBS Lett. 45,* 26.

Cassio, D., and Waller, J. P. (1971a), *FEBS Lett. 12,* 309.

Cassio, D., and Waller, J. P. (1971b), *Eur. J. Biochem. 20,* 283.

Fersht, A. R. (1975), *Biochemistry 14,* 5.

Fersht, A. R., Ashford, J. S., Bruton, C. J., Jakes, R., Koch, G. L. E., and Hartley, B. S. (1975), *Biochemistry 14,* 1.

Holler, E., and Calvin, M. (1972), *Biochemistry 11,* 3741.

Holler, E., Rainey, P., Orme, A., Bennett, E. L., and Calvin, M. (1973), *Biochemistry 12,* 1150.

Jakes, R., and Fersht, A. R. (1975), *Biochemistry 14,* 3344.

Kim, S. H. (1975), *Nature (London) 256,* 679.

Koch, G. L. E., Boulanger, Y., and Hartley, B. S. (1974), *Nature (London) 249,* 316.

Kula, M. R. (1973), *FEBS Lett. 35,* 299.

Lawrence, F. (1973), *Eur. J. Biochem. 40,* 493.

Mahler, H. R., and Cordes, E. H. (1969), in Biological Chemistry New York, N.Y., Harper & Row, p 201.

Rouget, P., and Chapeville, F. (1971), *Eur. J. Biochem. 23,* 443.

Waterson, R. M., and Konigsberg, W. H. (1974), *Proc. Natl. Acad. Sci. U.S.A. 71,* 376.

Yaniv, M., and Gros, F. (1969), *J. Mol. Biol. 44,* 1.

Yarus, M., and Berg, P. (1969), *J. Mol. Biol. 42,* 171.

DEUXIEME PARTIE

INTRODUCTION A L'ARTICLE 2

L'article précédent a permis de montrer l'importance des couplages synergiques pour la réaction d'activation de la méthionine. Certains couplages comme par exemple celui entre la méthionine et l'adénosine ne mettent pas en jeu d'ion métallique. Cependant, les couplages les plus importants en intensité nécessitent la présence d'un ion divalent (1,2). On peut dès maintenant noter que l'ion métallique joue non seulement un rôle dans la promotion de couplages synergiques majeurs mais aussi dans la catalyse elle-même. Ainsi la vitesse maximale de formation de l'aminoacyl adénylate est en l'absence de métal au moins trois ordres de grandeur plus lente qu'en présence de magnésium. Le rôle du métal dans la catalyse proprement dite, c'est-à-dire en fait la géométrie de l'état de transition, est difficilement accessible par l'expérience mais peut être mieux comprise par la connaissance des états intermédiaires ou des analogues de l'état de transition.

Jusqu'à présent, seul le magnésium a été étudié comme activateur de la méthionyl tARN synthétase. Toutefois l'ion Mg^{2+} ne fournit aucune observable ni par lui-même, ni par son action sur les atomes voisins. L'article suivant substitue l'ion paramagnétique Mn^{2+} à l'ion Mg^{2+} dans le site d'activation de la méthionine. La comparaison de ces deux ions tant du point de vue de la réaction d'activation que de celui de la promotion des effets synergiques permet de mieux comprendre le mécanisme enzymatique. D'autre part cette étude permet de caractériser des complexes abortifs de l'enzyme et de substrats ou de parties de substrats ayant des propriétés voisines de complexes productifs. L'étude de ces analogues abortifs de complexes intermédiaires de la réaction sera alors possible par résonance magnétique.

REFERENCES

[1] BLANQUET S., FAYAT G. and WALLER J.P. (1974). J. Mol. Biol. 94, 1-15.

[2] FAYAT G., FROMANT M. and BLANQUET S. (1976). soumis pour publication.

ARTICLE 2

METHIONYL-tRNA SYNTHETASE FROM *ESCHERICHIA COLI* : SUBSTITUTING MAGNESIUM BY MANGANESE IN THE L-METHIONINE ACTIVATING REACTION.

François HYAFIL and Sylvain BLANQUET

Ecole Polytechnique - Laboratoire de Biochimie

Laboratoire Associé n° 240 du Centre National de la Recherche Scientifique

91120 - PALAISEAU (France)

Postal address : François HYAFIL - The Biological Laboratories, Harvard University, 16 Divinity Avenue, Cambridge - Mass. 02138 - U.S.A.
Sylvain BLANQUET - Laboratoire de Biochimie - Ecole Polytechnique - 91128- Palaiseau Cedex.

Acknowledgements : This work has been carried out in the Laboratory of Doctor J.P. WALLER whose continuous support and stimulating criticism are gratefully acknowledged.
This study was supported in parts by grants from the Délégation Générale à la Recherche Scientifique et Technique and by the Commissariat à l'Energie Atomique.

Code number for the enzyme : Methionyl-tRNA synthetase (L-methionine : tRNA ligase (AMP) : E C 6.1.1.10).

Abbreviations : AA stands for aminoacid and more peculiarly for L-methionine
AAol for L-methioninol
PP for pyrophosphate
Ado for Adenosine
E for enzyme
AA∿AMP for methionyl-adenylate
EPR is electron paramagnetic resonance
When required, the equilibrium constants are symbolized with the help of lower and upper indices i.e. K_A^B represents the equilibrium constants of the ligand A with the enzyme saturated by the ligand B.
EDTA ethylene diaminotetracetic acid

SUMMARY

While Mg^{2+} can be efficiently replaced by Ni^{2+}, Co^{2+} and Mn^{2+} in the ATP-PP isotopic exchange reaction catalysed by methionyl-tRNA synthetase from *Escherichia coli*, the latter ion was selected for a detailed analysis of the L-methionine activation reaction. In order to avoid artefactual results due to the slow aggregation of Mn^{2+} with pyrophosphate, this process was investigated by EPR and conditions were determined where it does not interfere with enzymatic experiments. The thermodynamical parameters derived from steady-state (ATP-PP isotopic exchange, fluorescence at equilibrium) or prestationnary (fluorescence stopped-flow) experiments are compared to those obtained in the presence of Mg^{2+} (Hyafil et al., 1976, Biochemistry 15, 3678-3685).

While the standard ΔG for the reaction (E.Met.ATP-Me^{2+} $\rightleftarrows$ E.Met∿AMP.PP-Me^{2+}) is close to zero in the case of Mg^{2+}, Mn^{2+} slows down the rate of adenylate reversion and thus shifts the reaction towards the latter species. The ΔG for the formation of the E.Met∿AMP complex does not depend on the metal used, suggesting that the divalent ion does not participate to the structuration of this complex. Substituting Mn^{2+} for Mg^{2+} decreases notably the dissociation constant of PP-Me^{2+} from the E.Met∿AMP.PP-Me^{2+} species and from the abortive transition state analog E.Met.Adenosine.PP-Me^{2+}. Similarly the dissociation constant of ATP-Me^{2+} from another transition state analog E.Methioninol.ATP-Me^{2+} is decreased by Mn^{2+}. Involvment of the purine N7 atom in the binding of the metal ion to the active site of methionyl-tRNA synthetase is ruled out with the use of 7-deaza-adenosine.

The role of the metal in the catalytic process of methionine activation and its relevance to the specificity of the reaction is then discussed in the light of the results obtained without metal and with Mg^{2+} and Mn^{2+}.

INTRODUCTION

Reaction (1) catalysed by aminoacyl tRNA synthetases requires the presence of an added metal ion, usually magnesium, when measured as the rate of the ATP-PP isotopic exchange reaction (for review see [1,2]).

$$E + AA + ATP \xleftrightarrow{Me^{2+}} E.AA\sim AMP + PP \qquad (1)$$

Mechanistic studies using the ATP-PP isotopic exchange have shown that, in this reaction, Mg^{2+} is only involved as ATP-Mg^{2+} and PP-Mg^{2+} chelates |3|. Studies on the role of the metal ion in the course of the reversible aminoacid activation reaction have been so far confined to a comparison of the exchange rates measured in the presence of different metallic cations (for review see, |4,5|).

Recently, the adenylating sites of several aminoacyl-tRNA synthetases have been shown to develop synergistic couplings between analogs or parts of the aminoacid and ATP-Mg^{2+} molecules lacking either the carboxylate or/and the α-phosphate negative charges [6,7]. These couplings are believed to provide an uptake of free energy which would enable the ATP-Mg^{2+} and aminoacid molecules to be accomodated within the site and resemble the transition state of the reaction despite their antagonistic negative charges at the carboxylate and α-phosphate positions.

In the case of methionyl-tRNA synthetase from *Escherichia coli*, synergistic and antagonistic couplings have been shown to cancel each other and to result in uncoupled bindings of L-methionine and ATP-Mg^{2+} to form the ternary enzyme:methionine:ATP complex |8|. Detailed studies have brought out the important role

of the magnesium ion in the fullfillment of such couplings [6,9]. At the present time, the role of metal may be understood as a modulator of the phosphate negative charges within the site and as a stabilizer of the reactive or inhibitory transient complexes of the enzyme. Further knowledge of the mechanism of couplings from the viewpoint of the metal ion is likely to give new insights into the catalytic processes involved in adenylate synthesis.

In the present work, we demonstrate that manganese, cobalt and nickel as divalent ions are able to promote the reversible activation of L-methionine by methionyl-tRNA synthetase from *Escherichia Coli*. The mechanisms of reaction (1) and of the formation of dead-end synergistic complexes are studied in detail with the manganese ion. The resulting parameters are compared to the values obtained with magnesium [6,8,9,10] and are discussed.

Methionyl-tRNA synthetase may be studied as a native dimer or a pseudo monomer obtained by limited tryptic proteolysis of the native enzyme [11]. Both the native and the trypsin-modified enzymes possess one adenylating site per polypeptide chain Each of the two sites of the native enzyme have been shown to be equivalent to the unique site of the proteolytic fragment in the process of adenylate formation [8,10]. The present work is devoted to the trypsin-modified enzyme since this enzymatic species is presently the object of studies aimed at elucidating its primary and tertiary structure [12,13,14]. However, some of the experiments relative to the mechanism of adenylate formation are performed on both the native and the modified enzymes.

MATERIALS AND METHODS

Homogeneous native methionyl-tRNA synthetase was purified using a published procedure from *Escherichia Coli* strain EM 20031 carrying the F32 episome [15]. Homogeneous trypsin modified methionyl-tRNA synthetase was derived from the native enzyme as described earlier [11]. The enzymes were stored at -15°C in phosphate buffer pH 7.6 containing 50 % glycerol. Enzyme concentrations were determined from absorbancies at 280 nm [15]. ATP (Na) salt was purchased from Boehringer, Tubercidin from Sigma, 8 aminoadenosine from Calbiochem and L-methioninol from Fluka. Adenosine, L-methionine, pyrophosphate (Na), $MnCl_2\ (H_2O)_6$, $MgCl_2\ (H_2O)_6$, and imidazole are from Merck. The latter was recrystallyzed in methanol. Nucleosides and nucleotides concentrations were determined using their absorbancies [16].

(^{32}P) pyrophosphate was delivered by the Commissariat à l'Energie Atomique or the Radiochemical Center (Amersham). Purity of the labeled pyrophosphate was checked by Dowex chromatography as described elsewhere [10]. The amount of exchangeable labeled pyrophosphate was determined by measuring the isotopic plateau of the ATP-PP exchange in the presence of a hundred-fold excess of ATP over PP.

The amounts of radioactivity recovered as pure pyrophosphate on Dowex or converted into labelled ATP in the latter experiment were quite reliable and indicated around 90 % purity for the batches used.

All of the experiments were performed at 25°C in standard buffer containing 20 mM Imidazole-HCl at pH 7.6 and 10 mM 2-mercaptoethanol. The EDTA content, if any, is specified for each experiment.

Fluorescence at equilibrium.

Fluorescence measurements at equilibrium were performed in standard buffer at 25°C [8]. . The proteic fluorescence was excited at 295 nm and recorded at 332 nm. The quartz cell (1 cm x 0.4 cm, Hellma) was filled with 0.8 ml of a trypsin-modified enzyme solution (0.5 µM). Saturation curves were obtained by adding successive aliquots of 0.005 ml of the buffer containing the ligand under study. All titration curves were corrected for dilution and for inner-filter effects. Levels of fluorescence are expressed as percentages of the free enzyme fluorescence.

Stopped-flow.

Rapid mixing experiments were performed as described earlier [8].The proteic fluorescence was excited at 295 nm and registered at 90° through MTO (A340b) and Corning C.S.0.54 filters. Relaxations were obtained by 1:1 mixing of 0.2 ml volumes of reactants. The enzyme concentrations after mixing were 0.16 µM and 0.37 µM respectively in the cases of the native and the trypsin modified enzymes. Experimental curves were fitted to single exponentials using a three-parameters iterative regression program.

ATP-PP isotopic exchange.

The stock solutions of native and trypsin-modified enzymes were diluted in standard buffer containing 0.2 mg/ml bovine serum albumin . The reaction was started by addition of 0.025 ml of these enzyme solutions to 0.075 ml of a solution containing the other reactants in standard buffer [10].Final concentrations of enzyme were of the order of 1 nM for the determination of the rate of exchange

and of the order of 100nM for the determination of the isotopic plateau. After incubation at 25°C, the reaction is stopped with 2.5 ml of 0.35 % perchloric acid in 50 mM sodium acetate (pH 4.5) containing 0.4 % w/v activated charcoal plus 100 mM PP. After adsorbtion of the labeled ATP, the norite was filtered on Whatman n° 1 filter disks, washed and counted on an IDL Crystal scintillation counter.

Electron Paramagnetic Resonance.

Measurements were performed on a Thomson TSN 254 spectrometer operating at 9,500 MHz in a 0.2 ml quartz cell with a capillary containing diphenyl picrylhydrazyl as external standard. The modulation field had a 6 kHz frequency and a 20 Gauss amplitude. The power incident on the cavity was about 300 mW. The free manganese concentration was followed as the amplitude of one of the peaks of the Mn^{2+} hyperfine structure. Data were corrected for base line deviation. Temperature of the sample was 25°C.

All the calculations were performed on a Wang 2 200 B computer.

TABLE 1

ACTIVATION BY METAL IONS OF THE ATP-PP ISOTOPIC EXCHANGE CATALYSED BY METHIONYL-tRNA SYNTHETASE FROM E.COLI.

METAL	CONCENTRATION mM	ACTIVATION %
Mg^{2+}	5	100
Mn^{2+}	5	25
Co^{2+}	5	95
Ni^{2+}	5	35
Ca^{2+}	5	0
Cu^{2+}	5	0
Zn^{2+}	1	0
Ba^{2+}	5	0
Eu^{3+}	2	0
Sm^{3+}	2	0

The experiments were monitored in standard buffer containing 0.1 mM EDTA, 2 mM ATP, 2 mM AA and 2 mM PP. Incubations were performed at 25° C in the presence of native methionyl-tRNA synthetase.The activation is expressed as a percentage of the initial velocity of exchange measured in the presence of magnesium.

RESULTS

1 - SUBSTITUTING MAGNESIUM (II) BY MANGANESE (II)

Effect of metals on the isotopic ATP-PP exchange reaction catalysed by methionyl-tRNA synthetase.

The ability of various metals to catalyse the L-methionine activation reaction when monitored by the ATP-PP exchange assay, is presented in Table 1. The Mn^{2+} ion is able to substitute for Mg^{2+} in the reaction. In addition, Ni^{2+} and Co^{2+} are shown to act with fairly good efficiencies. The other tested ions, do not behave as activators of methionyl-tRNA synthetase. Moreover, the Ca^{++}, Cu^{++} and Ba^{++} ions inhibit the ATP-PP exchange insured by the presence of 5 mM Mg^{2+}.

Our ultimate goal being magnetic resonance studies on the role of metal in the adenylating site of methionyl-tRNA synthetase, the manganese ion was selected for further experiments since its paramagnetic properties are particularly convenient to observe (for review, see [17]). Another advantage provided by the manganous ion resides in the fact that it promotes structuration and aminoacylation of $tRNAs^{Met}$ as efficiently as magnesium (Blanquet and Waller, unpublished).

Interaction of Mn^{2+} with the relevant ligands.

The intensity of the EPR spectrum of free Mn^{2+} ion is decreased by several orders of magnitude when this ion binds a ligand [18]. This behaviour can be used to monitor the amount of free Mn^{2+} in solution. Equilibrium constants between Mn^{2+} and various substrates or compounds which are relevant to our experiments were determined in this way and are shown in Table 2. Since all measurements were performed in standard buffer, the significant complexation of Mn^{2+} by imidazole

TABLE 2

EQUILIBRIUM CONSTANTS OF MANGANESE (II)

WITH THE COMPOUNDS INVOLVED IN THE PRESENT STUDY.

Imidazole.HCl pH 7.6	L-Methionine	L-Methioninol	2-Mercapto-ethanol	ATP	PP	Ado
65 mM	135 mM	195 mM	∿ 8 M	0.8±0.1μM (1 site)	1.5±0.4μM (1^{st} site) 44 ±24 μM (2^{nd} site)	∿150 mM

The dissociation constants were measured by EPR in the Imidazole-HCl 20 mM (pH 7.6) buffer. Results are corrected for the chelation of Mn^{2+} by this buffer. Temperature of the sample was 25°C.

With the exception of the values relative to ATP and PP which are calculated from Scatchard plots (Figure 1), the values for the other compounds are determined with the assumption of a 1:1 stoichiometry.

In the case of adenosine, the value reported should be considered as tentative, due to the low solubility of this nucleoside (20 mM in our standard conditions).

$10^{-6} \times [Mn^{2+}\,bound] / [Mn^{2+}\,free] \times [PP\,total]$
B
A
0.6
0.4
0.2
2.0
1.5
1.0
0.5
$[Mn^{2+}\,bound] / [PP\,total]$
1.0
0.5
$[Mn^{2+}\,bound] / [ATP\,total]$
0.8
0.6
0.2
$10^{-6} \times [Mn^{2+}\,bound] / [Mn^{2+}\,free] \times [ATP\,total]$

FIGURE 1 : INTERACTION OF Mn^{2+} WITH ATP AND PP AS STUDIED BY EPR.

The experiments are performed at 25° C in standard buffer.

Panel A : Scatchard plot of the binding of Mn^{2+} to ATP.

The total $MnCl_2$ concentration was 4 µM or 10 µM and the ATP concentration varied from 0 to 25 µM. Linear regression of the experimental data (continuous line) indicates 0.93 ± 0.04 Mn^{2+} ion bound per ATP molecule with a dissociation constant of 0.82 ± 0.10 µM.

Panel B : Scatchard plot of the binding of Mn^{2+} to PP.

The experimental data were measured by varying the PP concentration from 0.01 to 0.2 mM and the $MnCl_2$ concentration from 0 to 0.3 mM. In the conditions where no aggregation process occured (i.e. PP below 0.1 mM), the experimental data (—⬡—) were fitted to a "two-class-of-sites" anticooperative model. The continuous line represented in the figure corresponds to the binding of 0.87 ± 0.12 Mn^{2+} ion per pyrophosphate molecule with a dissociation constant of 1.5 ± 0.4 µM (strong class) and of 1.05 ± 0.12 Mn^{2+} ion per pyrophosphate molecule with a dissociation constant of 44 ± 24 µM (weak class).

The aggregation of Mn^{2+} and PP was followed as a function of time by incubating 0.1 mM PP with 0.15 (—△—), 0.18 (—◇—) and 0.25 mM (—⧖—) Mn^{2+} and 0.2 mM PP with 0.2 mM Mn^{2+} (—□—). The arrows describe the state of aggregation in these experiments after 15 min (➔) 30 min (⟶) and 60 min (⟹) incubation.

was taken into account. Scatchard plots of the interaction of Mn^{2+} with ATP and PP are presented in Figure 1. It must be noted that the EPR spectrum of the bound species ATP-Mn^{2+} and PP-Mn^{2+} were sufficiently weak not to interfere with the free Mn^{2+} determination. In the range of concentrations used, ATP displays a unique binding site for Mn^{2+} with a dissociation constant of 0.8 ± 0.1 µM while pyrophosphate can bind two manganese ions with dissociation constants of 1.5 ± 0.4 and 44 ± 24 µM respectively.

Consequences of the aggregation of PP with Mn^{2+}.

Coopermann and Mark [19] have reported that manganese and pyrophosphate have a tendancy to slowly aggregate in dilute solutions. In order to avoid artifactual results due to this property, EPR was used to reinvestigate the aggregation process in our standard conditions. In the presence of excess manganese, no significant aggregation occurs with PP concentration below 0.1 mM even in the time-range of the hour. With solutions containing more than 0.1 mM PP, addition of excess manganese results in a slow time-dependent consumption of free metal which tends to saturate two sites of the pyrophosphate (Fig. 1B). In the upper range of pyrophosphate concentration (above 1mM), aggregation is accomplished within the dead time (a few minutes) of the EPR measurement. Two sites for Mn^{2+} per pyrophosphate molecule are then titrated. Overstepping of this 2:1 stoechiometry results in the precipitation of $(PP\text{-}Mn^{2+}_2)_n$ aggregates.

During the time dependent ATP-PP isotopic exchange, the radioactive ATP is ruled by the following relation [20]

$$ATP^{*} = ATP^{*}_{\infty} \left(1 - \exp\left(- w.t. \frac{(PP)+(ATP)}{(PP).(ATP)}\right)\right) \qquad (2)$$

$$\text{with} \qquad ATP^{*}_{\infty} = \frac{PP^{*}_{o}}{1 + \frac{(PP)}{(ATP)}} \qquad (3)$$

In these relations (ATP) and (PP) are the total concentrations of ATP and PP ; ATP^{*} is the radioactivity incorporated as ATP at time t, ATP^{*}_{∞} the radioactivity incorporated as ATP at isotopic equilibrium ; PP^{*}_{o} is the total amount of radioactivity initially added in the form of labeled pyrophosphate. The turnover rate of exchange, v, is independent of t, the time of incubation. Figure 2 illustrates the consequences of aggregation. In the case of Mn^{2+}, the kinetics for radioactive ATP formation are biphasic. In addition to a fast exponential phase, a slower one corresponds to the rate limiting release (half life time of 150 minutes) of the radioactive PP which has been trapped within the aggregates.Extrapolation of this second phase at zero time yields ATP^{*}_{∞} and through equation (3), the amount of unaggregated PP actually involved in the isotopic reaction. It may be noted that calculation of the rate of exchange, v, defined by (4) requires the determination of ATP^{*}_{∞}

$$v = - \frac{1}{t} (PP) \frac{ATP^{*}_{\infty}}{PP^{*}_{o}} \text{Ln} \left(1 - \frac{ATP^{*}}{ATP^{*}_{\infty}}\right) \qquad (4)$$

$$v \simeq \frac{1}{t} (PP) \frac{ATP^{*}}{PP^{*}_{o}} \qquad (5)$$

The linear approximation (5) is valid only if ATP^{*} is negligible in front of the ATP^{*}_{∞} concentration. Consequently it should not be used without prior determination of the actual ATP^{*}_{∞} in the conditions of the test, particularly in the case of manganese.

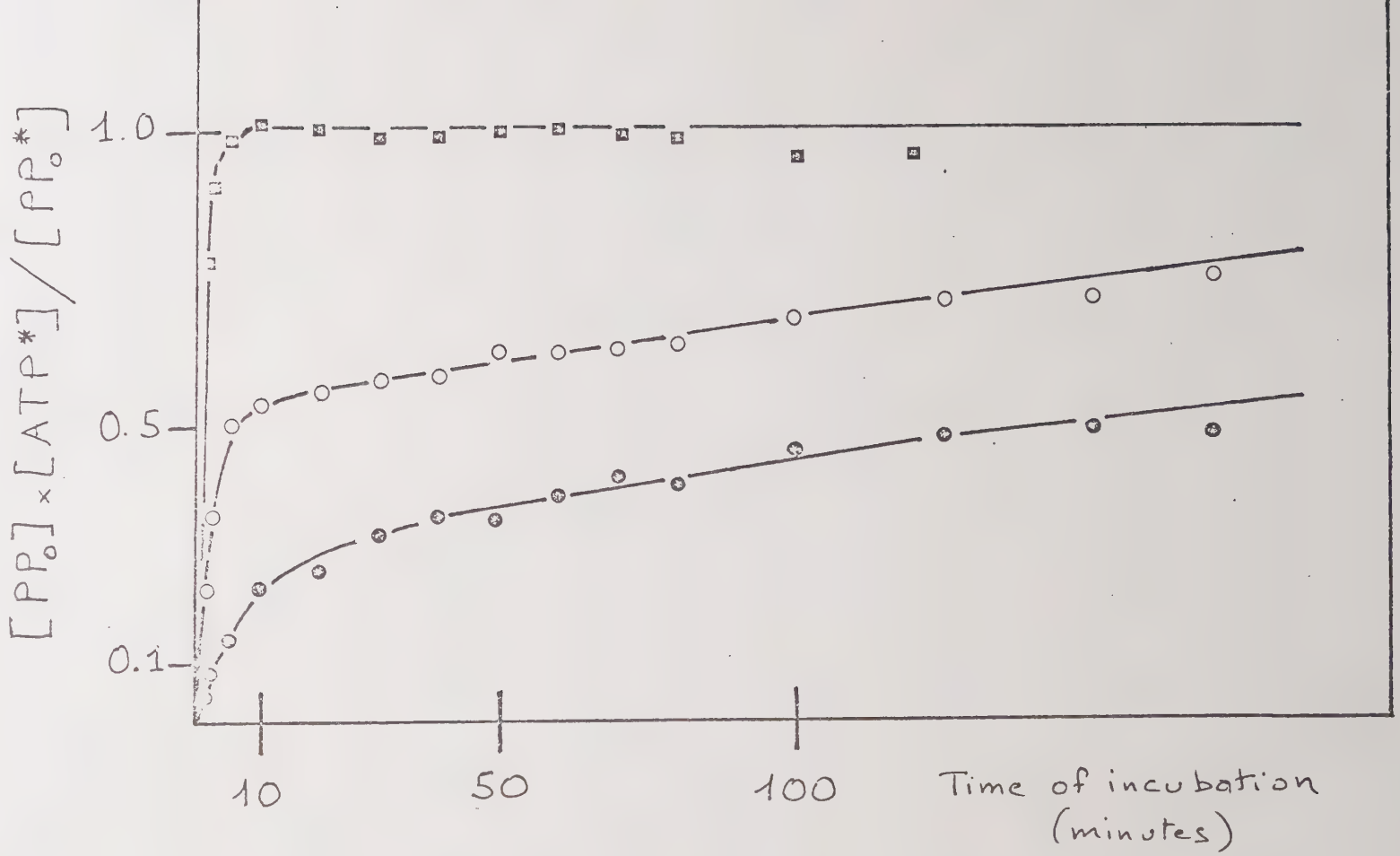

FIGURE 2 : INCORPORATION OF RADIOACTIVITY INTO ATP DURING THE TIME-COURSE OF THE ATP-PP ISOTOPIC EXCHANGE.

Experiments were performed at 25° C in standard buffer with 0.1 mM EDTA in the presence of 2 mM ATP, 2 mM PP, 2 mM L-methionine and catalytic amounts of purified methionyl-tRNA synthetase. The metal contents were 7 mM $MgCl_2$ (—■—) 4 mM $MnCl_2$ (—○—) and 10 mM $MnCl_2$ (—●—)

Non involvment of the adenosine-N7 position.

In solution, the manganese ion interacts with the phosphate groups of ATP and, through a water bridge, with the nitrogen atom in position 7 of the purine ring [21,22]. In the case of magnesium, data remain conflicting [21,23]. However a direct interaction between the Mg^{2+} ion and the purine has been reported which concerns the N1 or N3 positions of the ring [24]. Such differences in the mode of metal-purine interaction, if they still hold in the active site of methionyl-tRNA synthetase, would affect the validity of the substituting of Mn^{2+} for Mg^{2+} in further mechanistic and structural studies. In order to investigate this point, inbitory effects of adenosine and 7-deaza-adenosine (tubercidin) in the ATP-PP exchange reaction have been compared as a function of the divalent metal.

According to the general formalism developped in the case of such inhibited reactions [25], the reciprocal of the exchange rate, Et/v is a linear function of the inhibitor concentration (I). In the presence of a saturating amount of amino-acid, the slope of this function is ruled by :

$$\frac{d(Et/v)}{d(I)} = \frac{1}{k_{app}} \frac{Keq}{(ATP)} \left(\frac{1}{K_{I.AA}} + \frac{(PP\text{-}Me^{2+})}{K_{I.AA.PP\text{-}Me^{2+}}}\right) = \frac{1}{k_{app}} \frac{Keq}{(ATP)} \frac{1}{K_{I.AA}} \left(1 + \frac{PP\text{-}Me^{2+}}{K^{I.AA}_{PP\text{-}Me^{2+}}}\right) \quad (6)$$

where $K_{I.AA} = \dfrac{(E)(I)(AA)}{(E.I.AA)}$,

$$K_{I.AA.PP\text{-}Me^{2+}} = \frac{(E)(I)(AA)(PP\text{-}Me^{2+})}{(E.I.AA.PP\text{-}Me^{2+})}$$

and $$K^{I.AA}_{PP\text{-}Me^{2+}} = \frac{(E.I.AA)(PP\text{-}Me^{2+})}{(E.I.AA.PP\text{-}Me^{2+})}$$

TABLE 3

EFFECT OF THE NUCLEOSIDE ON THE EQUILIBRIUM CONSTANT OF PP-Me^{2+} WITH THE TRYPSIN-MODIFIED ENZYME:METHIONINE:NUCLEOSIDE TERNARY COMPLEX.

Nucleoside / Me^{2+}	Adenosine	Tubercidine	8-Amino-adenosine
Mg^{2+}	220±25 µM	240±100µM	4.4±2.1µM
Mn^{2+}	23.0±0.4µM	14.5±2.6µM	6.3±1.5µM

This table presents values for the dissociation constants of PP-Me^{2+} from the enzyme:methionine:nucleoside:PP-Me^{2+} complex i.e. :

$$\frac{(E.Nucleoside.AA)(PP\text{-}Me^{2+})}{(E.Nucleoside.AA.PP\text{-}Me^{2+})}$$

The values and their standard errors were determined by ATP-PP isotopic exchange according to the method described in the text. The experimental conditions were as follows : L-methionine 2 mM, ATP 0.25 mM, EDTA 0.1 mM. Adenosine, Tubercidine and 8-amino-adenosine were varied respectively from 0 to 2 mM, 0 to 1 mM and 0 to 0.04 mM. The pyrophosphate was varied in parallel from 0.1 to 0.03 mM and from 0.015 mM to 0.1mM respectively in the presence of 7 mM $MgCl_2$ and in the presence of 0.45 mM $MnCl_2$.

K_{eq} and k_{app} are defined in Table 4.

Thus, at constant AA and ATP concentrations, the secondary plot of the slope versus the PP concentration yields a line which intercepts the abscissa axis at the $K^{I.AA}_{PP-Mn^{2+}}$ value. Data pertaining to this experiment are presented in Table 3. They demonstrate that substituting tubercidin to adenosine does not affect significantly the binding of either PP-Mg^{2+} or PP-Mn^{2+} to the ternary enzyme:methionine:nucleoside complex. Thus, it appears that neither Mg^{2+} nor Mn^{2+} requires the N7 position of the purine ring in order to stabilize the dead-end synergistic complex (E.I.AA.PP-Me^{2+}) which is believed to simulate the transition state of the methionine activation reaction [8]. Consequently, the N7 atom of the purine appears not to be directly involved in the binding of the metal ion in the course of the activation reaction catalysed by methionyl-tRNA synthetase. Furthermore, fluorescence studies at equilibrium of the couplings on the enzyme between methionine and adenosine or tubercidin (using the methodology described in part 3) reveal that substitution by a carbon atom of the N7 position of adenosine affects neither the binding of the nucleoside nor the strength of its coupling to methionine binding.

2 - MECHANISM OF THE L-METHIONINE ACTIVATION REACTION IN THE PRESENCE OF MANGANESE (II).

ATP-PP isotopic exchange analysis. The mechanism of the activation reaction (scheme I) catalysed by methionyl-tRNA synthetase has already been resolved in the presence of Mg^{2+} with the help of the ATP-PP isotopic exchange [10].

LEGEND OF TABLE 4

The k_{app} term is defined as elsewhere [10] with, v, the initial rate of the ATP-PP exchange. The data are derived from the single or combined following experiments :

(a) Fluorescence titration of the enzyme by aminoacid (Figure 3A).

(b) Fluorescence titration of the enzyme : aminoacid complex by ATP-Mn^{2+} in the presence of various buffering PP-Mn^{2+} concentrations (Figure 3C, 4A).

(c) Fluorescence titration of the enzyme : ATP-Mn^{2+} complex by AA in the presence of various buffering PP-Mn^{2+} concentrations (Figure 3D, 4B).

(d) Fluorescence titration of E.AA~AMP by PP-Mn^{2+} in the presence of saturating AA and ATP-Mn^{2+} concentrations (Figure 3B).

(e) Multilinear resolution of the relation (7) by isotopic ATP-PP exchange.

TABLE 4

THERMODYNAMICAL PARAMETERS OF THE REVERSIBLE ACTIVATION REACTION OF METHIONINE CATALYSED BY NATIVE AND TRYPSIN-MODIFIED METHIONYL-tRNA SYNTHETASES IN THE PRESENCE OF MANGANESE (II).

	Native enzyme	Modified enzyme	Type of analysis
$K_{AA} = \frac{(E)(AA)}{(E.AA)}$		60 ± 2 µM	(a)
	88 ± 31 µM	80 ± 15 µM	(e)
$K_{ATP} = \frac{(E)(ATP\text{-}Mn^{2+})}{(E.ATP\text{-}Mn^{2+})}$		1.3 ± 0.2 mM	(a)+(b)+(c)
	1.5 ± 0.9 mM	1.6 ± 0.6 mM	(e)
$\frac{K_{eq}.K_x}{K_{ATP}} = \frac{(E.ATP\text{-}Mn^{2+})(AA)}{(X)}$	-	9.0 ± 0.9 µM	(c)
$\frac{K_{eq}.K_x}{K_{AA}} = \frac{(E.AA)(ATP\text{-}Mn^{2+})}{(X)}$	-	195 ± 7 µM	(b)
$K_{eq} = \frac{(E)(AA)(ATP\text{-}Mn^{2+})}{(E.AA \sim AMP)(PP\text{-}Mn^{2+})}$	-	780 ± 200 µM	(a)+(b)+(c)+(d)
	640 ± 300 µM	680 ± 240 µM	(e)
$K_x = \frac{(E.AA\sim AMP)(PP\text{-}Mn^{2+})}{(X)}$	-	9.6 ± 0.8 µM	(b)
		14.5 ± 3.9 µM	(c)
		15.6 ± 1.3 µM	(d)
	16 ± 4 µM	17 ± 4 µM	(e)
$k_{app} = \frac{v}{(E.AA \sim AMP)(PP)}$	$0.7 \pm 0.2 \mu M^{-1} s^{-1}$	$1.7 \pm 0.4 \mu M\ s^{-1}$	(e)

Scheme I

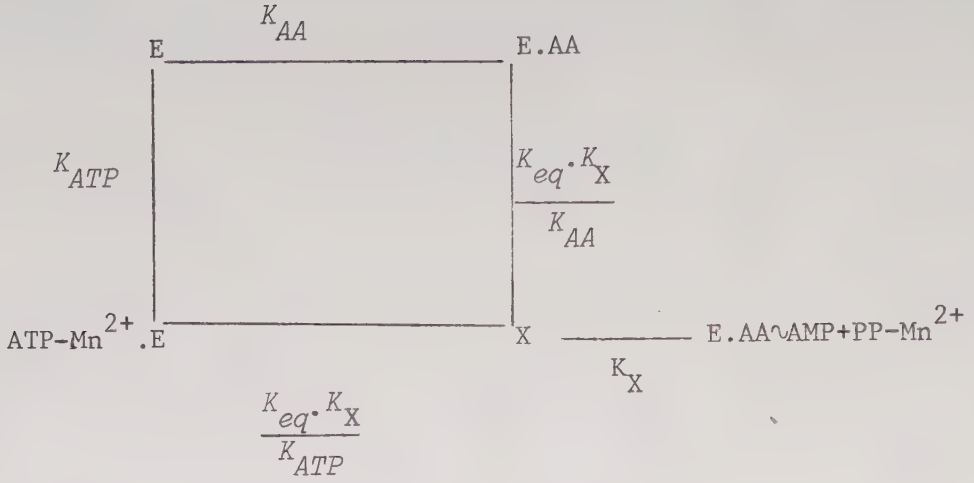

The rate of exchange, v, is ruled by (7) where all of the thermodynamical constant are as defined in Table 4 :

$$\frac{(E_t)}{v} = \frac{1}{k_{app}} \left(\frac{1}{(PP)} + \frac{1}{K_x} + \frac{K_{eq}}{K_{AA}.(ATP)} + \frac{K_{eq}}{K_{ATP}.(AA)} + \frac{K_{eq}}{(AA).(ATP)} \right) \qquad (7)$$

Relationship (7) was resolved by permutation of the ATP, PP and AA concentrations. In order to avoid artefacts due to the aggregation of pyrophosphate with manganese, the concentration of total pyrophosphate in the assay never exceeded 0.1 mM and a strict $(Mn^{2+})=(ATP)+(PP)+(EDTA)$ stoechiometry was respected. It was systematically verified by determination of the isotopic plateau that in these conditions no significant aggregation occurs during the experiments. The rat of exchange was then determined according to relation (4) in the following ranges of concentrations:AA from 0.01 to 2 mM,ATP from 0.1 to 4 mM,PP from 0.05 to 0.1 mM

In these conditions, plots of Et/v versus 1/(AA) at constant (ATP) and (PP) were always linear, thus providing evidence that the k_{app} term remains constant in the range of methionine under study [10, 20]. The experimental values were analysed according to relation (7) with the help of a multiparameter multivariable iterative linear regression. Resulting parameters are presented in Table 4. Similar thermodynamical constants are found in the case of the native and of the trypsin-modified enzymes. As expected, the k_{app} values vary as the number of active sites per molecule of enzyme [10].

Fluorescence at equilibrium.

Tryptophan fluorescence of methionyl-tRNA synthetase has been used in order to resolve the mechanism of the activation reaction in the presence of magnesium [10]. Substituting manganese to magnesium does not affect significantly the fluorescence variations which correspond to the different steps of the activation reaction. Consequently, experiments are presented in Figure 3 which lead to a resolution of the mechanism at equilibrium. Titration of the enzyme by L-methionine is presented in panel A. The presence of up to 7 mM $MnCl_2$ lowers the fluorescence yield of the enzyme : methionine complex but does not affect significantly its dissociation constant. Titrations of the E.AA complex by ATP-Mn^{2+} in the presence of different buffering PP-Mn^{2+} concentrations (i.e. (PP-Mn^{2+}) $\gg$ sites concentration) are presented in panel C. The corresponding dissociation constants, K, are ruled by (8), when calculated according to scheme I.

$$K = \frac{K_{eq}}{K_{AA}} \quad \frac{(PP)}{1+\frac{(PP)}{K_x}} \qquad (8)$$

relative fluorescence Ø (%)
A
B
C
D
130
120
110
100
90
80
200
400
100
300
500
2000
6000
250
500
750
100
300
500
2000
6000
(Ø-Ø₀)/[AA] (mM)⁻¹
(Ø-Ø₀)/[PP-Mn²⁺] (mM)⁻¹
(Ø-Ø₀)/[ATP-Mn²⁺] (mM)⁻¹
(Ø-Ø₀)/[AA] (mM⁻¹)

FIGURE 3 : FLUORESCENCE ANALYSIS AT EQUILIBRIUM OF THE REVERSIBLE METHIONINE ACTIVATION REACTION CATALYSED BY TRYPSIN-MODIFIED METHIONYL-tRNA SYNTHETASE.

The proteic fluorescence $\emptyset$ is plotted as a linear function of $(\emptyset-\emptyset_o)/(L)$ where $\emptyset_o$ is the fluorescence of the enzyme before titration by the ligand L, and where (L) is the free ligand concentration in the cell calculated with the assumption of a unique binding site on the enzyme [8,10]. The dissociation constants for the equilibria are measured by the absolute slopes of the lines obtained.

Panel A : Titration of the enzyme by methionine in the presence (—— o ——) and in the absence (—— • ——) of 7 mM $MnCl_2$.

Panel B : Titration by PP of the enzyme : methionyl-adenylate complex obtained in the presence of methionine (2 mM), ATP (0.75 mM) and manganese (0.8 mM).

Panel C : Titration by ATP-Mn^{2+} of the enzyme saturated with methionine (2mM) in the presence of various buffering PP-Mn^{2+} concentrations.

Panel D : Titration by AA of the enzyme saturated with ATP-Mn^{2+} (3.75 mM) in the presence of various buffering PP-Mn^{2+} concentrations.

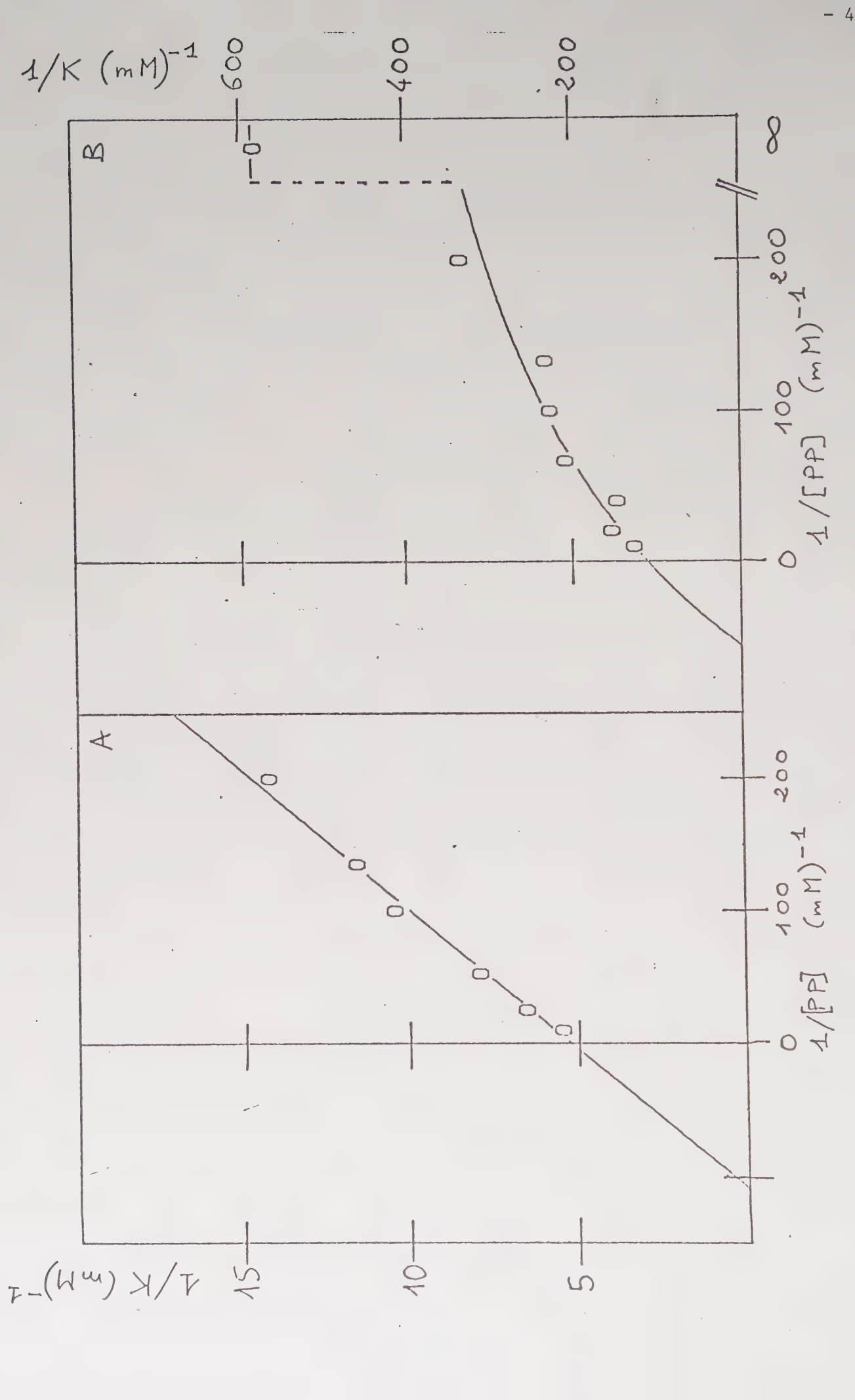
1/K (mM)-1
600
400
200
B
0
1/[PP] (mM)-1
100
200
A
15
10
5
1/K (mM)-1

FIGURE 4 : FLUORESCENCE AT EQUILIBRIUM;SECONDARY PLOT.

The dissociation constants determined as shown in Figure 3C and 3D are analysed in function of the buffering pyrophosphate-manganese concentration according to scheme I.

Panel A : Analysis of the titrations of E.AA by ATP-Mn^{2+}. Double reciprocal plot of the dissociation constant versus PP-Mn^{2+}. The experimental data are fitted to equation (8) (continuous line).

Panel B : Analysis of the titrations of E.ATP-Mn^{2+} by AA. Double reciprocal plot of the dissociation constant versus PP-Mn^{2+}. The infinite value of 1/PP corresponds to the titration in the presence of the only contaminating pyrophosphate. The experimental data are fitted to equation (9) (continuous line).

Plot of 1/K versus $1/(PP\text{-}Mn^{2+})$ (Fig. 4A) yields the $K_{eq}.K_x/K_{AA}$ and K_x values (Table 4). The reciprocal titrations of the $E.ATP\text{-}Mn^{2+}$ complex by L-methionine in the presence of different buffering $PP\text{-}Mn^{2+}$ concentrations are shown in Fig. 3D. Saturation of the enzyme by $ATP\text{-}Mn^{2+}$ requires an important amount of ATP (3.75 mM in the presented experiments) in which unavoidable contaminating pyrophosphate occurs. Thus, the dissociation constants, K, obtained in this set of experiments were fitted to a general equation(9) :

$$K = \frac{K_{eq}}{K_{ATP}} \cdot \frac{(PP)+(PP)_c}{1+\frac{(PP)+(PP)_c}{K_x}} \qquad (9)$$

where the contaminating pyrophosphate concentration, $(PP)_c$, is taken into account. The corresponding double reciprocal plot is shown in Fig. 4B and the data derived from the fit are presented in Table 4. It may be noted that the fitted value for $(PP)_c$ is equal to 3.4 µM and corresponds to a 1 °/oo contamination of the ATP solution.

The K_X value may be directly determined by titrating with $PP\text{-}Mn^{2+}$ the E.AA∿AMP complex insured by the presence of saturating amounts of $ATP\text{-}Mn^{2+}$ and AA (Fig. 3B).

Stopped-flow analysis.

Scheme I does not describe completely the adenylation mechanism since the species X contains unresolved isomers. Stopped-flow fluorescence technique has been recently applied to resolve the rate constants of the central

equilibrium which rules the reaction in the presence of magnesium [8]. According to this work, the overall mechanism for L-methionine activation may be described by scheme II in which ligand bindings are in rapid preequilibria relative to the reaction rates k_f and k_b. In this model, X is resolved into the E.AA.ATP-Mn^{2+} and E.AA∿AMP.PP-Mn^{2+} species which correspond to a minimal order of degeneracy.

Scheme II

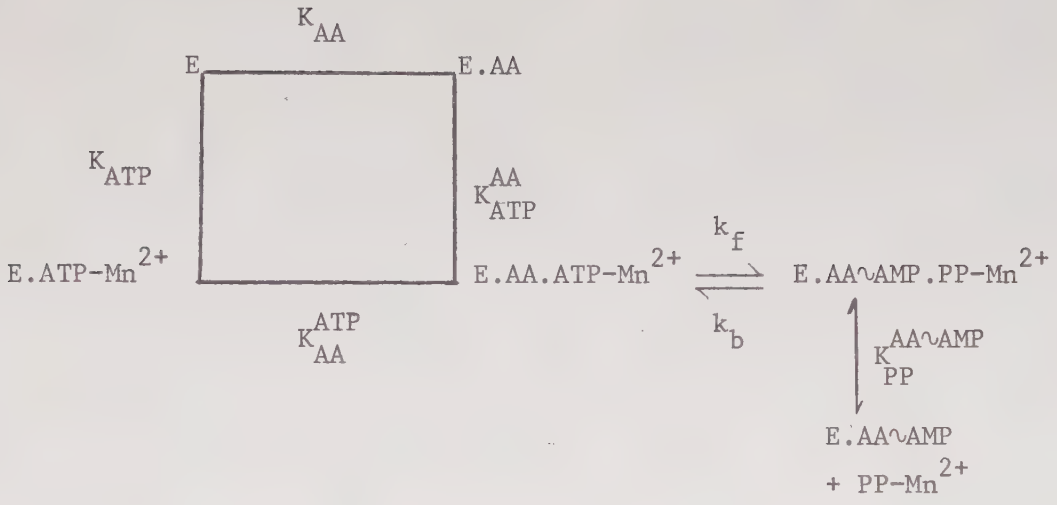

As demonstrated previously [8], the time constant, k, of the exponential fluorescence relaxation which is associated to adenylate synthesis or reversion, is ruled by (10)

$$k = k_f \left\{ 1 + \frac{K_{ATP}^{AA}}{(ATP\text{-}Mn^{2+})} + \frac{K_{AA}^{ATP}}{(AA)} + \frac{K_{AA} \cdot K_{ATP}^{AA}}{(AA).(ATP\text{-}Mn^{2+})} \right\}^{-1} + k_b \left\{ 1 + \frac{K_{PP}^{AA\sim AMP}}{(PP\text{-}Mn^{2+})} \right\}^{-1} \qquad (10)$$

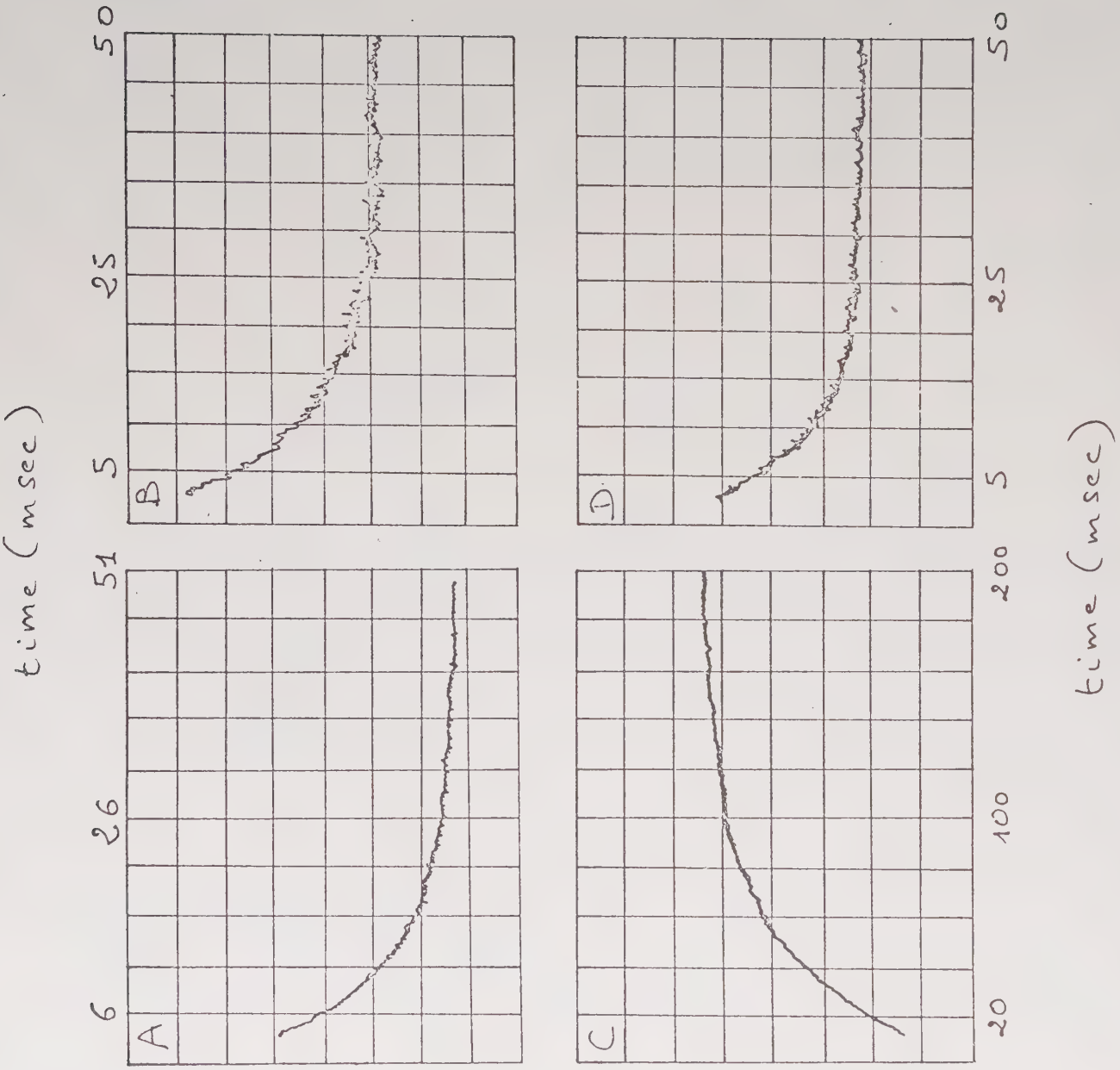
time (msec)
A
6
26
51
B
5
25
50
C
20
100
200
D
5
25
50
time (msec)

FIGURE 5 : OSCILLOSCOPE TRACINGS FOR THE FORMATION OF THE METHIONYL-tRNA SYNTHETASE : METHIONYL~ADENYLATE COMPLEX AND ITS REVERSION.

Experiments were performed in standard buffer containing 0.1 mM EDTA and 0.1 mM $MnCl_2$. The time scales take into account a 2.5 ms dead time of the apparatus. The rise time is 1 ms for panel C and 0.1 ms for the others. The voltage unit of the oscillograms is 50 mV/div.

Panels A and D : Rapid 1:1 mixing of a solution containing 0.74 µM trypsin modified methionyl-tRNA synthetase plus 2.5 mM L-methionine and 1 µM (panel A) or 100 µM (panel D) pyrophosphate with a solution containing the same concentrations of methionine and pyrophosphate plus 12 mM ATP-Mn^{2+}. The amplitude of signals at equilibrium are respectively equal to 0.95 V and 1.0 V after substracting the buffer signal.

Panel B : Rapid 1:1 mixing of a solution containing 0.74 µM trypsin-modified methionyl-tRNA synthetase plus 4 mM ATP-Mn^{2+} and 1 µM PP with a solution containing the same ATP-Mn^{2+} and pyrophosphate concentrations plus 1 mM methionine. Final signal is 1.8 V.

Panel C : Rapid 1:1 mixing of a solution containing 0.74 µM trypsin-modified methionyl-tRNA synthetase plus 2.5 mM methionine, 50 µM ATP-Mn^{2+} and 200 µM free Mn^{2+} with a solution containing the same concentrations of methionine and ATP-Mn^{2+} plus 200 µM pyrophosphate. Final signal is 1.05 V.

LEGEND OF TABLE 5

The parameters determined in the presence of manganese were obtained as indicated in the text.

Comparative values obtained in the presence of 7 mM $MgCl_2$ are from [8], k_f is the rate of reaction from E,AA.ATP-Mn^{2+} to E.AA∿AMP,PP-Mn^{2+} while k_b is the inverse one.

$$K_{ATP}^{AA} = (E.AA).(ATP\text{-}Mn^{2+})/(E.AA.ATP\text{-}Mn^{2+}),$$

$$K_{AA}^{ATP} = (E.ATP\text{-}Mn^{2+}).(AA)/(E.AA.ATP\text{-}Mn^{2+})$$

and $$K_{PP}^{AA\sim AMP} = (E.AA\sim AMP)(PP\text{-}Mn^{2+})/(E.AA\sim AMP.PP\text{-}Mn^{2+})$$

The other thermodynamical parameters are defined in Table 4.

TABLE 5

STOPPED-FLOW ANALYSIS OF THE REVERSIBLE ACTIVATION REACTION OF METHIONINE CATALYSED BY NATIVE AND TRYPSIN-MODIFIED METHIONYL-tRNA SYNTHETASES IN THE PRESENCE OF MANGANESE (II).

	Manganese		Magnesium
	Native enzyme	Modified enzyme	Modified enzyme
k_f	$210 \pm 8\ s^{-1}$	$170 \pm 9\ s^{-1}$	$259 \pm 9\ s^{-1}$
k_b	$28.7 \pm 1.2\ s^{-1}$	$27.9 \pm 1.4\ s^{-1}$	$223 \pm 7\ s^{-1}$
k_f/k_b	7.32 ± 0.60	6.09 ± 0.63	1.11 ± 0.07
K_{ATP}^{AA}	1.45 ± 0.10 mM	1.41 ± 0.12 mM	1.50 ± 0.10 mM
K_{AA}^{ATP}	-	60 ± 10 µM	80 ± 9 µM
$K_{PP}^{AA\sim AMP}$	13.4 ± 1.3 µM	20.6 ± 2.7 µM	214 ± 11 µM
$K_x = \frac{K_{PP}^{AA\sim AMP}}{(1+\frac{k_b}{k_f})}$	11.8 ± 2.1 µM	17.7 ± 4.2 µM	113 ± 11 µM
$\frac{K_{eq}\ K_x}{K_{AA}} = \frac{K_{ATP}^{AA}}{(1+\frac{k_f}{k_b})}$	174 ± 26 µM	199 ± 38 µM	700 ± 100 µM
$\frac{K_{eq}\ K_x}{K_{ATP}} = \frac{K_{AA}^{ATP}}{(1+\frac{k_f}{k_b})}$	-	8.5 ± 1.7 µM	37.5 ± 5.7 µM

Formation of the enzyme-bound adenylate was performed either by 1:1 mixing of ATP-Mn^{2+} with a saturated E.AA complex (Fig. 5A) or of AA with a E.ATP-Mn^{2+} complex (Fig. 5B), in the presence, in both cases, of buffering amounts of PP-Mn^{2+}. Reversion of the preformed enzyme-bound adenylate in one syringe was insured by 1:1 mixing with PP-Mn^{2+} contained in the other syringe (Fig. 5C). In all of these experiments the PP concentration never exceeded 0.25 mM and the stoichiometry (Mn^{2+}) = (PP)+(ATP)+(EDTA) was always respected after mixing. Respective concentrations of pyrophosphate and manganese in each syringe were chosen in order to avoid aggregation prior to mixing (Legend to Figure 5C).

Comparison of panels A and B in figure 5 indicates that, in agreement with scheme II, the order of substrates addition does not modify the observed rate constant for adenylate formation (k=130 s^{-1} for the relaxation in A and 125 s^{-1} in B). The model is also verified by the fact that the rate constant at saturating amounts of all substrates (Fig. 5D, k=165 s^{-1}) is actually the sum of those at saturating PP-Mn^{2+} and AA, low ATP-Mn^{2+} (Fig. 5C, k=26 s^{-1}), and saturating ATP-Mn^{2+} and AA, low PP-Mn^{2+} (Fig. 5A, k=130 s^{-1}). The data shown in Table 5 were obtained by varying (AA), (ATP-Mn^{2+}) and (PP-Mn^{2+}) respectively from 0.005 to 2 mM, 0.03 to 6 mM and 0.001 to 0.25 mM, and fitting the rate constants to equation (10), either globaly or by a set of independent regressions [8].

As shown in Table 5 magnesium insures similar values for the rates of isomerisation k_f and k_b and consequently an isomerisation constant k_f/k_b close to 1. In contrast,with manganese, the lower value of k_b displaces the central reaction towards the E.AA∿AMP.PP-Mn^{2+} complex. Comparison of the data also shows that changing the metal does not affect significantly the uncoupled binding of AA and ATP-Me^{2+} within the catalytic site. Only the central reaction and the pyrophosphate binding to the E.AA∿AMP complex are modified to a significant extent.

3 - SUBSTITUTING MAGNESIUM (II) BY MANGANESE (II). METHIONYL-tRNA SYNTHETASE DEAD-END SYNERGISTIC COMPLEXES.

Evidence for couplings between ligands within the active site of methionyl-tRNA synthetase from *Escherichia coli* has been recently reported. [6, 9]. Analysis of these phenomena reveals that coupling between ligands behaves as a function of the distribution of the carboxylate and phosphate negative charges which are introduced into the site by methionine and 5'-nucleotides. Moreover, the role of the divalent magnesium ion on the distribution of these charges has been emphasized.

It was thus important to investigate the metal specificity in these effects. Consequently, the tryptophan fluorescence enhancement induced by the binding of L-methionine or L-methioninol in the presence of variable concentrations of coupled partners was used in order to resolve the corresponding equilibria. It may be recalled that, in the presence of a partner S, the apparent dissociation constant, K_d, for the aminoacid or alcohol, AA, is ruled by the following hyperbola :

$$K_d = K_{AA} \frac{1 + (S)/K_S}{1 + (S)/K_S^{AA}} \qquad (11)$$

where $K_{AA} = \frac{(E)\ (AA)}{(E.AA)}$, $K_S = \frac{(E)\ (S)}{(ES)}$ and $K_S^{AA} = \frac{(E.AA)\ (S)}{(E.AA.S)}$

and where the extent of coupling is defined by K_{AA}/K_{AA}^S.

Enzyme:methioninol:ATP-Mn^{2+} complex.

L-methioninol binding is markedly coupled to the presence of ATP-Mn^{2+} in the active site of methionyl-tRNA synthetase. As shown in Figure 6A, increasing

B
A
dissociation constant of methionine (μM)
100
10
1
(logarithmic scale)
1
2
3
4
10
20
[ATP-Mn2+] (mM)
[Mn2+] (mM)

FIGURE 6 : SYNERGISTIC COUPLING OF L-METHIONINOL AND ATP-Mn^{2+} WITHIN THE SITE OF TRYPSIN-MODIFIED METHIONYL-tRNA SYNTHETASE.

The equilibrium constant of methioninol with the enzyme was determined with the help of proteic fluorescence in the presence of various amounts of ATP-Mn^{2+} (panel A). The inhibitory effect of free manganese on methioninol binding is illustrated in panel B where the dissociation constant for methioninol has been plotted as a function of the total manganese added in the absence (—— O ——) or in the presence of 0.065 mM (—— ◐ ——), 0.65 mM (—— ◑ ——) and 4 mM (—— ● ——) ATP.

amounts of ATP-Mn^{2+} enhance the affinity of the enzyme for the aminoalcohol. The data obtained in the presence or absence of Me^{2+} are compiled in Table 6. The extent of synergistic coupling between L-methioninol and ATP is notably increased by the presence of metal, particularly in the case of manganese.

It has been noticed that in the case of magnesium, the presence of the free metal ion inhibits the fixation of L-methioninol [9]. Investigation of the inhibition pattern caused by free Mn^{2+} in the presence of various ATP concentrations provides further insight into this phenomenon (Fig. 6B). The presence of free Mn^{2+} appears to inhibit competitively the fixation of L-methioninol with a K_i equal to 5 mM, which is independent of the ATP-Mn^{2+} concentration present in the solution. These results clearly argue for the existence of at least two metal binding sites on the enzyme : ATP complex. One metal ion is brought into the active site as an ATP-Me^{2+} while the other binds the enzyme weakly and competes with methioninol binding. The latter ion does not interfere with the extent of the coupling between methioninol and ATP-Mn^{2+}.

Enzyme : Methionine (or methioninol) : adenosine : PP-Mn^{2+} complex.

Pyrophosphate and methionine bindings are coupled on the enzyme:adenosine complex in the presence of magnesium [6], while the corresponding coupling involving methioninol instead of methionine does not require magnesium [9]. Investigation of these couplings in the presence of manganese is complicated by the aggregation of PP-Mn^{2+}. However, the effect of Mn^{2+} on the methioninol-adenosine-pyrophosphate coupling can be resolved on the following grounds : at concentrations of pyrophosphate (10 mM) and adenosine (10 mM) which are saturating for the coupling in the absence of metal, addition of up to 2.5 mM Mn^{2+} does not change the equilibrium constant of L-methioninol with the trypsin-modified enzyme. In the same

conditions, the equilibrium constant of L-methionine has dropped from 12 µM in the absence of Mn^{2+} down to 0.5 µM in the presence of 2.5 mM Mn^{2+}. It is thus likely that the manganese ion does not affect significantly the dissociation constant of methioninol from the enzyme:methioninol:adenosine:pyrophosphate complex. This assumption is also supported by the fact that addition of manganese (up to 3 mM) to an enzyme:adenosine:pyrophosphate complex (18 mM Ado, 5 mM PP) which is 50 % saturated by methioninol does not modify the saturation fraction by more than 10 %. Therefore, we assume the following equality :

$$\frac{(E.Ado.AAol)(PP)}{(E.Ado.AAol.PP)} = \frac{(E.Ado.AAol)(PP\text{-}Mn^{2+})}{(E.Ado.AAol.PP\text{-}Mn^{2+})} \qquad (12)$$

Thus, from (12) and from analysis of the dissociation constants for L-methioninol obtained in the presence of adenosine with PP-Mn^{2+} concentrations varying from 0 to 0.18 mM, the scheme for the synergistic coupling between L-methioninol and PP-Mn^{2+} on the enzyme : adenosine complex may be resolved. Pertaining parameters are shown in Table 6 with, for comparison, corresponding values measured in the presence and in the absence of magnesium.[9]

LEGEND OF TABLE 6

The equilibrium constants in the presence of manganese were determined with their standard errors as indicated in the text. The values relative to the absence or presence of 7 mM magnesium are from [6] and [9]. Both in the case of Mg^{2+} and Mn^{2+} a competitive behaviour of the free metallic ion on methioninol binding has been reported [9]. However the extents of coupling involving the aminoalcohol do not depend on the free metal concentration. Thus in the case of $K_{AAol}^{Ado,PP}$ and K_{AAol}^{ATP}, the given values are related to the absence of free metal.

The K_{PP}^{Ado} value corresponding to the absence of metal is taken equal to $K_{PP}^{Ado,AA}$ since in this case PP is not coupled to AA binding on the enzyme:adenosine complex [6].

TABLE 6

EFFECT OF METAL ION ON SYNERGISTIC COUPLING BETWEEN LIGANDS WITHIN THE ACTIVE SITE OF TRYPSIN MODIFIED METHIONYL-tRNA SYNTHETASE.

	No metal	Magnesium II	Manganese II
K_{AA}	59 ± 3 μM	60 ± 4 μM (Mg^{2+}=7mM)	63 ± 5 μM (Mn^{2+}=7mM)
K_{AA}^{Ado}	9 ± 1 μM	9 ± 1 μM	10.5 ± 2 μM
$K_{AA}^{Ado.PP}$	9 ± 1 μM	0.2 ± 0.1 μM	0.11 ± 0.04 μM
K_{AAol}	330 ± 15 μM	460 ± 15 μM (Mg^{2+}=7mM)	840 ± 90 μM (Mn^{2+}=7mM)
K_{AAol}^{Ado}	110 ± 20 μM	120 ± 20 μM (Mg^{2+}=7mM)	275 ± 35 μM (Mn^{2+}=7mM)
$K_{AAol}^{Ado.PP}$	10.8 ± 1.7 μM	20 ± 5 μM	14 ± 4 μM
K_{AAol}^{ATP}	18 ± 5 μM	6 ± 2 μM	1.0 ± 0.2 μM
K_{ATP}	250 ± 60 μM	1.3 ± 0.2 mM	1.5 ± 0.2 mM
K_{ATP}^{AAol}	13.5 ± 1 μM	30 ± 1.5 μM	4.6 ± 0.2 μM
K_{PP}^{Ado}	700 ± 500 μM	6 ± 3 mM	1.9 ± 0.4 mM
$K_{PP}^{Ado.AAol}$	89 ± 23 μM	185 ± 43 μM	180 ± 10 μM
$K_{PP}^{Ado.AA}$	700 ± 500 μM	246 ± 21 μM	19 ± 2 μM

The coupling of L-methionine and PP-Mn^{2+} on the enzyme:adenosine complex is also complicated by the aggregation of the PP-Mn^{2+} species at concentrations over 0.2 mM. However, from the results of Table 3 and from fluorescence titration of the enzyme by methionine in the presence of adenosine (18 mM) plus PP-Mn^{2+} concentrations varying from 0 to 0.15 mM, an accurate value for $K^{Ado.AA}_{PP-Mn^{2+}}$ can be derived (Table 6). Knowledge of the K^{Ado}_{AA} value and of the $K^{Ado}_{PP-Mn^{2+}}$ value (from the above experiments with L-methioninol) enables to resolve completely the coupling scheme, the parameters of which are presented in Table 6.

DISCUSSION

Inhibition of methioninol binding by a divalent metal ion ([9] and this work), (Fig.6) has indirectly shown the existence of a weak site on the enzyme for this divalent ion. In the range of metal concentrations which are studied here (0 - 30 mM), the binding of Mn^{2+} appears competitive (K_I = 5 mM) with that of methioninol. In contrast, the slight interference of the free metal ion concentration with the binding of L-methionine argues for possible accomodation of the metal and aminoacid together on the enzyme. It may be noted that the affinity of Mn^{2+} for this metal binding site is weak and remains unmodified upon addition of ATP-Mn^{2+} to the enzyme. Furthermore this site is shown not to interfere with the extent of synergistic coupling between ATP-Mn^{2+} and methioninol. In most if not all of the experiments presented here, no free Mn^{2+} was present to saturate this site to a significant extent. Therefore we assume that it has little if any role in the catalytic and synergistic mechanisms discussed below. Moreover, preliminary EPR and water proton relaxation rate studies indicate no manganese binding to free trypsin-modified methionyl-tRNA synthetase with an equilibrium constant lower than 1 mM.

The metal ion is thus likely to enter the active site of the enzyme in the form of chelate with ATP or PP. Such ATP-Me^{2+} and PP-Me^{2+} chelates may undergo structural modifications on binding to the protein. An evidence is given by the behaviour of the N7 atom of the purine ring, which is essential in solution for the interaction of the Mn^{2+} ion with either the ATP molecule [22] or the Ado+PP combination (F.H. unpublished). As attested by the similar properties of adenosine and tubercidin, this N7 atom does not play a critical role in the active site of methionyl-tRNA synthetase. On the other hand, it is shown in

Table 6, that the ATP molecule has a six fold enhanced affinity for the enzyme as compared to ATP-Me^{2+}. Another way to handle these thermodynamical parameters is to compute the relative affinities of the metal ion for the ATP molecule and for the enzyme:ATP complex. From the definitions of K_{ATP} and $K_{ATP-Me^{2+}}$ it may be shown that the metal ion has a six times lower affinity for the enzyme:ATP complex than for ATP alone. Such a destabilization of the ATP-Me^{2+} complex could be accounted for by the suppression of a part of the interaction of the metal ion with the enzyme-bound nucleotide. Furthermore, this destabilization renders unlikely the possibility that a metal-protein bridge occurs on the ternary enzyme:ATP-Me^{2+} complex.

The parameters of Table 6 have been also used in order to compare the relative affinities of Mn^{2+} and Mg^{2+} towards different complexes of the enzyme and ligands (Table 7). For instance, Mg^{2+} and Mn^{2+} are shown to have a twofold weaker affinity for the quaternary E.AAol.Ado.PP complex than for Ado plus PP in solution. Introduction of the methionine carboxylate group strengthens the affinity of the metal ion for the E.AA.Ado.PP complex so that it becomes forty times stronger than for PP+Ado in the case of Mn^{2+}, and four times in the case of Mg^{2+}.(Table7) If a negative charge is brought into E.AAol.Ado.PP complex as the α-phosphate of ATP, (E.AAol.ATP) a similar three fold enhancement is only observed in the case of Mn^{2+} binding to ATP. The latter case is particularly interesting since the role of the methionine backbone (its side group and α aminogroup) can be pointed out through a comparison of the E.AAol.ATP and E.ATP species. Indeed it appears from Table 7 that upon binding of methioninol to the E.ATP complex, the binding of both metals to the enzyme-bound ATP is strengtened. Furthermore a tenfold greater enhancement of the binding of Mn^{2+} relative to Mg^{2+} is observed for both the E.AAol.ATP and the E.AA.Ado.PP complexes which contains respectively the α-phosphate group of ATP and the carboxylate of methionine.

TABLE 7

Metal binding to ATP and pyrophosphate.
Role of the enzyme and of coupling partners.

Relative efficiency of metal binding	Magnesium	Manganese
$\frac{(ATP)(Me^{2+})}{(ATP.Me^{2+})} / \frac{(E.ATP)(Me^{2+})}{(E.ATP.Me^{2+})} =$	0.2	0.2
$\frac{(PP)(Me^{2+})}{(PP.Me^{2+})} / \frac{(E.AA.Ado.PP)(Me^{2+})}{(E.AA.Ado.PP.Me^{2+})} =$	4	40
$\frac{(PP)(Me^{2+})}{(PP.Me^{2+})} / \frac{(E.AAol.Ado.PP)(Me^{2+})}{(E.AAol.Ado.PP.Me^{2+})} =$	0.5	0.5
$\frac{(ATP)(Me^{2+})}{(ATP.Me^{2+})} / \frac{(E.AAol.ATP)(Me^{2+})}{(E.AAol.ATP.Me^{2+})} =$	0.4	3
$\frac{(E.ATP)(Me^{2+})}{(E.ATP.Me^{2+})} / \frac{(E.AAol.ATP)(Me^{2+})}{(E.AAol.ATP.Me^{2+})} =$	2	18

Data of the Table are calculated from Table 6.

A rationale for these findings can be provided on the following grounds. The binding of the aminoacid backbone to the enzyme triggers a primary synergistic process where the binding of the nucleoside moiety is enhanced [9]. A spectroscopic track of this process may be the enhancement of the enzyme fluorescence by addition of methionine or analogs of methionine lacking the carboxylate function. When both the aminoacid backbone and the nucleoside and pyrophosphate moieties of ATP are present within the active site of methionyl-tRNA synthetase, introduction of a negative charge under the form of the methionine carboxylate or of the 5'-ATP α-phosphate improves the binding of the metal ion to the complex. A possible mechanism is that the metal ion is attracted by a negative charge provided either directly by the added ligands or indirectly by the protein itself. In the previous case, the divalent ion can be stabilized by its interaction with the α phosphate or the carboxylate negative charge perhaps through a second sphere complex of the metal (ion pair) [26]. An alternative possibility is that the introduction of a negative charge triggers the opening of a preexisting ion pair on the protein. The so liberated positive group interacts with the introduced negative charge to form a new ion pair while the liberated negative group is free to interact, again in an ion pair, with the divalent ion. This mechanism would be by many features similar to that suggested by Holler and his coworkers in the cases of phenylalanyl- and isoleucyl-tRNA synthetases [7]. Whatever the true mechanism is, if the metal ion forms an ion pair with a negative ligand, its stability constant is likely to be greater for Mn^{2+} (ionic radius 0.80 Å) than for Mg^{2+} (0.65 Å). This could explain the stronger stabilization observed with the manganous ion.

One of the aims of this work was to determine the L-methionine activation

kinetics in the presence of manganese and to compare it with the previously described kinetics in the presence of magnesium [8]. Such a comparison can be made on the basis of our prestationnary state experiments and is conveniently expressed as a Gibbs free energy diagramm (Figure 7). It appears from this diagram that the mechanism of formation of the anhydride bond between the aminoacid and the nucleotide, as reflected in the L-methionine and ATP-Me^{2+} binding steps and in the energy of the transition state of the reaction, is not affected by the substitution of one metal ion for another. The E.AA.ATP-Me^{2+} complexes are thus likely to be stabilized by metal ions irrespective of the nature of the metal involved. Their geometry should not resemble exactly those of the above discussed dead-end complexes for which stabilizations depending on the metal used have been demonstrated. A difference between the two classes of complexes (productive and dead-end) can be accounted for by the distortions resulting from a supplementary negative charge in the productive complexes. In contrast, the E.AA∿AMP.PP-Me^{2+} complex is accurately simulated by the E.AA.Ado.PP-Me^{2+} and the

E.AAol.ATP-Me^{2+} species. Indeed, PP-Me^{2+} displays, in the case of each metal, the same dissociation constants from the abortive E.AA.Ado.PP-Me^{2+} and from the productive E.AA∿AMP.PP-Me^{2+} species. It may be noted that in these cases, both the aminoacid backbone and the nucleoside moiety are present in the complexes, and that in either case a single negative charge occurs into the active site (methionine carboxylate and methionyl-adenylate phosphate groups respectively). Thus, it may be safely assumed that PP-Me^{2+} couples to the binding of AA∿AMP as it does in the case of the AA+Ado combination.

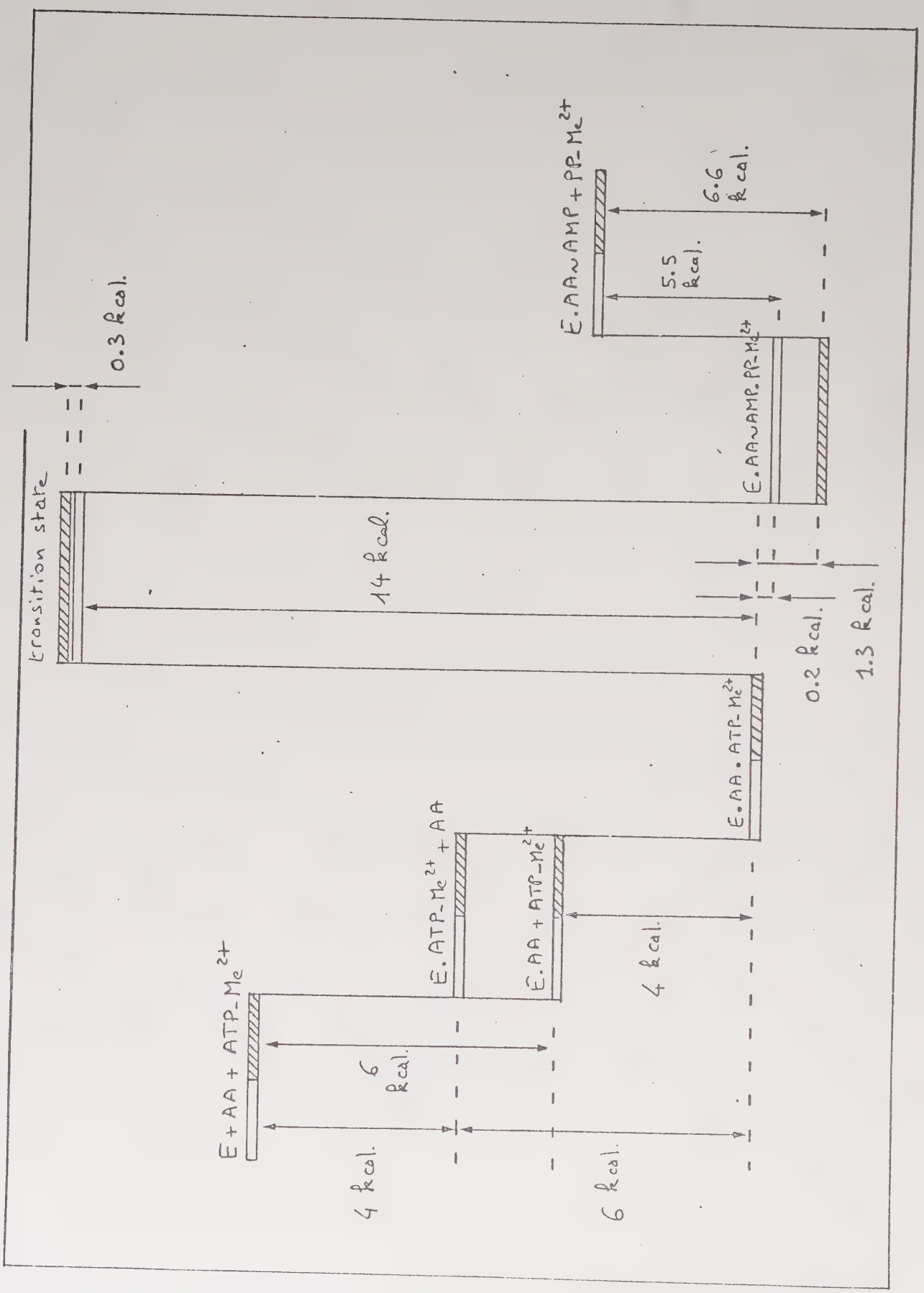
transition state
0.3 Kcal.
14 Kcal.
E.AA~AMP+PP-Me2+
5.5 Kcal.
6.6 Kcal.
E.AA~AMP.PP-Me2+
0.2 Kcal.
1.3 Kcal.
E.AA.ATP-Me2+
4 Kcal.
E.AA + ATP-Me2+
E.ATP-Me2+ + AA
6 Kcal.
4 Kcal.
6 Kcal.
E+AA+ATP-Me2+

FIGURE 7 : GIBBS FREE ENERGY DIAGRAMM OF THE REVERSIBLE L-METHIONINE ACTIVATION REACTION CATALYZED BY TRYPSIN-MODIFIED METHIONYL-tRNA SYNTHETASE. COMPARISON OF MAGNESIUM (II) AND MANGANESE (II).

The diagramm, which is calculated in the case of the modified enzyme, is derived from the stopped-flow studies summarized in Table 5. The change in free energy upon binding a substrate to an enzymatic species is calculated by : $\Delta G = -RT \, LnK$, where K is the dissociation constant of the substrate from its complex with the enzymatic species under consideration. Energies of the transition state are calculated according to the transition state theory, with

$$\Delta G_{f(or\ b)} = -RT \, Ln\left(\frac{h}{k.T} \cdot k_{f(or\ b)}\right)$$

The diagramms calculated for magnesium (▭) and manganese (▨) are given a common arbitrary origin at the $E+AA+ATP-Me^{2+}$ state.

The only significant difference between the two metals in the activation reaction is the greater stability of the E.AA~AMP.PP-Me^{2+} species in the case of manganese as compared to magnesium. In spite of this, as shown in Figure 7 the free energy of the enzyme-bound methionyl-adenylate does not depend on the divalent ion. This result, supports the assumption that the metal ion participates little, if any, to the structuration of the enzyme:methionyl-adenylate complex.

Stadtman [27] and Mahler and Cordes [28] have estimated between 3.5 and 6 kcal the energy difference upon adenylation of acetate to yield acetyl-AMP plus pyrophosphate from acetate and ATP. Assuming similar values in the case of methionyl-AMP synthesis in solution provides an energy uptake between 8.5 kcal and 11 kcal upon binding of methionyl-AMP to methionyl-tRNA synthetase (Fig.7). Such a value corresponds to a dissociation constant (between 10 nM and 600 nM) for methionyl-AMP which is in the same range as determined previously [29].

The manganese ion was reported to substitute for magnesium in the reactions catalysed by other activating enzymes (for review, see [4, 5]). However, in most cases, manganese stimulates the hydroxamate formation rather than the isotopic ATP-PP exchange reaction. This finding can be related to the demonstration, in the present report, that Mn^{2+} simulates better Mg^{2+} in the enzyme:methionyl-adenylate synthesis than in the reversion of this complex by PP-Me^{2+}.

Apart from the broad class of aminoacyl-tRNA synthetases, a variety of enzymes proceed through an enzyme-bound acyl-AMP (for review see, [27]). A possible aim for these intermediates has been proposed by Hopfield [30, 31] as a proofreading step where discrimination between the correct and incorrect

substrates can be achieved before incorporation into the products. In the case of aminoacyl-tRNA synthetases, advantage would be taken of an enhanced stability of the cognate aminoacyl-adenylate on the enzyme relative to non-cognates in order to select the proper aminoacid. In the presence of pyrophosphate, the E.AA∿AMP-PP-Me^{2+} species is likely to be verified to a lesser extent since it is stabilized by the synergistic coupling between AA∿AMP and PP-Me^{2+} in the active site of the enzyme. The validity of Hopfield's hypothesis would thus depend on the assumption that a low cellular pyrophosphate concentration drives the E.AA∿AMP.PP-Me^{2+} $\rightleftharpoons$ E.AA∿AMP+PP-Me^{2+} equilibrium towards the latter species. Recent measurements of the intracellular pyrophosphate concentrations in various *Escherichia coli* strains [31] do not support this assumption.

Substitution of Mg^{2+} by Mn^{2+} would further displace the above equilibrium towards the E.AA∿AMP.PP-Me^{2+} species even in the presence of a low free pyrophosphate intracellular concentration. Thus, in the case of Mn^{2+}, the only species for which the proofreading scheme applies, i.e. E.AA∿AMP is unlikely to occur with enough probability to insure proofreading.

This mechanism could be related to the observation that, in the case of several DNA polymerases, Mn^{2+} promotes the incorporation of ribonucleotides and improper deoxyribonucleotides ([32] and references therein). There again the proofreading step might be obliterated by the stabilization of an "unverified" E.dXMP.PP-Mn^{2+} complex. Such misincorporations are thought to provide the molecular basis for mutagenic effect of the manganese ions.

REFERENCES

[1] SÖLL D. and SCHIMMEL P.R. (1974). In the Enzymes Vol.X (P.D.Boyer,Ed.) Academic Press (N.Y. and London) pp. 489-538.

[2] KISSELEV L.L. and FAVOROVA O.O.(1974). In Adv. in Enzymology Vol.40 (A.Meister, Ed.).John Wiley & Sons (N.Y.-London-Sydney-Toronto). pp. 141-238.

[3] COLE F.X. and SCHIMMEL P.R. (1970). Biochemistry 9, 3143-3148.

[4] SCRUTTON M.C. (1973). In Inorganic Biochemistry Vol.I (G.L.Eichorn Ed.) Elsevier (Amsterdam-London-N.Y.) pp. 381-437.

[5] LOFTFIELD R.B. (1971). In Protein Synthesis (E.H.Mac Conkey,Ed.) M.Dekker publisher New-York Chap.1, pp. 1-88.

[6] BLANQUET S., FAYAT G. and WALLER J.P. (1975). J. Mol. Biol. 94, 1-15.

[7] HOLLER E., HAMMER-RABER B., HANKE T. and BARTMANN P. (1975). Biochemistry 14, 2496-2503.

[8] HYAFIL F., JACQUES Y, FAYAT G., FROMANT M., DESSEN P. and BLANQUET S.(1976). Biochemistry 15, 3678-3685.

[9] FAYAT G., FROMANT M. and BLANQUET S. submitted for publication.

[10] BLANQUET S., FAYAT G. and WALLER J.P. (1974). Eur.J.Biochem. 44, 343-351.

[11] CASSIO D. and WALLER J.P. (1971). Eur. J. Biochem. 20, 283-300.

[12] BRUTON C.J., JAKES R. and KOCH G.L.E. (1974). F.E.B.S. Letters 45, 26-28.

[13] ZELWER C., RISLER J.L. and MONTEILHET C. (1976). J. Mol. Biol. 102, 93-101.

[14] GULIK A., MONTEILHET C., DESSEN P. and FAYAT G. (1976). Eur. J. Biochem. 64, 295-300.

[15] CASSIO D. and WALLER J.P. (1971). F.E.B.S. Letters 12, 309-312.

[16] LAWRENCE F., SHIRE D.J. and WALLER J.P. (1974). Eur. J. Biochem. 41, 73-81.

[17] DWEK R.A. (1973). N.M.R. in Biochemistry, Clarendon Press Oxford.

[18] COHN M. and TOWNSEND J. (1954). Nature 173, 1090.

[19] COOPERMAN B.S. and MARK D.H. (1971) Biochem.Biophys.Acta 252, 221-234.

[20] COLE F.X. and SCHIMMEL P.R. (1970). Biochemistry 9, 480-489.

[21] COHN M. and HUGHES T.R. (1962). J. Biol. Chem. 237, 176-181.

[22] GLASSMANN T.A., COOPER C., HARRISON L.W. and SWIFT T.J. (1971). Biochemistry 10, 843-851.

[23] HAPPE J.A. and MORALES M. (1966). J. Am. Chem. Soc. 88, 2077-2078.

[24] KUNTZ G.P.P. and SWIFT T.J. (1973). Fed. Proc. Am. Soc. Exp. Biol. 32, 546.

[25] BLANQUET S., FAYAT G., POIRET M. and WALLER J.P. (1975). Eur. J. Biochem. 51, 567-571.

[26] MILDVAN A.S., NOWAK T. and FUNG C.H. (1973). Ann. N.Y. Acad. Sci. 222, 192-210.

[27] STADTMAN E.R. (1973). In the Enzymes Vol. VIII (P.D. Boyer Ed.) Academic Press (N.Y.-London) pp. 1-49.

[28] MAHLER H.R. and CORDES E.H. (1969). In Biological Chemistry p. 201. Harper and Row (N.Y. Evanston & London) and John Weatherhill inc. (Tokyo).

[29] BLANQUET S., FAYAT G., WALLER J.P. and IWATSUBO M. (1972). Eur. J. Biochem. 24, 461-469.

[30] HOPFIELD J.J(1974). Proc. Nat. Acad. Sci. U.S. 71,4135-4139.

[31] HEINONEN J. (1974). Anal. Biochem. 59, 366-374.

[32] KORNBERG A. (1974). DNA Synthesis, W.H. Freeman & Co. San Francisco.

TROISIEME PARTIE

INTRODUCTION A L'ARTICLE 3

La mesure des temps de relaxation d'un substrat s'échangeant entre un site paramagnétique et un environnement extérieur diamagnétique peut permettre de connaître les distances entre l'ion paramagnétique et les différents noyaux du substrat. Cette méthode a permis de mesurer les distances Mn^{2+}-phosphores dans le complexe ATP-Mn^{2+} [1-4] et de proposer que l'ion manganèse chélate un oxygène de chacun des trois phosphores de la chaîne triphosphate. De plus, le manganèse interagirait probablement par l'intermédiaire d'une molécule d'eau, avec l'atome d'azote en position 7 de la base purique [5] (Figure 1). On peut noter que les techniques de relaxation nucléaire donnent accès à des distances moyennes métal-noyau (plus exactement à la moyenne de la puissance sixième de la distance métal noyau) qui peuvent ne pas avoir de signification précise s'il n'y a pas une conformation unique.

Il est probable que, dans le cas de substrats liés à des enzymes il y a une conformation unique ou tout au moins que peu de déplacements par rapport à la conformation d'énergie la plus basse. Les mesures de relaxation nucléaires sont donc susceptibles de donner de bons résultats. Toutefois le peu de sensibilité de la R.M.N. et, dans le cas d'études sur le proton, la nécessité de séparer les protons du substrat de ceux de l'enzyme exigent un grand excès de substrat par rapport à l'enzyme. Une limitation de cette technique est donc que la relaxation du substrat sur l'enzyme puisse être séparée de celle extérieure à l'enzyme. Ceci est possible dans le cas des enzymes possédant un site fort pour le métal, le substrat n'étant alors relaxé que s'il est dans son site, ou bien pour les substrats ne fixant pas le métal.

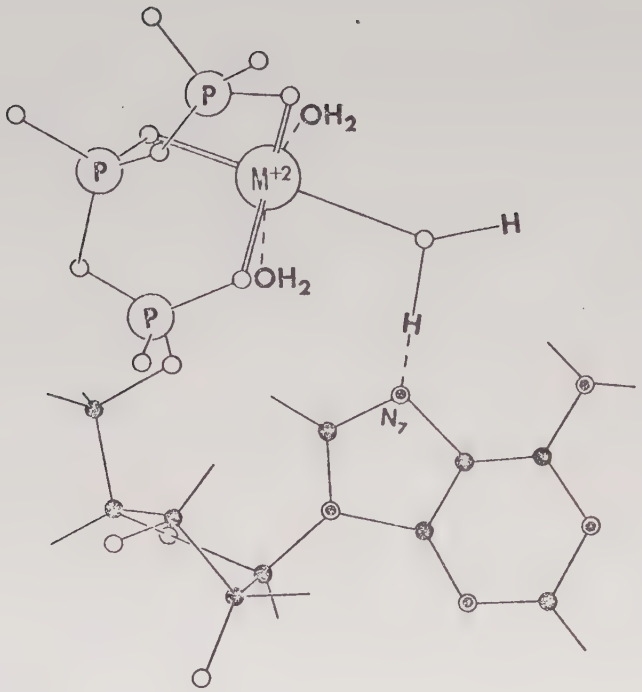

Figure 1 : Structure du complexe ATP-métal proposée par Glassman et al. [5] sur la base d' études de RMN. Une molécule d'eau forme un "pont" entre le métal et le N7 de la purine.

La méthionyl tARN synthétase ne possède pas de site fort pour le manganèse. De plus la molécule d'ATP, comme sa décomposition en adénosine + pyrophosphate, fixent le manganèse hors de l'enzyme. On peut pourtant, grâce aux propriétés synergiques de la méthionyl-tARN synthétase, trouver des conditions où la contribution paramagnétique sur l'enzyme n'est pas voilée par la contribution paramagnétique hors de l'enzyme. L'article suivant présente une étude entreprise dans ces conditions. Il montre que la molécule d'ATP-Mn^{2+}, qui est le véritable substrat de la réaction d'activation change de conformation en se fixant à l'enzyme. En particulier, l'interaction entre la purine et le métal divalent est abolie dans le site actif de la méthionyl tARN synthétase. Ce résultat nous permet de penser que les interactions métal-purine ne sont pas, une propriété de la molécule d'ATP essentielle quant à son rôle catalytique. Ceci nous rappelle une fois de plus le danger d'extrapoler aux sites actifs d'enzymes les conformations de substrats isolés.

REFERENCES

[1] COHN M. and HUGHES T.R. (1962). J. Biol. Chem. 237, 176-181.

[2] STERNLICHT H., SHULMAN R.G. and ANDERSON E.W. (1965). J. Chem. Phys. 43, 3123-3132.

[3] BROWN F.F., CAMPBELL I.D., HENSON R., HIRST C.W.J.and RICHARDS R.E. 1973). Eur. J. Biochem. 38, 54-58.

[4] SLOAN D.L. and MILDVAN A.S. (1976). J. Biol. Chem. 251, 2412-2420.

[5] GLASSMAN T.A., COOPER C., HARRISON L.W. and SWIFT T.J. (1971). Biochemistry 10, 843-851.

ARTICLE 3

THE L-METHIONINE ACTIVATION SITE OF METHIONYL tRNA SYNTHETASE FROM *ESCHERICHIA COLI*:ABSENCE OF INTERACTION BETWEEN THE METAL ION AND THE PURINE RING OF ATP.

François HYAFIL[a*] and Jean-Marie BERNASSAU[b]

[a]Laboratoire de Biochimie and [b]Laboratoire de Synthèse Organique
Ecole Polytechnique - 91128-PALAISEAU CEDEX - FRANCE -

*to whom correspondence should be addressed at The Biological Laboratories, Harvard University, 16 Divinity Avenue,Cambridge Mass.02138, U.S.A.

INTRODUCTION

In a previous report, we have studied manganese ions as a substitute for magnesium in the L-methionine activation site of methionyl tRNA synthetase from *Escherichia coli* |1|. The properties of both metals were shown to be quite similar with respect to both the methionine activation reaction and the formation of dead-end synergistic complexes |2, 3|. Among these, the enzyme:methionine:adenosine:pyrophosphate-metal (E.AA.Ado.PP-Me^{2+})* abortive complex was shown to simulate the enzyme:methionyl-adenylate:pyrophosphate-metal (E.AA∿AMP.PP-Me^{2+}) productive complex as regards its geometric , charge and thermodynamic properties |1,4|. In this paper we use the effect of the paramagnetic manganous ion on the longitudinal relaxation times of neighbouring protons to show that the metal does not chelate the purine ring of adenosine in the E.AA.Ado.PP-Mn^{2+} complex.

*Abbreviations : E is enzyme, AA = methionine, Ado = adenosine,
AA∿AMP = methionyl-adenylate,
PP = pyrophosphate, NMR = Nuclear Magnetic Resonance,
EPR = Electron Paramagnetic Reconance.

MATERIALS AND METHODS

Native methionyl tRNA synthetase is purified as described earlier [5] and converted into its trypsin-modified fragment [6]. The C_4 proton of imidazole is exchanged to a deuterium by heating an imidazole solution in D_2O at 90° C for 24 hours. This partially deuterated 5M imidazole solution is neutralized with HCl until a pH meter reading of 7.45 is reached after 1/500 dilution in D_2O. This 10 mM Imidazole-HCl buffer is used in all experiments since its NMR spectrum does not interfer with that of the ring protons of adenosine. The purified enzyme, stored in 20 mM potassium buffer at pH 7.5 containing 10 mM 2-mercaptoethanol and 50 % glycerol, is extensively dialized against the imidazole buffer and concentrated by ultrafiltration if necessary.

The experiments are performed in 5 mm tubes at 20°C in a Varian XL 100 NMR spectrometer operating in the Fourier Transform mode with a disk. The methodology used in 180° - τ - 90° T_1 measurement method is described elsewhere [7]. The T_2 are estimated from the half-height width. The EPR spectra are obtained in a Thomson TSW 254 spectrometer operating at 9500 MHz. The spectra are digitalized every 10 gauss and the base line substracted.

The theory of relaxation of a nucleus exchanging between a bulk solution and a paramagnetic site is well documented and comprehensively reviewed (for example in [8]). Briefly, τ_M being the residence time of the studied molecule on the paramagnetic site and f the fraction of molecules seeing the paramagnetic ion, the paramagnetic contribution to the longitudinal (fT_{1p}) or to the transverse

(fT_{2p}) relaxation time is ruled by (1) :

$$(1) \quad fT_{ip} = T_{iM} + \tau_M \qquad i = 1,2$$

In the case of Mn^{2+} macromolecular complexes we can neglect the hyperfine contribution to the relaxation [8] T_{iM} is then governed by the dipolar interaction and can be expressed by (2) :

$$(2) \quad T_{iM} = \left(\frac{C}{r}\right)^6 fi\ (\tau_c) \qquad i = 1,2$$

where C is a constant depending upon the nature of the observed nucleus, r is the ion-nucleus average distance and the fi's are functions of τ_c, of the frequency and of the magnetic field. The expressions and plots of the fi's and of f_2/f_1 can be found in [8]. τ_c , the correlation time, is governed by (3) :

$$(3) \quad \tau_c^{-1} = \tau_M^{-1} + \tau_e^{-1} + \tau_R^{-1}$$

i.e. by, the shortest of the following times τ_M, τ_e the electronic relaxation time, and τ_R the rotation correlation time of the complex, an upper estimation of which results from Stokes Einstein's law. For water protons the right term in Eq (2) must be multiplied by $q < 12$, the number of protons in the first hydration sphere of Mn^{2+}.

RESULTS

Electron paramagnetic resonance fails to detect any site with a dissociation constant below 1 mM for Mn^{2+} on trypsin-modified methionyl-tRNA synthetase. Addition of methionyl-tRNA synthetase to a 20 µM $MnCl_2$ solution enhances the relaxation of the water protons. However, up to a concentration of 0.2 mM enzyme this enhancement remains proportional to the enzyme concentration (at 0.2 mM enzyme = $\varepsilon \simeq 2$). The observed enhancement could thus arise from a non specific effect or from a metal site with low affinity. Similar enhancements are found in the additional presence of saturating amounts of methionine or of methionine and adenosine. Thus, methionyl tRNA synthetase does not appear to possess a strong site for a metallic ion at least in the absence of ATP or pyrophosphate (see below).

Table 1 presents the relaxation data for the dead-end complex E.AA.Ado.PP-Mn^{2+}, the concentration of which is known [1] from the total enzyme and PP Mn^{2+} concentrations. The paramagnetic effect outside the enzyme (i.e. that of the Ado.PP-Mn^{2+} complex) is substracted from the measured effect to yield the contribution of the enzyme complex to the shortening of relaxation times. The H8 proton of adenosine is strongly relaxed in the Ado.PP-Mn^{2+} complex indicating a structure probably resembling that of ATP-Mn^{2+} [9,11]. Experiments were conducted with tubercidine (7 deaza-adenosine), similar to adenosine with respect to its enzymatic properties [1] but for which no direct or indirect interaction is possible between the metal ion and position 7 of the purine ring. As shown in Table 1, there is still formation of a tubercidine.PP-Mn^{2+} ternary complex in which the H2 proton of the purine ring is now the most strongly relaxed.

TABLE

Nucleoside	Proton	Enzyme: methionine: nucleoside: PP-Mn^{2+} complex				Nucleoside: PP-Mn^{2+} complex	
		fT_{1p}^{-1} (s^{-1})	fT_{2p}^{-1} (s^{-1})	Distance lower limit(Å)	Distance Estimation (Å)	$f'T_{p}^{-1}$(a) (s^{-1})	Distance Estimation (Å)
Adenosine	H_2	69 ± 21	N.D	9.7	11.9 ± 0.6	56 ± 8	6.5 ± 0.5 (d) 5.5 ± 0.8 (e)
	H_8	240 ± 10 (b)	N.D	7.2	9.8 ± 1.0	100 ± 21	4.5 ± 0.5 (d) 3.8 ± 0.6 (e)
	H_1'	78 ± 8	N.D	10.0	11.7 ± 1.2	7 ± 7	6.2 ± 0.6 (d)
	HDO	$(2.69 \pm 0.14)10^6$	$(2.87 \pm 0.32)10^7$	-	2.87 ± 0.05 (c)	$(5.9 \pm 0.3)10^5$	2.87 ± 0.05 (c)
Tubercidine	H_2	61 ± 11 (b)	62 ± 32 (b)	9.7	12.1 ± 1.4	155 ± 10	6.6 ± 0.7 (f)
	H_7	93 ± 19	480 ± 33	8.8	11.4 ± 1.4	17 ± 4	5.8 ± 0.8 (f)
	H_8	96 ± 14	354 ± 32	8.9	11.4 ± 1.3	37 ± 10	5.3 ± 0.5 (f)
	H_1'	62 ± 12	N.D	9.6	12.1 ± 1.4	23 ± 5	5.8 ± 0.6 (f)
	HDO	$(2.51 \pm 0.42)10^6$	$(2.2 \pm 0.24)10^7$	-	2.87 ± 0.05	$(6.4 \pm 0.5)10^5$	2.87 ± 0.03 (c)

(a) Since the real value of f is not known the relaxations are normalized using $f' = (\text{Nucleoside})_{total}/(Mn^{2+})_{total}$.

(b) This term arises from the difference of two rather large contributions and can be subject to large errors.

(c) Hypothesis.

(d) (e) Distances calculated for the ATP-Mn^{2+} complex in [9] and [10] respectively.

(f) Distances calculated for the Tubercidine-triphosphate-Mn^{2+} complex in (11).

N.D. Not determined.

Manganese proton distances as estimated from the relaxation behaviour.

This table presents the paramagnetic contributions to the relaxation rates and the estimated Mn^{2+}-proton distances in the enzyme.methionine.nucleoside.PP-Mn^{2+} complexes. The experiments are performed in the presence of 2 mM nucleoside, 40 µM trypsin-modified methionyl tRNA synthetase, 1 mM methionine and 0 to 40 µM PP-Mn^{2+} in imidazole-DCl buffer (10 mM) at 20°C. The nucleoside.PP-Mn^{2+} complexes are investigated in the same conditions but without enzyme. The contribution of these complexes to the observed rate is estimated from the dissociation constants of PP-Mn^{2+} from the E.AA.Ado (Tub).PP-Mn^{2+} complex which are found to be 20 (15) µM [1]. A lower limit to the proton Mn^{2+} distance is found by minimizing the right term of Eq(4). T_{1pH} and T_{1pHDO} are the observed paramagnetic contributions to the relaxation of the considered proton and of HDO respectively. σ_{1H} and σ_{1HDO} are their standard errors and T_{2p} and σ_2 are the shortest contribution to T_2 observed with its standard errors The lower limit is thus found by the expression :

$$2.82 \left(\frac{T_{1pH} - 2\sigma_{1H} - T_{2p} - 2\sigma_2}{T_{1pHDO} + 2\sigma\ HDO} \times \frac{1}{q} \right)^{1/6}$$

An upper limit of q is taken to be 10 (at least one water molecule exchanged).

It can be noticed that relevant data on tubercidine triphosphate [11] do not show this greater relaxation of the H_2 proton in the presence of Mn^{2+} but show a larger shift of H_2 in the presence of Ni^{2+}. In our case, we cannot estimate metal proton distances in the nucleoside : PP-Mn^{2+} complex since we do not know the (nucleoside) (PP-Mn^{2+})/(nucleoside : PP-Mn^{2+}) equilibrium constant and thus we cannot calculate f . However, this equilibrium constant is well over 10 mM, so that the lower is the adenosine concentration, the lower is the paramagnetic contribution outside the enzyme.

The H_2 proton of the purine ring is the only observed proton for which a significant contribution to the longitudinal relaxation time is observed in the diamagnetic enzyme:nucleoside:methionine complex ($(f\ T_{1d})^{-1} \simeq 20\ s^{-1}$). This contribution might well arise through dipolar relaxation by enzyme protons indicating that the H_2 proton is at, or close to, a specific point of attachment of the purine ring on the protein. This is in agreement with previous data from this laboratory [12] indicating a weak inhibition, or no inhibition at all, of the ATP-PP isotopic exchange by analogs of adenosine modified in the "2" position. In contrast, introduction of bulky groups at the "8" position does not alter the binding of adenosine. This fits well with the fact that no diamagnetic relaxation is observed for the H_8 proton.

No further diamagnetic relaxation of the nucleoside protons were observed in the E.AA.Nucleoside.PP-Mg^{2+} complexes. There is thus good evidence that the observed relaxation of the E.AA.nucleoside.PP-Mn^{2+} complexes arises from the paramagnetic effect of the Mn^{2+} ion and not from diamagnetic effects due to the formation of the E.AA.nucleoside.PP-Mn^{2+} dead end complex.

The relaxation data from Table 1 can be used to attempt to derive Mn^{2+} - proton distances in the E.AA.Ado.PP-Mn^{2+} complex. A lower limit of these distances can be obtained using Eq.4, as illustrated in the legend of Table 1.

$$(4) \quad r_{Mn} - H = r_{Mn} - HDO \left(\frac{T_{1MH}}{T_{1M\ HDO}} \times \frac{1}{q} \right)^{1/6}$$

Equation 4 assumes identical τ_c's for the studied protons and for the water protons . This holds true since τ_c for the water protons is unlikely to be governed by the residence time of the water molecules. For a more precise evaluation of the distances, it is necessary to derive the correlation time τ_c. The rotational correlation time of the enzyme calculated by Stoke's law sets an upper limit of τ_c to 2×10^{-8}s. The highest T_1/T_2 ratio can be used to set a lower limit of τ_c to 6×10^{-9}s. Using these limits introduces only a 9 % incertitude on the distances since they depend on the sixth root of f_1 (τ_c). The estimated distances are presented in Table 1 assuming no contribution of the exchange rate τ_M to T_{1M}. They preclude any direct or indirect interaction of the manganous ion with the purine ring in the active site of methionyl tRNA synthetase. Furthermore the difference between the conformation of the ATP-Mn^{2+} in solution and that of adenosine in the complex cannot be confined

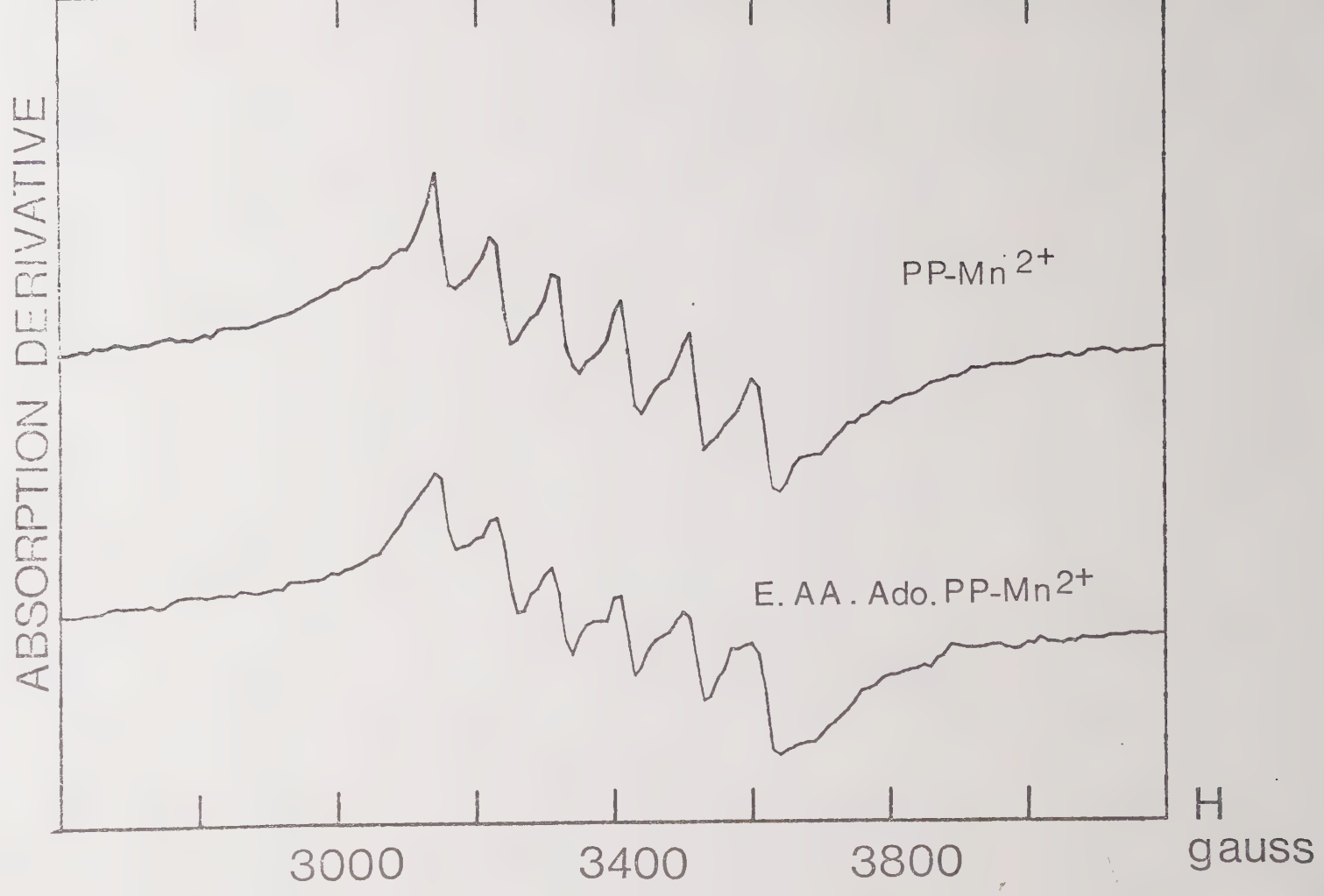

FIGURE 1 : EPR spectrum in the X band of the E.AA.Ado-PP-Mn^{2+} complex.

Top spectrum : 0.2 mM PP plus 0.1 mM Mn^{2+}. Bottom spectrum as top spectrum but in addition 2 mM L-methionine, 10 mM Adenosine and 0.095 mM trypsin-modified methionyl tRNA synthetase. Temperature 25°C . These spectra arise from the digital substraction of the base line from the recorded spectra.

to a mere rotation about the glycosidic bond (i.e. an anti → syn transition). In fact, the Mn^{2+}-proton distances are too long and not precise enough to provide information on the purine conformation about the glycosidic bond.

Proton relaxation enhancement measurements (Joyce and Cohn, Yaniv and Cohn, unpublished but quoted in [13])on tryptophanyl and valyl tRNA synthetases have indicated an enzyme.substrate.metal bridge in the E.ATP-Mn^{2+} complexes. This should also be the case of methionyl tRNA synthetase since there is no strong binding site for the metal and the affinity of ATP-Mn^{2+} for the enzyme is weaker than that of ATP [1]. It was stated in a previous report [1] that further stabilization of the metal ion in the dead-end synergistic complex could originate from the interaction of the metal ion with a single negative charge in the active center of the enzyme. Whether this charge is contributed by the protein itself or by the substrates was not resolved. We tried and approach this problem through the EPR spectra of Mn^{2+} in the dead-end synergistic complexes. Figure 1 compares a situation where 65 % of the Mn^{2+} is under the form of E.AA.ADO.PP-Mn^{2+} complex to the spectrum of PP-Mn^{2+} (unaggregated form : see [1]). In a same fashion, Figure 2 compares the spectrum of the E.methioninol-ATP-Mn^{2+} complex (81 % complex, 19 % ATP-Mn^{2+}) with that of ATP-Mn^{2+}. In both cases, the EPR spectrum of the dead-end synergistic complex is not significantly different from that of free PP-Mn^{2+} or ATP-Mn^{2+}. This indicates little distortions in the symmetry of the manganous ion environment when participating to the complex. However, this does not preclude a metal:protein interaction since spectra resembling those of Mn^{2+} in the dead-end complexes of methionyl tRNA synthetase have been reported for binary complexes of Mn^{2+} with strong metal binding enzymes [14].

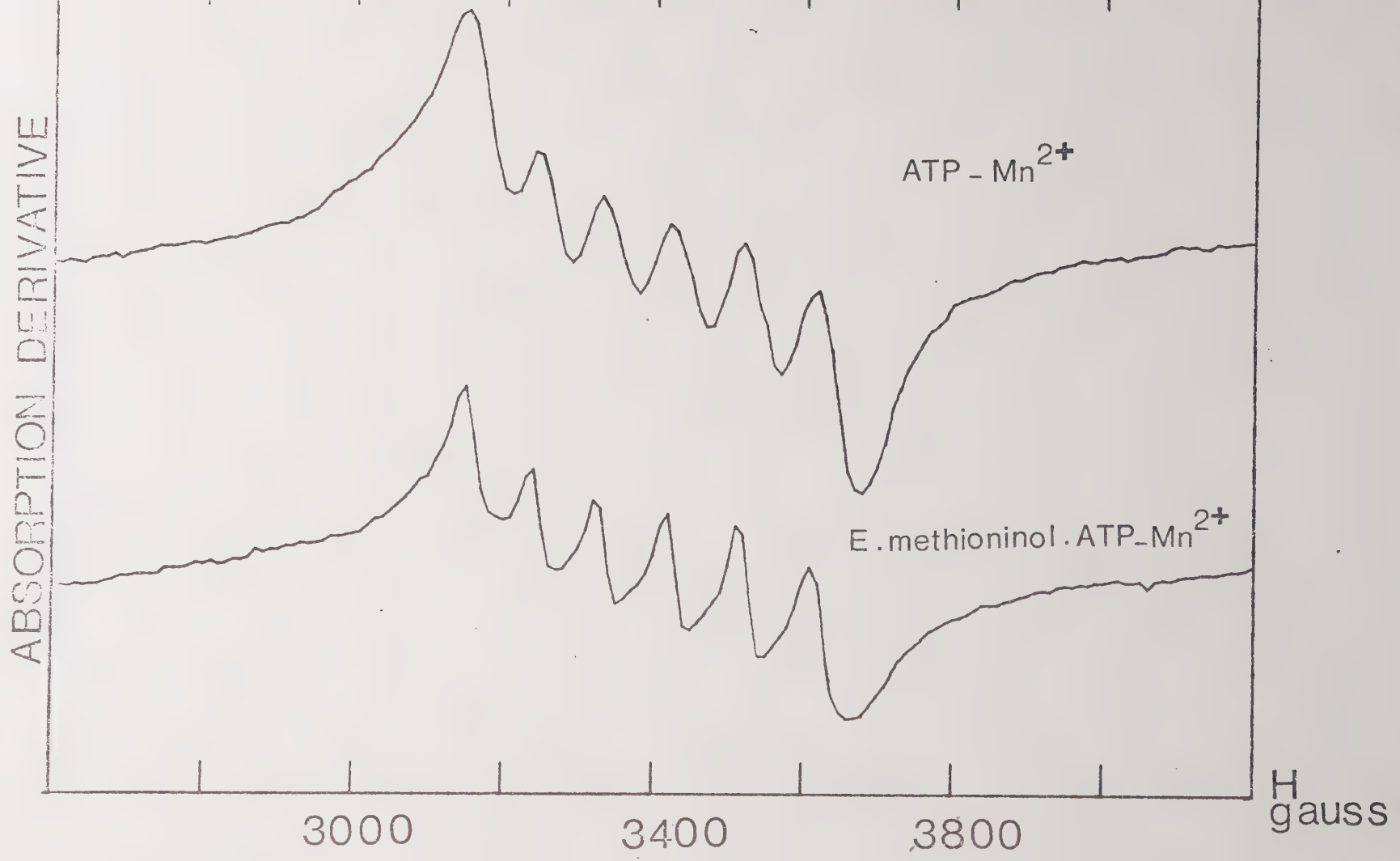

FIGURE 2 : EPR sepctrum of the X band of the E.methioninol.ATP-Mn^{2+} complex.

Top spectrum : 0.25 mM ATP plus 0.1 mM Mn^{2+}. Bottom spectrum 0.15 mM ATP plus 0.1 mM Mn^{2+} and in addition 2 mM L-methioninol and 0.095 mM trypsin-modified methionyl tRNA synthetase. Same conditions as Figure 1.

DISCUSSION

Szent-Györgyi proposed on intuitive grounds [15,16] that a metal ion could interact with both the triphosphate moiety and the purine ring of adenosine in the ATP-Me^{2+} complex. Such a situation would permit charge transfers between the energy rich phosphate bonds and the purine ring, facilitating the cleavage of the phosphate bonds. Since that time, NMR has permitted to measure distances in the ATP-Mn^{2+} complex [9,10,17] and to propose models of interaction between the metal ion and the purine ring of ATP [11]. It may be relevant to note that NMR measurements allow the determination of average distances (actually of the average of r^6) and thus cannot provide meaningful results if the molecule exists in more than one conformation. For instance, a measured distance of 4 Å between the Mn^{2+} ion and the H_8 proton of adenosine can be interpreted in terms of water bridging between the N_7 and the Mn^{2+} ion [11]. It could equally well mean that Mn^{2+} interacts directly ($dM_n - H_8 = 3$ Å) with the N_7 during 15 % of the time and does not interact at all with the purine during the remaining time.

The conformation of enzyme-bound nucleotides has been determined through NMR techniques in a few cases [10, 18]. These investigations were performed on enzymes with strong metal binding sites, since the paramagnetic contribution outside the enzyme can be easily eliminated. The derived distances fail to show any direct or indirect interaction between Mn^{2+} and the purine ring. This result can be understood since the loss in energy in taking the purine apart from the metal can be paid for by the high free energy of the metal-enzyme interaction.

Methionyl tRNA synthetase is, to our knowledge, the first enzyme without strong metal binding site for which information can be gained regarding the conformation of the enzyme-bound nucleotide. This was possible on two grounds : (1) by "splitting" the ATP-Mn^{2+} molecule into adenosine plus PP-Mn^{2+} in order to minimize the relaxation outside the enzyme and (2) by using synergism in order to increase the proportion of enzyme:complex-bound manganese. Our results show that, despite ATP-Me^{2+} being the true substrate of the activation reaction, no metal-purine interaction occurs in the active site of methionyl tRNA synthetase. It remains to be seen whether the absence of interaction between metal ions and the purine ring can be generalized to the other enzymes using ATP-Me^{2+} as a substrate. This would suggest that the purine metal interaction stabilizes weakly, if at all, the ATP-Me^{2+} molecule.

REFERENCES

(1) HYAFIL F. and BLANQUET S. Submitted for publication.

(2) BLANQUET S., FAYAT G. and WALLER J.P. (1975). J. Mol. Biol. 94, 1-15.

(3) FAYAT G., FROMANT M. and BLANQUET S. Submitted for publication.

(4) HYAFIL F., JACQUES Y., FAYAT G., FROMANT M. DESSEN P. and BLANQUET S. (1976). Biochemistry 15, 3678-3685.

(5) CASSIO D. and WALLER J.P. (1971). FEBS Letters 12, 309-312.

(6) CASSIO D. and WALLER J.P. (1971). Eur. J. Biochem. 20, 283-300.

(7) BERNASSAU J.M. and HYAFIL F. Submitted for publication.

(8) DWEK R.A. (1973). Nuclear Magnetic Resonance in Biochemistry Clarendon Press - Oxford.

(9) STERNLICHT H., JONES D.E. and KUSTIN (1968). J. Am . Chem. Soc. 90, 7110.

(10) SLOAN D.L. and MILDVAN A.S. (1976). J. Biol. Chem. 251, 2412-2420.

(11) GLASSMANN T.A., COOPER C., HARRISON L.W. and SWIFT T.J. (1971) Biochemistry 10, 843-851.

(12) LAWRENCE F., SHIRE D.J. and WALLER J.P. (1974). Eur. J. Biochem., 41, 73-81.

(13) MILDVAN A.S. (1970). In the Enzymes (Vol.II) Third Edition (P.D. Boyer ed.) Academic Press New-York-London, pp. 445-536.

(14) REED G.H. and COHN M. (1973). J. Biol. Chem. 248, 6436-6442.

(15) SZENT GYÖRGYI A. (1957). Bioenergetics Academic Press N.Y. pp. 64-73.

(16) SZENT GYÖRGYI A. (1960). Introduction to a Submolecular Biology Academic Press (New-York and London) pp. 115-121.

(17) BROWN F.F., CAMPBELL I.D., HENSON R., HIRST C.W.J. and RICHARDS R.E. (1973). Eur. J. Biochem. 38, 54-58.

(18) SLOAN D.L., LOEB A.L., MILDVAN A.S. and FELDMANN R.J. (1975). J. Biol. Chem. 250, 8913-8920.

ANNEXE

INTRODUCTION A L'ARTICLE 4

Cette annexe traite d'un problème rencontré lors de la mesure simultanée de plusieurs temps de relaxation longitudinaux dans un spectromètre à transformée de Fourier. La méthode la plus courante consiste en la séquence 180° - τ - 90° dite Inversion - Recovery. Elle est illustrée dans la Figure 1.

La magnétisation longitudinale M_o $(1 - 2_{exp}(\tau/T_1)$ est projetée par l'impulsion de 90° dans le plan xOy. L'observation de la magnétisation dans le plan xOy pour différentes valeurs de τ permet de mesurer T_1. Le but de notre étude est d'optimiser les valeurs de τ pour mesurer T_1 avec le maximum précision en un minimum de temps. Une méthode de simulation du problème grâce à un générateur aléatoire gaussien de bruit ne permet pas d'obtenir de solution en un temps raisonnable de calcul sur IBM 370/168. Nous sommes donc conduits à chercher une fonction mathématique approximant l'erreur statistique moyenne commise dans une expérience donnée. La minimisation de cette fonction permet de décrire les conditions optimales pour la mesure simultanée de tous les T_1 compris dans une gamme donnée.

FIGURE 1

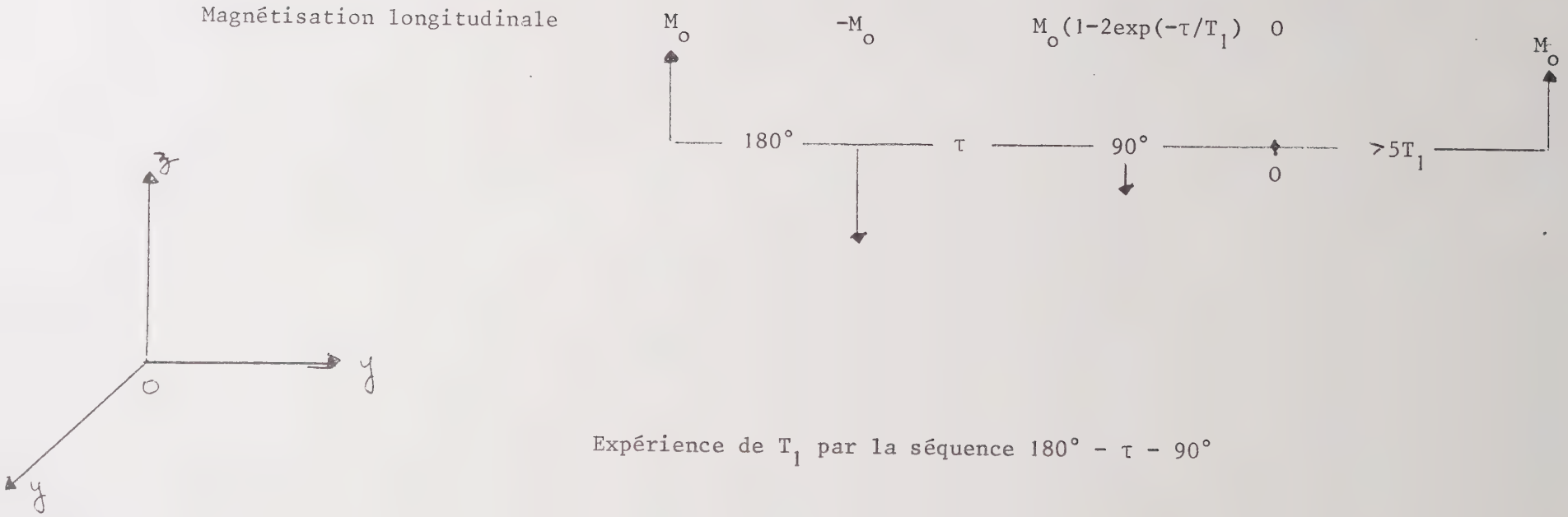

Expérience de T_1 par la séquence 180° - τ - 90°

ARTICLE 4

Choice of the τ sequence in T1 measurements by Inversion Recovery.

Jean-Marie BERNASSAU* and François HYAFIL** [a]

Laboratoire de Synthèse Organique (*) and Laboratoire de Biochimie (**), Ecole Polytechnique - 91120 PALAISEAU (France).

[a] Present address : The Biological Laboratories - Harvard University 16 Divinity Avenue - Cambridge - Mass. 02138-- U.S.A.

SUMMARY

In this study, we optimize the values of τ, the delay between the 180° and the 90° pulse in an inversion recovery experiment, to get as much precision as possible on the determination of longitudinal relaxation times in a given time of experiment. A function of the τ_i's is constructed, approximating at first order the variance of the relative error on T_1. This function is shown to be close agreement with that derived by a simulation of the problem through a random generator of gaussian noise. The function is then minimized in the case of the measurement of a single T_1 value or of a set of T_1 values for which limits are set up. In peculiar it is discussed whether one or more experiments are needed for measurements of relaxation times in a wide range of values. The whole set of results is summarized in Figure 7 which can be used as a "recipe" for the design of T_1 experiments.

INTRODUCTION

Fourier Transform NMR spectroscopy allows the simultaneous determination of Spin lattice (T_1) relaxation times of different lines of an NMR spectrum. Choice of a specific pulse sequence (Inversion Recovery, Saturation Recovery, etc...) and critical factors for the accuracy of a T_1 determination have been recently discussed by Levy and Peat (1). The Inversion Recovery ($180° - \tau - 90°$) method is the less sensitive to external factors and is the one usually available on commercial spectrometers. In this paper we design optimal sets of τ values for measuring T_1's by the Inversion Recovery method.

Choice of the Regression Method.

Assuming an exponential relaxation, the variation of the longitudinal magnetization after a 180° pulse is ruled by :

$$m = m_\infty (1-2e^{-\lambda\tau}) \qquad [1]$$

If the 180° pulse is not perfect, or the recurrence rate too fast, [1] becomes :

$$m = m_\infty (1-ae^{-\lambda\tau}) \qquad [2]$$

where a may differ from 2. In the absence of noise, the observed

signal s would obey the same relation :

$$s = s_\infty (1-ae^{-\lambda\tau}) \qquad [3]$$

we can rewrite [3]

$$s = \mu + \nu e^{-\lambda\tau} \qquad [4]$$

where $\mu = s_\infty$ and $\nu = -2a\ s_\infty$.

Most calculations of T_1 values are based on semilogarithmic plots of $s_\infty - s$ versus τ. This method is extremely sensitive to the accuracy of the s_∞ value. Therefore, it is better to treat λ, μ and ν as parameters on the same footing and to determine them together by optimizing the fit of the experimental data to the theoretical curve [4], for instance using a three-parameters least square regression. As show below, the three parameters least squares fit allows accurate determination of T_1's even with rather poor signal/noise ratios. Similar conditions would not allow the use of semilogarithmic plots unless tedious measurement of a precise s_∞ value is achieved.

In the following analysis we assume perfect exponential behaviour of the magnetization. Such is the case of most T_1 measurements in organic chemistry. It may be noticed that errors in the pulse width corresponding to a 180° flip do not affect the exponential character of the relaxation (1). Various computing programs have been devised (2-4) for the least square fit. We have written fortran and basic versions of a fast (vide infra) least square fit method which are available upon request.

Measurement of a the T_1 of a single peak.

In the following we will assume that all the experimental uncertainties on s can be represented by gaussian noise of standard deviation σ.The conventional peak to peak noise can be estimated to 4 σ. It is important that the accumulation of spectra with different τ values should be performed in a random order and not, for example, in the order of increasing τ values.In these conditions,the effects of systematic errors arising from drifts in temperature, spectrometer sensitivity, homogeneity etc... will be minimized. The following sections will apply only if systematic errors remains small compared to the electronic noise. σ is then proportionnal to $N^{-1/2}$ if N is the number of transients.

Therefore, we shall consider the experimental trace as sum of a signal which varies according to Eq[4] with unknown parameters λ, μ, ν to which is added a gaussian noise, whose standard deviation σ is proportionnal to $N^{-1/2}$.

We first simulated the experimental situation by adding to s given by Eq [2] , with known s_∞ and λ, a random gaussian noise. The rate constant λ_1 derived from these curves by regression analysis is then compared to λ. By making several trials with the

same set of values and different noise samples, all with the same standard deviation σ, we obtain a distribution of λ_1's. When the number of trials increases undefinitely we verified that the average of λ_1 is λ. The root mean square, R, of $(\lambda_1-\lambda)/\lambda$ can then be thought as a good measurement of the accuracy of the experiment. Thus a way of comparing two different sets of τ values is to compare the R values obtained for each of them. In order to compare R values for different noises and different numbers of experimental points, we will normalize R to

$$F = \frac{R}{\sigma \left(\frac{\sum_i (\tau_i + w)}{w} \right)^{1/2}} \qquad [4]$$

where the τ_i's are the pulse intervals and w the waiting time is set to $5/\lambda$ Eq.|4| takes into account the fact that the S/N ratio varies as the square root of the number of transients and that $\sum_i (\tau_i + w)$ is the total time of the experiment. F is thus a function of σ and of the τ_i's and our goal is to find for a given value of σ the set of τ_i's which renders F minimal. A problem in this method is that an accurate estimate of F requires a great number of trials. This is illustrated in Fig.1 where the averages and the root mean squares of five determinations of F are plotted against the number of trials, n. In fact the convergence of F towards its limit is achieved as $n^{-1/2}$. Even with a fast computer program (10.000 trials on 10 experimental points in one minute of C.P.U.) the use of a standard minimization procedure to find the minimum of F would take too much computer time. We are

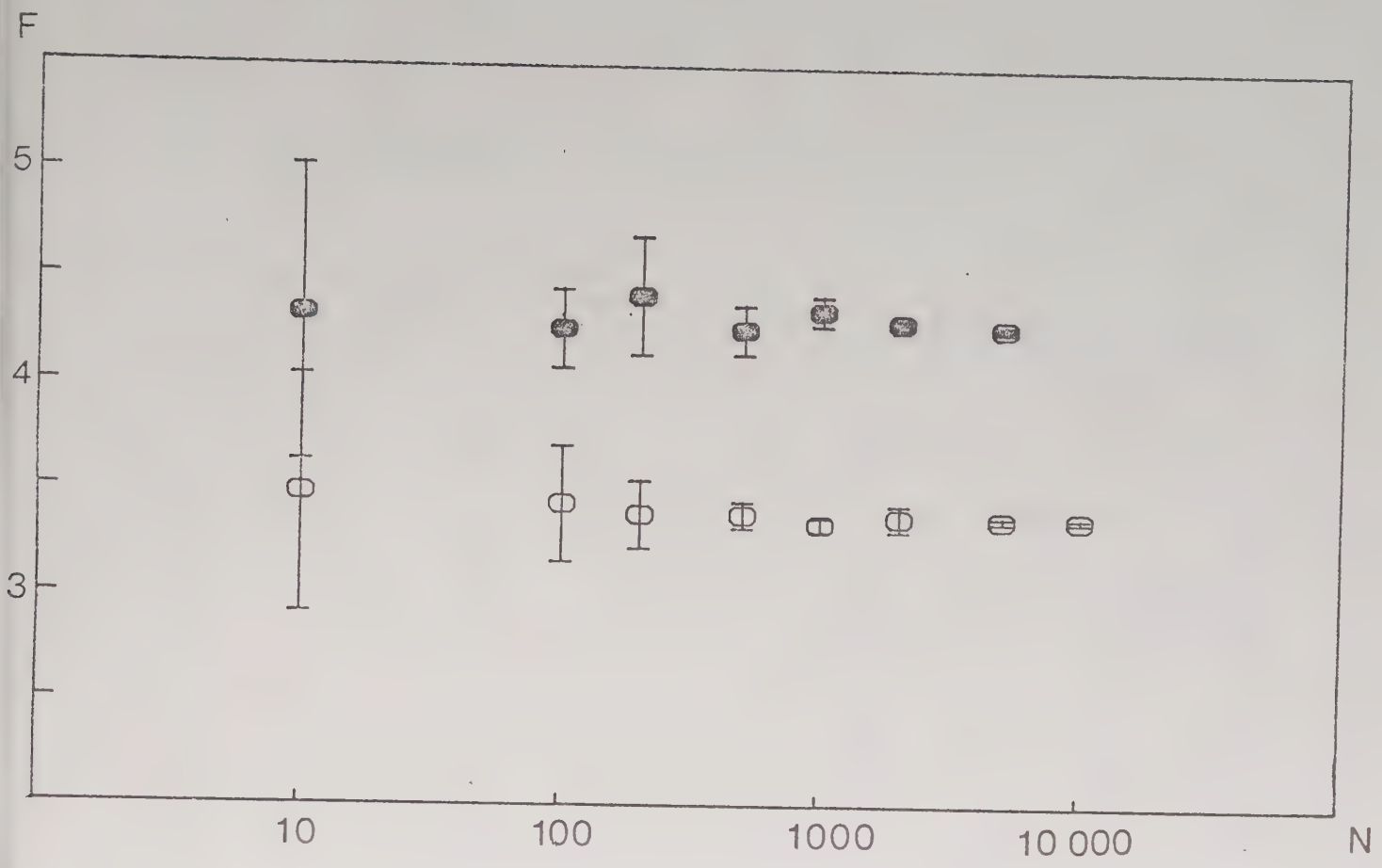

Fig. 1 : Influence of the number of experiments on the simulated value of F.

This figure represents the average and the standard deviation of 5 determinations of F by the simulation described in the text as the number of experiments increases from 10 to 10.000. White points refers to the best solution obtained by minimization, black points to a cut of the τ axis in 10 values corresponding to equal segments in the s axis. For both sets $\sigma = 0.005$.

therefore led to develop a mathematical approximation of our function F.

Variance analysis.

In one of the above trials, λ, μ and ν are the parameters of the theoretical curve. If we add a gaussian noise, least squares fit will provide simulated values λ_1, μ_1 and ν_1. We can then define $\bar{\lambda}$, $\bar{\mu}$, $\bar{\nu}$ the relative errors on λ, μ and ν by :

$$\begin{aligned} \lambda_1 &= \lambda\ (1 + \bar{\lambda}) \\ \mu_1 &= \mu\ (1 + \bar{\mu}) \\ \nu_1 &= \nu\ (1 + \bar{\nu}) \\ s_i &= g(\tau_i) + \bar{s} = \mu + \nu e^{-\lambda\tau_i} + \bar{s} \end{aligned} \qquad [5]$$

s_i is the value of the signal at the point τ_i (Fig. 2).

The least square method determines $\bar{\lambda}$, $\bar{\mu}$, $\bar{\nu}$ such [6] is minimum

$$\sum_i [s_i - g(\tau_i)]^2 \text{ where } g(\tau_i) = \mu + \nu e^{-\lambda\tau_i} \qquad [6]$$

Each term of [6] can be developped at first order

$$s_i - g(\tau_i) = s_i + \bar{s}_i - [\mu(1 + \bar{\mu}) + \nu(1 + \bar{\nu})\ e^{-\lambda(1+\bar{\lambda})\tau_i}]$$

$$= s_i \ldots - \nu\nu e^{-\lambda\tau_i} + \nu\lambda\bar{\lambda}\tau_i e^{-\lambda\tau} \qquad [7]$$

so that [6] becomes

$$\sum_i (\bar{s}_i - \mu\bar{\mu} - \nu\bar{\nu}e^{-\lambda\tau_i} + \nu\lambda\bar{\lambda}e^{-\lambda\tau_i})^2 \text{ minimum} \qquad [8]$$

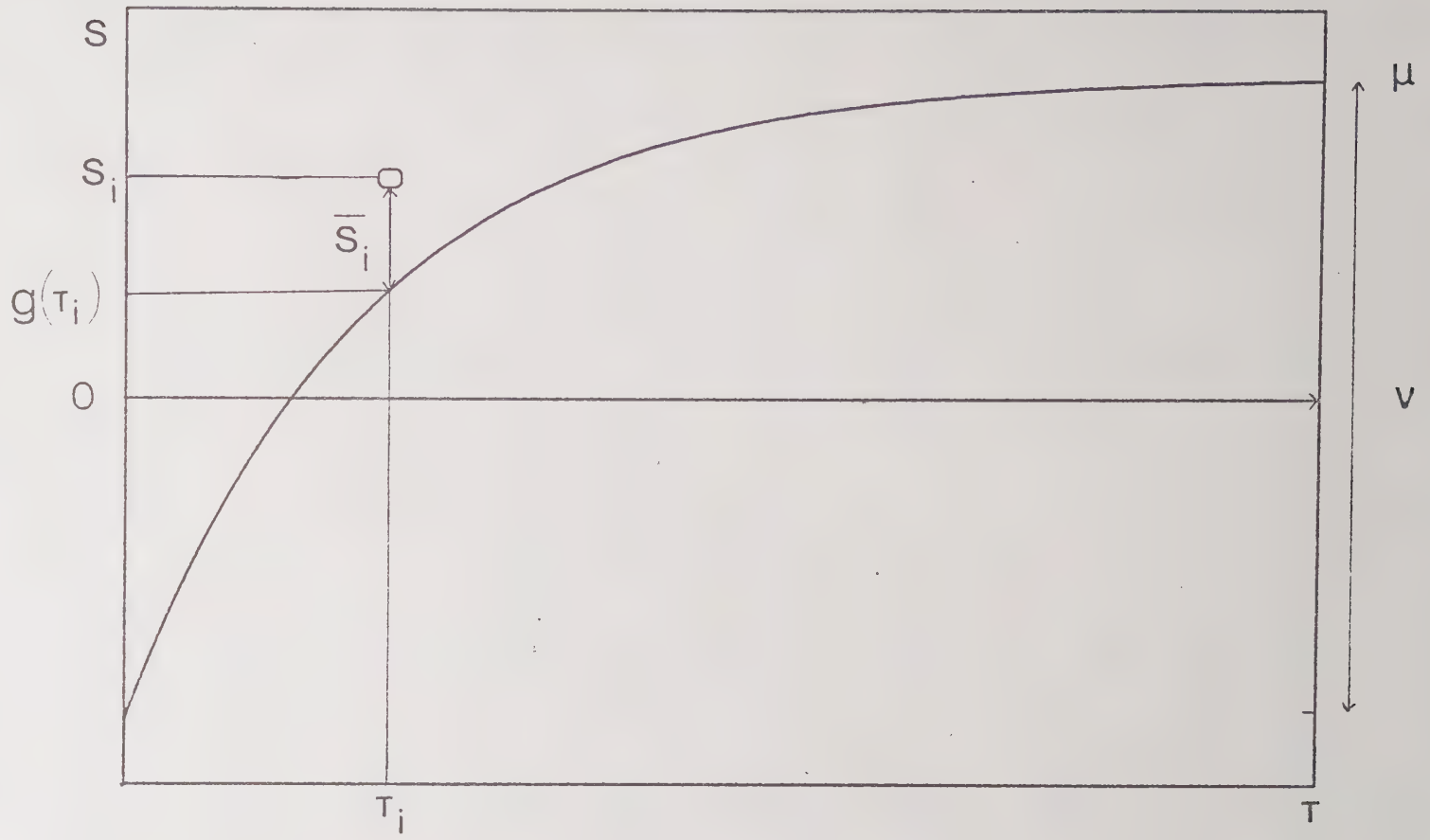

Fig. 2 : Illustration of the notations of the text.

$g(\tau_i)$ is the value of $g(\tau) = \mu + \nu e^{-\lambda\tau}$ for $\tau = \tau_i$. s_i is the observed signal and $\bar{s}_i$ difference between $g(\tau_i)$ and S_i.

[8] can be solved by equaling its partial derivatives to zero.

$$\left.\begin{array}{ll} \frac{\partial}{\partial\bar{\lambda}} & \sum_i (\bar{s}_i - \mu\bar{\mu} - \nu\bar{\nu}e^{-\lambda\tau_i} + \nu\lambda\bar{\lambda}e^{-\lambda\tau_i})\ \nu\lambda\tau_i e^{-\lambda\tau_i} = o \\ \frac{\partial}{\partial\bar{\mu}} & \sum_i (\bar{s}_i - \mu\bar{\mu} - \nu\bar{\nu}e^{-\lambda\tau_i} + \nu\lambda\bar{\lambda}e^{-\lambda\tau_i})\ \mu = o \\ \frac{\partial}{\partial\bar{\nu}} & \sum_i (\bar{s}_i - \mu\bar{\mu} - \nu\bar{\nu}e^{-\lambda\tau_i} + \nu\lambda\bar{\lambda}\tau_i e^{-\lambda\tau_i})\nu e^{-\lambda\tau_i} = o \end{array}\right\} \quad [9]$$

Leading to the linear system

$$(-\lambda^2\nu^2\textstyle\sum_i\tau_i^2 e^{-2\lambda\tau_i})\bar{\lambda} + (\lambda\mu\nu\sum_i\tau_i e^{-\lambda\tau_i})\bar{\mu} + (\lambda\nu^2\sum_i\tau_i e^{-\lambda\tau_i})\bar{\nu} = \lambda\nu\sum_i\tau_i e^{-\lambda\tau_i}\ \bar{s}_i$$

$$(-\lambda\mu\nu\textstyle\sum_i\tau_i e^{-\lambda\tau_i})\ \bar{\lambda} + (\mu^2\sum_i 1)\ \bar{\mu} + (\mu\nu\sum_i e^{-\lambda\tau_i})\ \bar{\nu} = \mu\sum_i \bar{s}_i \quad [10]$$

$$(-\lambda\nu^2\textstyle\sum_i\tau_i e^{-2\lambda\tau_i})\ \bar{\lambda} + (\mu\nu\sum_i e^{-\lambda\tau_i})\ \bar{\mu} + (\nu^2\sum_i e^{-\lambda\tau_i})\ \bar{\nu} = \nu\sum_i e^{-\lambda\tau_i}\ \bar{s}_i$$

Using the matricial notation [10] becomes

$$[\alpha_{jk}]\ \begin{bmatrix}\bar{\lambda}\\ \bar{\mu}\\ \bar{\nu}\end{bmatrix} = [b_j] \quad [11]$$

[11] can be solved as

$$\begin{bmatrix}\bar{\lambda}\\ \bar{\mu}\\ \bar{\nu}\end{bmatrix} = [a_{jk}][b_j] \text{ where } [a_{jk}] = [\alpha_{jk}]^{-1} \quad |12|$$

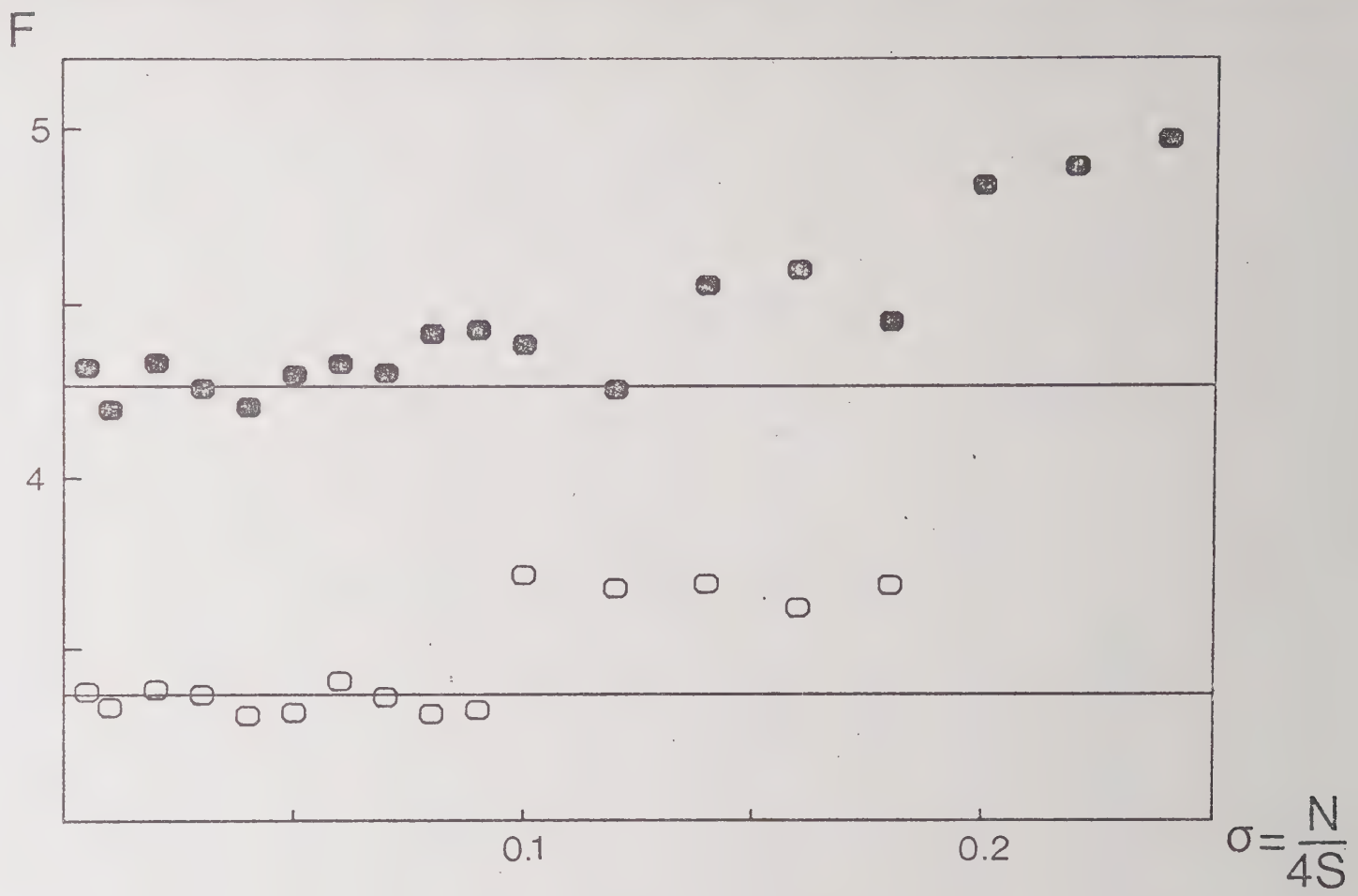

Fig. 3 : Comparison of the simulated and calculated values of F. The simulated values have been calculated using 1.000 experiments. White (respect. black) points refer to the best (respect. equal segments in the s axis) set of τ_i's. Continuous lines are the calculated values of F for these sets.

The above defined function R can thus be approximated at first order by the square root of the average value of ρ^2, the element corresponding to λ in the covariance matrix. The covariance matrix is :

$$[a_{jk}]\ [b_j]\ {}^t[b_j]\ {}^t[a_{jk}] \qquad [13]$$

so that ρ^2, its first line and first row element, can be expressed as :

$$\rho^2 = (a_{11}\ b_1 + a_{12}\ b_2 + a_{13}\ b_3)^2 \qquad [14]$$

Replacing b_i by their values and noting that

$$\langle \bar{s}_i^{\,2} \rangle = \sigma^2$$
$$\langle \bar{s}_i \bar{s}_j \rangle = 0 \qquad [15]$$

where < > means average value. We get

$$\langle \rho^2 \rangle = \sigma^2 \left[\tfrac{1}{2}\, a_{11}^2\ \alpha_{11} + a_{12}^2\ \alpha_{22} + a_{13}^2\ \alpha_{33} + a_{11}\ a_{12}\ \alpha_{21} + a_{11}\ a_{13}\ \alpha_{31} + 2a_{12}\ a_{13}\ \alpha_{32} \right] \qquad [16]$$
$$= \sigma^2\ f^2$$

Thus , to first order, F is given by

$$F = f/(\Sigma\ (\tau_i + w)/w)^{1/2} \qquad [17]$$

It may be relevant to note that F, the error on T_1 divided by the noise, depends only on the τ_i's and not on the value of the noise. Fig. 3 illustrates this result and compares the calculated value of F with that obtained by simulation. For reasonable noise

($N/S < 0.4$), the calculated and simulated values are in good agreement. Differences appear at larger noise values, for which the first order approximation breaks down. In the following section we shall minimize F in the space of the τ_i's.

Best set of τ values for the measurement of a T1.

We will discuss the case of the measurement of a single T_1 value with a waiting time of 5 T_1. Data in this section refers to T_1 = 1 sec. The solution for any value can be derived by a simple multiplication. We have used the Fletcher Powell (5) algorithm to minimize locally the function F in the field of the τ_i's with $\lambda = 1$. In order to make sure and find the absolute minimum on the whole space we have taken as starting points all the sets of τ_i's formed by taking for each i the values τ_i = 0.01, 0.5, 1,5.

We have also tried several intuitive and systematic starting points but they always lead to worse or equivalent solutions.

Penalizations are added to F in order to avoid solutions with no physical significance (e.g. negative τ values). Calculations are performed on sets of n τ_i's (n = 3 to 10, 12, 15, 20). For 20 τ_i's the computation takes ca.2 hours on an IBM 370/168. Pertaining data are presented in Table 1. It appears that in all cases only three different values of τ_i are necessary and that the best solution is obtained for n = 9. However the improvement over the n = 4 solution is neglectible.

More remarkable is the fact that the solutions for n = 8, 12, 20 are the two-, three-, and fivefold repetitions of the n = 4 solution.

Table 1

Number of τ values	Values of τ and N Times			Value of F
3	0.01	0.925	5.912	3.648
4	0.01	0.902 (x2)	6.198	3.366
5	0.01	0.888 (x3)	6.427	3.385
6	0.01 (x2)	0.812 (x3)	6.55	3.419
7	0.01 (x2)	0.912 (x3)	6.06 (x2)	3.434
8	0.01 (x2)	0.902 (x4)	6.198 (x2)	3.366
9	0.01 (x2)	0.894 (x5)	6.318 (x2)	3.360
10	0.01 (x3)	0.849 (x5)	6.38 (x2)	3.377
12	0.01 (x3)	0.902 (x6)	6.198 (x3)	3.366
15	0.01 (x3)	0.858 (x8)	6.390 (x4)	3.366
20	0.01 (x5)	0.902 (x10)	6.198 (x5)	3.366

Measurement of a single T_1.

This table shows the τ values to be used in the measurement of a T_1 of 1 with a waiting time of 5. The values in parenthesis indicate the number of times a particular value of τ is to be used.

Measurement of all T_1s in a given range.

The previously discussed case has indeed little practical significance since one is seldom concerned with the measurement of a single T_1. Moreover the exact value is obviously not known before the experiment.

A true experiment deals with the simultaneous measurement of several T_1's. A reasonable assumption for the following is that theoretical considerations and /or preliminary experiments have provided limits for the T_1 values. A straightforward criterion for a τ_i sequence would be the average value of F over the given T_1 range. The maximum value of F in the range provides a better criterion, however, since it gives a limit on the maximum error. Therefore we have minimized the maximum of F over various ranges of T_1's. The maximum of F over the range is obtained by computing F at 25 points (logarithmically spread) and by refining its value in the vicinity of the so-found maximum, by the golden section algorithm.

The maximum of F is then minimized by the Fletcher Powell program. For each range and each number of τ_i's about fifty starting sets of τ_i's were tried (each minimization requires from 10^4 to 10^5 computations of F). Table 2 shows the computed values of the "minimax" of F for ranges varying from T_1 max/T_1 min = 2 to 50. τ_i values corresponding to the "best" sets are compiled in Table 3. It appears that it is never necessary to use more that 7 τ_i's even for wide ranges of T_1's.

For comparison the minimization was performed using the average criterion for typical ranges of T_1's. The "minimax" and "average" best solutions are illustrated in Fig. 4 along with

Table 2

Number of τ_i's \ T1 Max	2	2.76	3.81	5.25	7.25	10	13.8	19.04	20.27	36.24	50
4	* 3.51	3.78	3.90	3.95	4.05	4.18	4.36	4.57	4.83	5.14	5.46
5	3.55	* 3.75	3.87	3.93	3.99	4.03	4.08	4.14	4.24	4.35	4.46
6	3.65	3.82	* 3.85	* 3.90	* 3.96	* 4.03	* 4.09	* 4.15	* 4.18	4.28	4.30
7	3.79	3.90	3.93	3.97	4.01	4.06	4.15	4.17	4.18	* 4.22	* 4.26
8	3.68	3.83	3.87	3.92	3.98	4.06	4.15	4.25	4.24	4.31	4.34
9	3.79	3.90	3.92	3.97	4.01	4.06	4.17	4.17	4.23	4.27	4.36
10	3.55	3.76	3.82	3.88	3.98	4.05	4.18	4.17	4.24	4.32	4.39

F values for the measurement of a range of T_1's.

Comparison of different numbers of τ values.

* Solution developped in Table 3.

Table 3

T1 Max	τ_1	τ_2	τ_3	τ_4	τ_5	τ_6	τ_7	F
2	0.01	1.35	1.35	10.7	-	-	-	3.51
2.76	0.01	1.19	1.36	2.90	16.3	-	-	3.75
3.81	0.01	1.22	1.32	3.42	3.54	21.9	-	3.85
5.25	0.01	1.24	1.78	4.11	5.02	29.7	-	3.90
7.25	0.01	1.21	2.14	4.74	6.71	41.3	-	3.96
10	0.01	1.05	2.56	5.50	9.43	55.3	-	4.03
13.8	0.01	1.02	2.93	6.92	12.86	71.9	-	4.09
19.04	0.01	1.05	3.50	9.11	17.6	91.4	-	4.15
26.27	0.01	1.16	4.36	11.9	22.6	124	-	4.18
36.24	0.01	0.94	2.59	7.79	17	35.1	203	4.22
50	0.01	1.05	3.05	9.87	22.9	44.1	254	4.26

τ values for the measurement of a range of T_1's.

This table gives the τ value for the best solutions of Table 2 (*).

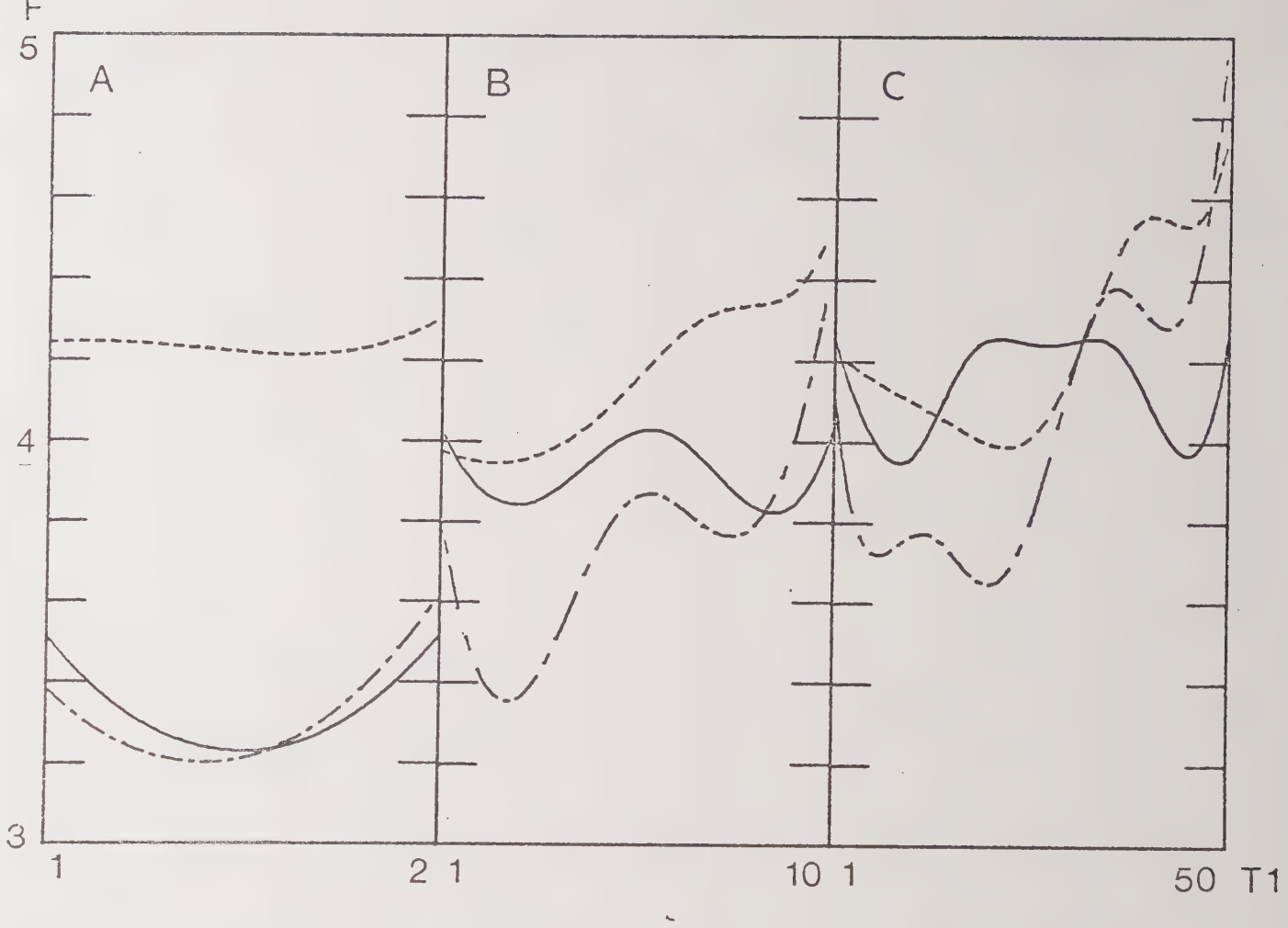

Fig. 4 : Comparison of minimisation methods.

This figure shows the variation of F as a function of the T1 value for T1 ranging from 1 to 2 (panel A) 1 to 10 (panel B) 1 to 50 (panel C).The represented curves are either the "minimax" solution for the corresponding range (continuous line), the "average" solution (-·-·-) and an "intuitive" set of τ_i's (- - -).

τ_i Values

Panel	Method *	τ_i values												
A	av	0.01	1.272	1.272	9.96	-	-	-	-	-	-	-	-	-
	int	0.01	0.25	0.5	1	1.5	2.3	3.5	5	7.5	12	50	-	-
B	av	0.01	0.01	1.728	1.728	1.728	1.728	6 455	6.455	6.455	43	43	-	-
	int	0.01	0.25	0.5	1	1.7	3	5	8	12	20	32	50	250
C	av	0.01	1.64	1.64	4.69	5.94	9.23	20.95	36.37	212	-	-	-	-
	int	0.01	0.2	0.4	0.7	1	1.5	2	2.8	10	-	-	-	-

* av = result of the minimization with the "average criterion

int = intuitive solution.

an "intuitive" set of τ values. It appears clearly that the mini-max algorithm gives uniform error over the range while the "average" can lead to high errors in parts of the range.

The question may be raised whether broad ranges of T_1 should be measured in one or two experiments. In a single experiment, where T_1's are to be measured from 1 to $\alpha 1$, the time necessary to achieve a given precision is proportional to

$$\Phi_1 (\alpha_1) = F^2 (\alpha_1) \times \alpha_1 \qquad [18]$$

If the same range of T_1's is measured using two experiments from 1 to α_o and from α_o to α. The total time is now proportional to

$$\Phi_2 (\alpha_o, \alpha_1) = F^2 (\alpha_o)\alpha_o + F^2 (\alpha_1/\alpha_o)\alpha_1 \qquad [19]$$

In order to compare these two expressions, we have approximated $F(\alpha_1)$ by an explicit function as shown in Fig. 5. We have then compared Φ_1 to Φ_2 for α_1 = 1 to 100 and α_o = 1 to α_1 . Fig 6 shows the points for which two experiments should be preferred. The time saved using two experiments is always small compared to the total time of the measurement (Fig.6).

Finally, it could be helpful to give an example of the use of Table 3 to show how to design a T1 experiment. Suppose a set of nuclei with T1's lying in the range from 1 to α. NT transients (90°) give a N/S ratio of 4σ. If we desire a precision p on the T1's of all the nuclei , the total time TT for the experiment can be deduced by

$$TT = NT \times \left(\frac{2F\alpha}{p}\right)^2 \times w \qquad [20]$$

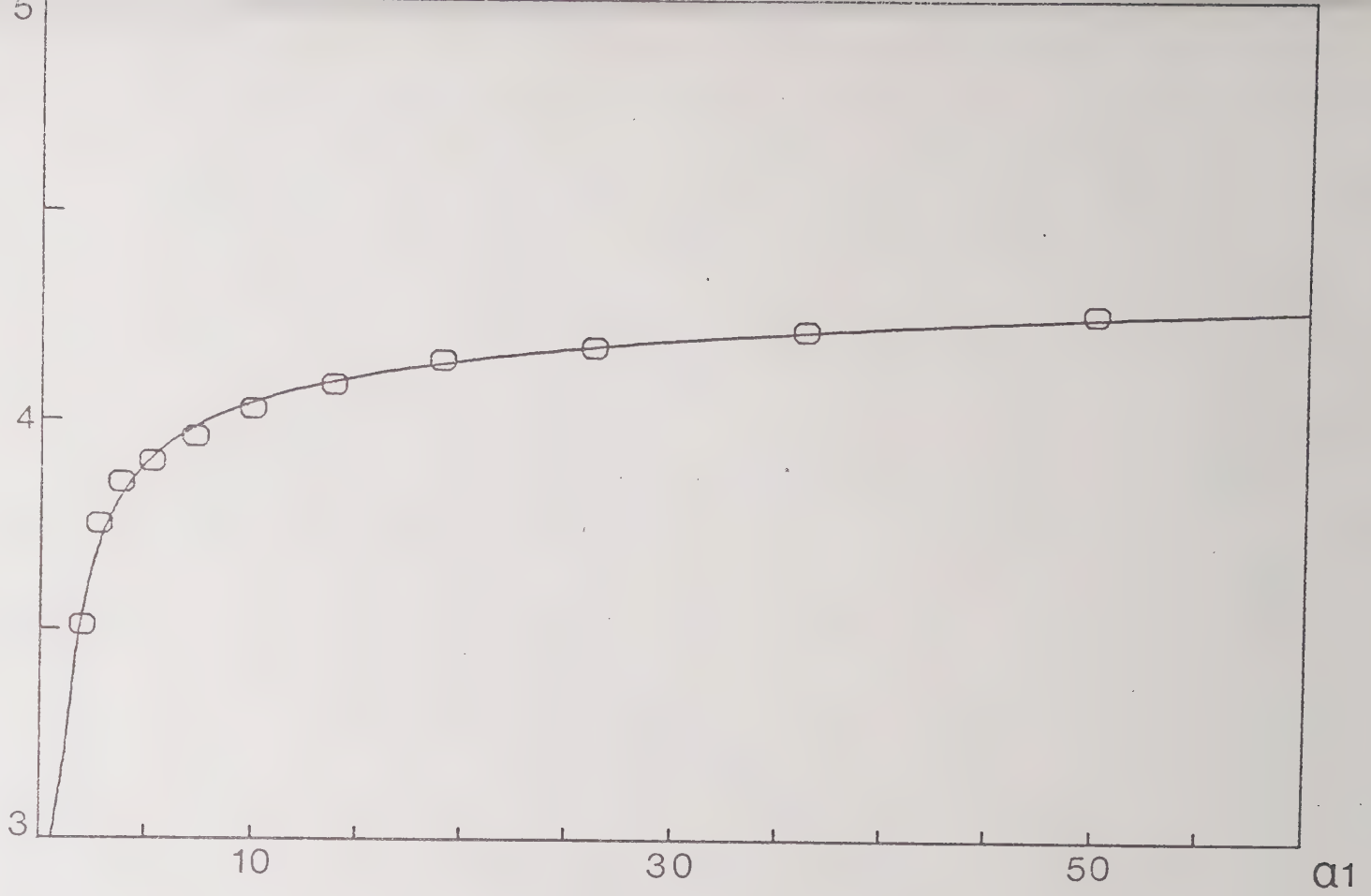

Fig. 5 : Best values of F.

The lowest values of Table 2 are plotted against α_1 the upper limit of the T1 range. The continuous line shows an explicit function approximating F : $F = 3.949 - 0.916/\alpha_1 + 0.082 \text{ Ln } (\alpha_1)$ where

$$\alpha_1 = \frac{T_1 max}{T_1 min}$$

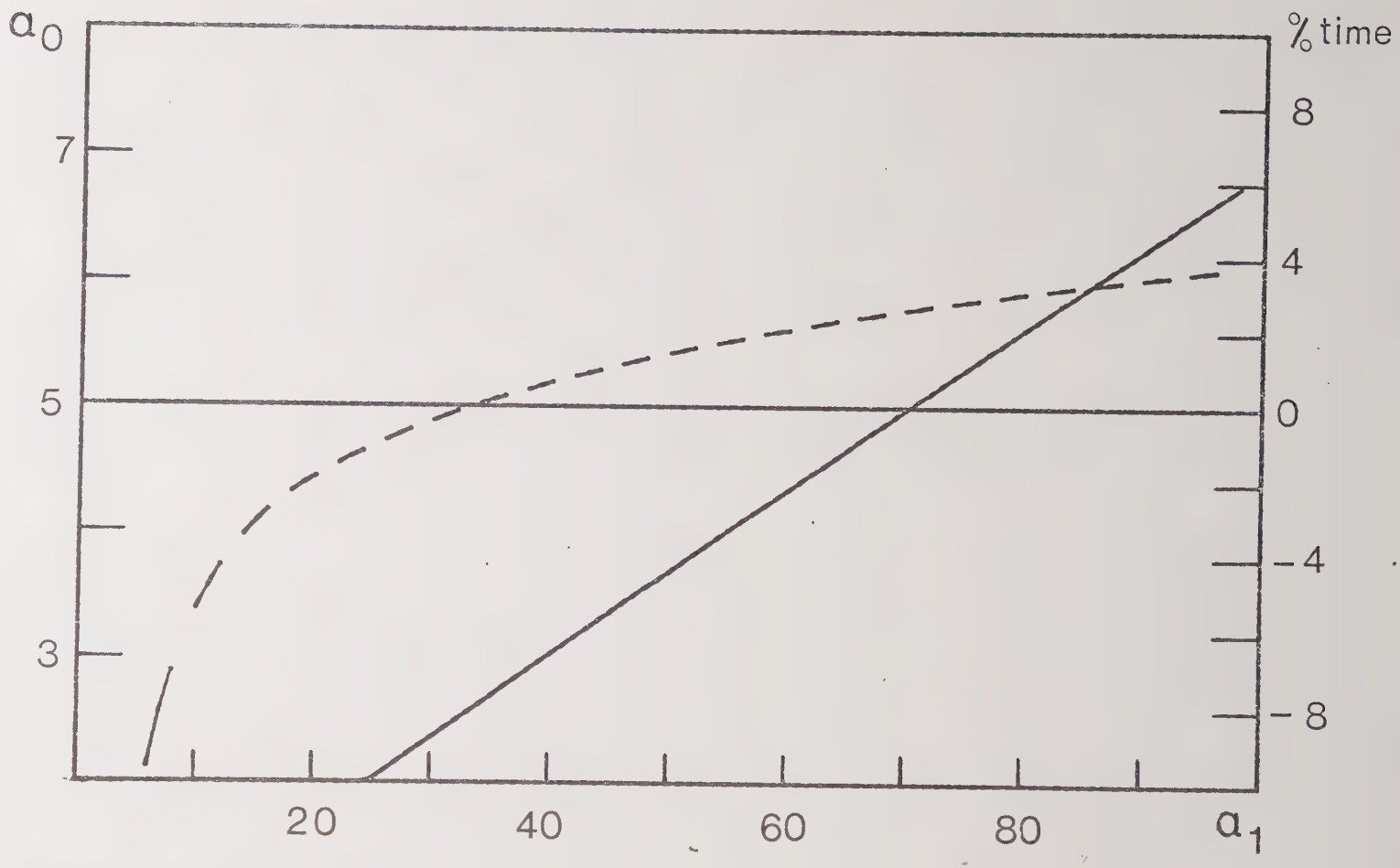

Fig. 6 : Comparison of a single and a double experiment. If two experiments with ranges 1 to α_o and α_o to α_1 are performed, instead of only one experiment in the range 1 to α_1, the continuous line indicates the best value of α_o to use. The dotted line shows the percentage of time saved (or lost for negative values) by performing two experiments instead of one.

The number of transients for each τ_i can be deviced by dividing TT by $\Sigma_i(w + \tau_i)$. Since the value of F is close to 4, The time for a T1 measurement with a given precision will approximatively be the time needed to get a N/S equal to twice this precision by pulsing 90° pulses every w..

Design of the experiment.

Figure 7 provides the necessary data to prepare a T_1 experiment. Set T_1 min. and T_1 max., the limits of the range of T_1 values to be measured. Read in panel A the τ values corresponding to your T_1min/T_1 max ratio and multiply them by T_1min Set your waiting time w to 5 T_1 max.

1) - If you desire a given precision on all the T_1 values. Let NT transients give a S/N ratio of 10. If you require a 5 % on the T_1's of all the nuclei, the number of transients for each τ_i can be calculated from Eq |20|.

Number of transients for each τ_i = NT x F^2 x $w/\sum_i(w + \tau_I)$

Whatever T_1 max/T_1 min, F^2 x $w/\sum_i(w + \tau_i)$ is close to 2.25. Thus for a 5 % precision on 95 % of the T_1 measurements, a signal over peak to peak noise ratio of 15 must be achieved on the completely relaxed (and completely inversed) spectrum . If a 10 % precision is required, just achieve 7.5 S/N ratio. We do not think that precisions better than 5 % can be significative in T_1 measurements since sample geometry, temperature control problems etc... become important.

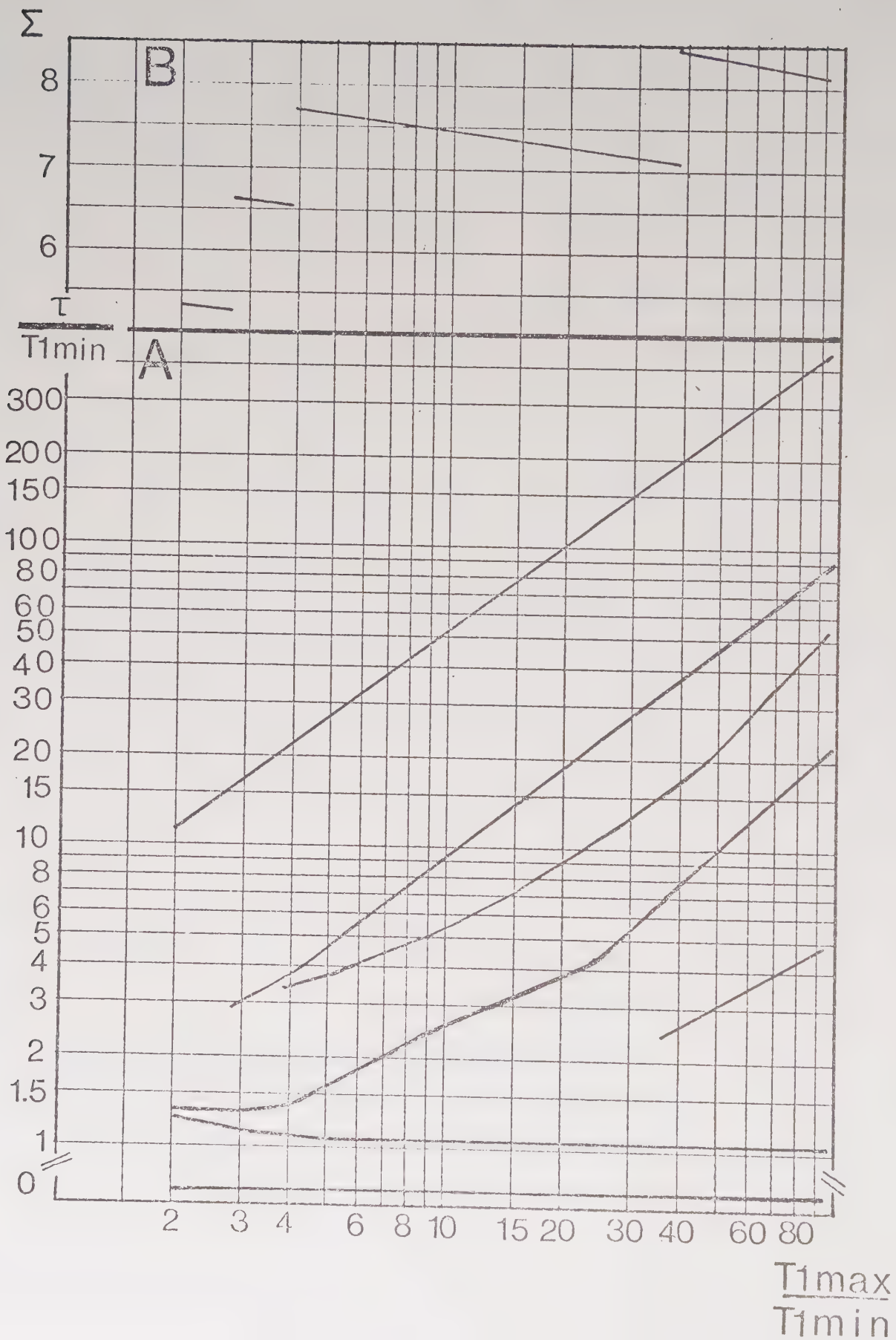
Σ
8
7
6
B
τ
T1min
A
300
200
150
100
80
60
50
40
30
20
15
10
8
6
5
4
3
2
1.5
1
0
2
3
4
6
8
10
15
20
30
40
60
80
T1max
T1min

Fig. 7 : Abacus for the design of a T_1 experiment.

Panel A : Read the τ/T_1 min values corresponding to your T_1max/T_1min value. If you desire a 5 % precision on 95 % of your T_1 measurements within this range, set the number of transients for each spectrum so that a signal/peak to peak noise ratio of 15 is achieved on the fully relaxed (and fully inversed) spectrum.

Panel B : If you have only the time TT free for your experiment, read the value of Σ corresponding to your T_1max/T_1min ratio. Then $TT/(5 \times T_1max \times \Sigma)$ is your number of transients for each of the spectra.

2) - If you have a given time TT for your experiment read in panel B the value of Σ corresponding to your T_1max/T_1min ratio. The ratio $TT/(5 \times T_1max \times \Sigma)$ will then give you the number of transients to be accumulated for each spectrum.

ACKNOWLEDGEMENTS

We are specially grateful to Dr. M. GUERON for his constant interest and advices during the course of this work and for critical reading of the manuscript.

We acknowledge Dr. G. RUCKEBUSCH for help in the mathematical treatment.

We thank Pr. M. FETIZON for his interest during this work.

BIBLIOGRAPHY

(1) G.C. Levy and I.R. Peat. J.Magn.Resonance 18. 500 (1975).

(2) R. Gerhards and W. Dietrich. J.Magn.Resonance 23. 21 (1976).

(3) W.S. Moore and T. Yalcin. J. Magn. Resonance 11. 50 (1973).

(4) D.L. De Fontaine, D.K. Ross and B. Ternai. J. Magn.Resonance 18. 276, (1975).

(5) Program obtained from the I.M.S.L. Library.